



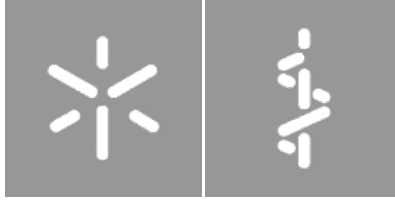
Universidade do Minho
Escola de Medicina

Nucleus Accumbens neuronal activity in associative learning

Catarina Vinhas Mósca Desevye

Catarina Vinhas Mósca Desevye

Nucleus Accumbens neuronal activity in associative learning



Universidade do Minho

Escola de Medicina

Catarina Vinhas Mósca Desevyve

**Nucleus Accumbens neuronal activity in
associative learning**

Dissertação de Mestrado
Mestrado em Ciências da Saúde

Trabalho efetuado sob a orientação de
Doutora Carina Isabel Soares da Cunha
e de
Doutora Ana João Gomes Rodrigues

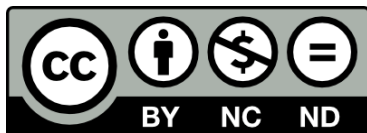
DIREITOS DE AUTOR E CONDIÇÕES DE UTILIZAÇÃO DO TRABALHO POR TERCEIROS

Este é um trabalho académico que pode ser utilizado por terceiros desde que respeitadas as regras e boas práticas internacionalmente aceites, no que concerne aos direitos de autor e direitos conexos.

Assim, o presente trabalho pode ser utilizado nos termos previstos na licença abaixo indicada.

Caso o utilizador necessite de permissão para poder fazer um uso do trabalho em condições não previstas no licenciamento indicado, deverá contactar o autor, através do RepositóriUM da Universidade do Minho.

Licença concedida aos utilizadores deste trabalho



Atribuição-NãoComercial-SemDerivações

CC BY-NC-ND

<https://creativecommons.org/licenses/by-nc-nd/4.0/>

Agradecimentos

Após a chegada ao fim desta etapa, quero agradecer a todas as pessoas que, de alguma forma, contribuíram para que pudesse concluir este trabalho de tese com sucesso.

À Doutora Ana João Rodrigues, minha orientadora, por me ter dado a oportunidade única de trabalhar nesta equipa, por me proporcionar todo o apoio e meios necessários para realizar esta dissertação. Agradeço ainda por todo o conhecimento e momentos de crescimento, pela disponibilidade contínua e pelo profissionalismo, exigência e rigor impostos.

À Doutora Carina Cunha, minha coorientadora, pela orientação, por todos os ensinamentos que me transmitiu, pelo auxílio e paciência incessantes. Obrigada por se ter mostrado sempre disponível a ajudar a resolver as dificuldades que se foram atravessando ao longo deste trabalho e pelas ideias e sugestões que me incitaram a melhorar. Obrigada por toda a ajuda, e dedicação que proporcionaram a realização deste trabalho de tese.

A todos os meus colegas de equipa, por se terem mostrado sempre disponíveis para me auxiliar. Obrigada pelos esclarecimentos e pela companhia ao longo do desenvolvimento desta dissertação.

A toda a equipa C2B, pelas discussões científicas, e, em particular, a todos os que sempre estiveram dispostos a ajudar quando necessário.

A todas as minhas amigas/os pelos momentos de convívio e por pelo apoio incondicional.

Por último, mas não menos importante, muito obrigada aos meus pais, pela educação que me deram, por todo carinho e por demonstrarem interesse pelo meu trabalho. Obrigada, por me apoiarem em todos os momentos e por me darem força e motivação para continuar!

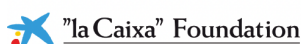
O trabalho apresentado nesta tese foi realizado no Instituto de Investigação em Ciências da Vida e Saúde (ICVS), da Universidade do Minho. O presente projeto recebeu financiamento através do Concelho Europeu de Pesquisa (ERC) no âmbito do programa de pesquisa e inovação Horizonte 2020 da União Europeia (contrato No 101003187); da Fundação “La Caixa” (ID 100010434, sob o acordo LCF/PR/HR20/52400020); da Fundação Portuguesa para a Ciência e Tecnologia (FCT) – projeto PTDC/MED-NEU/ 4804/2020 (ENDOPIO) e PTDC/SAL-TOX/6802/2020 (REMIND); da Fundação Bial (175/2020) e da Plataforma de Microscopia Científica do ICVS, membro da *PPBI - Portuguese Platform of Bioimaging* (PPBI -POCI-01-0145-FEDER-022122).



University of Minho
School of Medicine



ICVS/3B's
Associate Laboratory
University of Minho



STATEMENT OF INTEGRITY

I hereby declare having conducted this academic work with integrity. I confirm that I have not used plagiarism or any form of undue use of information or falsification of results along the process leading to its elaboration.

I further declare that I have fully acknowledged the Code of Ethical Conduct of the University of Minho.

Título: Atividade neuronal do núcleo accumbens na aprendizagem associativa

Resumo

Para sobreviver, os indivíduos aprendem sobre o que está em seu redor e ajustam-se para gerar um comportamento apropriado. Este processo é mediado em parte pelo núcleo accumbens (NAc), que é maioritariamente constituído por neurónios espinhosos médios GABAérgicos (MSNs), que expressam o recetor de dopamina D1 ou D2. Classicamente, os D1-MSNs estão associados a recompensa e os D2-MSNs a aversão; no entanto, estudos recentes questionam esta dicotomia, demonstrando que ambas as populações podem despoletar comportamentos associativos tanto positivos como negativos.

Nesta dissertação, pretendemos estudar qual é a relevância dos neurónios do tipo D1 ou D2 do NAc na aprendizagem associativa de recompensa/aversão. Inicialmente, identificámos conjuntos neuronais no NAc que representam respostas de recompensa em fases iniciais versus fases mais tardias de aprendizagem de comportamento Pavloviano. Para isto, examinamos o padrão de expressão de c-fos, uma proteína codificada por um gene de ativação imediata, que é frequentemente usada como marcador de atividade neuronal. Em paralelo, a atividade dos neurónios do NAc foi gravada durante o condicionamento pavloviano usando fotometria de fibra. Esta abordagem permitiu explorar como é que os neurónios do NAc codificam aprendizagem associativa.

Os nossos dados mostram que o NAc não apresenta alterações na densidade de células c-fos durante as fases inicial e tardia de aprendizagem, em comparação com a condição controlo. Gravações com fotometria de fibra para medir transientes de cálcio durante o condicionamento Pavloviano mostraram que a atividade “bulk” dos neurónios D1 e D2 é genericamente semelhante, mas com algumas diferenças durante a aprendizagem. Os neurónios D1 parecem desempenhar um papel particularmente relevante nos estádios iniciais do condicionamento pavloviano, uma vez que a sua atividade durante a apresentação da pista está aumentada nos “trials” iniciais. À medida que o processo de aprendizagem é consolidado, a atividade dos neurónios D1 e D2 diminui em resposta à pista e à recompensa. Finalmente, gravações com fotometria de fibra durante o condicionamento Pavloviano negativo mostraram que ambas as populações aumentam sua atividade em resposta à pista à medida que os animais associam a pista com o choque nas patas (consequência negativa), e também aumentam em resposta ao choque nas patas. Os nossos dados refutam a ideia da função dicotómica dos neurónios D1 e D2, sugerindo que estes neurónios desempenham um papel concorrente no processamento de recompensa e aversão.

Palavras-chave: aprendizagem associativa, choque na pata, estímulo condicionado, núcleo accumbens, sacarose

Title: Nucleus accumbens neuronal activity in associative learning

Abstract

To survive, individuals learn about their surroundings and adjust to generate appropriate behaviors. These processes are partially mediated by the nucleus accumbens (NAc), that is mainly composed by GABAergic medium spiny neurons (MSNs), that express either dopamine receptor D1 or D2. Classically, NAc D1-MSNs have been associated with reward, and D2-MSNs with aversion; however, recent studies challenge this view, showing that both populations can drive positive and negative associative learning.

Here, we aim to clarify what is the relevance of D1-/D2-neurons in reward/aversive (Pavlovian) associative learning. We identified NAc neuronal ensembles that represent early *versus* late Pavlovian conditioning by examining the pattern of expression of endogenous c-fos, an immediate early gene and marker of neuronal activity in B6 wild-type mice after the Pavlovian conditioning test. After, we recorded the activity of NAc neurons responsive to conditioned stimuli (CS), positive outcomes (sucrose) or to negative outcomes (shock) during positive/negative Pavlovian conditioning using fiber photometry in freely behaving mice. This approach allowed us to better understand how NAc neurons respond during associative learning.

Our data shows that the NAc does not present changes in c-fos⁺ cell density during early and late Pavlovian conditioning learning in comparison to control condition. Fiber photometry recordings of calcium transients during Pavlovian conditioning showed that D1- and D2-neurons exhibit a general similar pattern of bulk activity, with minor differences throughout learning. D1-neurons appear to play a particularly relevant role in the early stages of positive Pavlovian conditioning, as activity during CS presentation increases in the initial trials. As the learning process is consolidated, the activity of D1- and D2-neurons decreases in response to the cue and to the reward. Finally, fiber photometry recordings during negative Pavlovian conditioning showed that D1- and D2-neurons increase their activity in response to the CS as animals associate the CS with the unconditioned stimuli (US, shock), and it also increases in response to the US.

Our data contradicts the proposed model of a dichotomous function of D1- and D2-neurons and suggest that both populations play an important role in reward and aversion processing.

Key words: associative learning, conditioned stimuli, footshock, nucleus accumbens, sucrose

Table of contents

List of abbreviations and acronyms	ix
List of figures	xi
List of tables.....	xiii
CHAPTER 1 – Introduction	1
1. Introduction.....	2
1.1. Brain reward circuit	3
1.2 Cue outcome associative learning	4
1.3. Nucleus Accumbens	6
1.3.1 Neuroanatomy and neuronal populations of the NAc	6
1.4. Role of D1- and D2-MSNs in reward and aversion	9
1.4.1 Electrophysiology studies.....	10
1.4.2 Optogenetic studies.....	12
1.4.3 Calcium imaging studies- Fiber Photometry and miniaturized microscopes	14
CHAPTER 2 – Objectives.....	18
2. Objectives	19
CHAPTER 3 – Materials and Methods	20
3. Materials and Methods	21
3.1 Animals	21
3.2 D1 and D2-cre line: mating and genotyping.....	21
3.3 Surgery and optical fiber implantation	22
3.4 Behavioral experiments.....	22
3.4.1 Subjects.....	22
3.4.2 Pavlovian Conditioning	23
3.4.3 Pavlovian aversive conditioning.....	24
3.4.4. Locomotor behavior.....	25
3.5 Fiber Photometry recordings	25
3.6 Fiber photometry data analysis.....	26
3.7 Histology	27
3.7.1. Sacrifice and brain sectioning.....	27

3.7.2. Immunostaining	27
3.7.3 Image acquisition and analysis	28
3.8. Statistical analysis.....	29
CHAPTER 4 – Results	30
4. Results.....	31
4.1 NAc neuronal ensembles responding to early versus late associative learning	31
4.2 Distinct patterns of activity of D1- and D2-neurons in associative learning.....	35
4.2.1 D1-neurons respond to positive Pavlovian conditioning.....	35
4.2.2 D2-neurons respond to positive Pavlovian conditioning.....	42
4.2.3 D1-neurons activity changes in Pavlovian aversive conditioning.....	48
4.2.4. D2-neurons respond to Pavlovian aversive conditioning	54
CHAPTER 5 – Discussion, Conclusion and Future Perspectives	61
5.1 Discussion	62
5.2 Conclusion	67
5.3 Future perspectives.....	68
CHAPTER 6 – References	70
6. References.....	71
CHAPTER 7 – Supplementary information	91

List of abbreviations and acronyms

A2Ar: adenosine receptor 2a	GABA: <i>gamma</i> -aminobutyric acid
AAV: adeno-associated virus	GECI: genetically encoded calcium indicator
AAV5: adeno-associated virus serotype 5	GFP: green fluorescent protein
ACC: anterior cingulate cortex	GPe: external globus pallidus
AP: anteroposterior	GPi: globus pallidus internus
AUC: area under the curve	GuPPy: Guided Photometry Analysis in Python
BLA: basolateral nucleus of the amygdala	I.P.: intraperitoneal
Ca ²⁺ : calcium ions	ICSS: Intracranial self-stimulation
CeA: central nucleus of the amygdala	ICVS: <i>Instituto de Investigação em Ciências da Vida e Saúde</i> /Life and Health Sciences Research Institute
CeM: centromedial amygdala	IEG: immediate early gene
ChR2: Channelrhodopsin-2	iMSN: indirect pathway
CIN: cholinergic interneuron	ITI: inter trial interval
CPP: conditioned place preference	LDT: laterodorsal tegmental nucleus
Cre (or CreER): Cre recombinase enzyme	LH: lateral hypothalamus
CS: conditioned stimulus	LHb: lateral habenula
DA: dopamine	LTS: low-threshold spiking interneuron
DAPI: 4',6-diamidino-2-phenylindole	MAD: median absolute deviation
D1-MSN: medium spiny neuron expressing dopamine receptor D1	ML: mediolateral
D2-MSN: medium spiny neuron expressing dopamine receptor D2	mPFC: medial prefrontal cortex
DGAV: <i>Direção-Geral de Alimentação e Veterinária</i>	mRNA: messenger ribonucleic acid
dMSN: direct pathway	MSN: medium spiny neuron
Drd1: dopamine receptor D1	NAc: nucleus accumbens
Drd2: dopamine receptor D2	NAcc: nucleus accumbens core
DV: dorsoventral	NAcs: nucleus accumbens shell
dyn: dynorphin	NAcsLat: nucleus accumbens lateral shell
FBS: fetal bovine serum	NAcsMed: nucleus accumbens medial shell
FELASA: Federation for Laboratory Animal	PBS: phosphate buffered saline
FS: fast spiking interneuron	PBS-T: phosphate buffered saline with 0.3% triton x-100

PCR: polymerase chain reaction

PFA: paraformaldehyde

PFC: prefrontal cortex

PINP: Photostimulation-assisted Identification of
Neuronal Populations

RT: room temperature

scRNA: single-cell RNA sequencing

SEM: standart error of mean

SN: *substantia nigra*

vHPC: ventral hippocampus

VNAcMed: ventral nucleus accumbens medial
shell

VP: ventral pallidum

VTA: ventral tegmental area

US: unconditioned stimulus

WT: wild type

List of figures

Figure 1- Brain reward circuit.	4
Figure 2- Cue-outcome associative learning	6
Figure 3 - Inputs and outputs of the nucleus accumbens.	8
Figure 4 – Animals learn the association between cue and reward throughout training.	32
Figure 5 – Quantification of c-fos+ cell density in the NAc of mice at early learning (day 2).	33
Figure 6 - Quantification of c-fos+ cell density in the NAc of mice at late learning (day 12).	34
Figure 7 – Behavior of D1-cre mice injected with GCaMP6f during positive Pavlovian conditioning	36
Figure 8 – Activity of D1-neurons during Pavlovian conditioning.....	37
Figure 9 – Activity of D1-neurons decreases in response to the CS across days of training in the Pavlovian conditioning.....	39
Figure 10 - Activity of D1-neurons decreases in response to the US across days of training in the Pavlovian conditioning.....	40
Figure 11 –D1-neurons activity decreases in response to CS and US from day 1 to day 12 of Pavlovian conditioning.	41
Figure 12 – Behavior of D2-cre injected with GCaMP6f during positive Pavlovian conditioning.....	43
Figure 13 – Activity of D2-neurons during Pavlovian conditioning	44
Figure 14 – Activity of D2-neurons decreases in response to the CS across days of training in the Pavlovian conditioning.....	45
Figure 15 - Activity of D2-neurons decreases in response to the US across days of training in the Pavlovian conditioning.....	46
Figure 16 – D2-neurons activity decreases in response to CS and US from day 1 to day 12 of Pavlovian conditioning.....	47
Figure 17 – Behavior of D1-cre mice injected with GCaMP6f during Pavlovian aversive conditioning ...	48
Figure 18 – Average activity of D1-neurons during Pavlovian aversive conditioning	50
Figure 19 – Activity of D1-neurons during Pavlovian aversive conditioning	51
Figure 20 – Activity of D1-neurons increases in response to the CS.....	52
Figure 21 – Activity of D1-neurons increases in response to foot shock	53
Figure 22 – D1-neurons activity in day 1 and day 3 in response to CS and to US (shock)	54
Figure 23- Behavior of D2-cre mice injected with GCaMP6f during Pavlovian aversive conditioning.....	55
Figure 24 – Average activity of D2-neurons during Pavlovian aversive conditioning	56
Figure 25 – Activity of D2-neurons during Pavlovian aversive conditioning	57

Figure 26 – Activity of D2-neurons increases in response to the CS.....	58
Figure 27 – Activity of D2-neurons increases in response to foot shock	59
Figure 28 – D2-neurons activity in day 1 and day 3 in response to CS and to the US (shock).....	60

List of tables

Table 1 - Summary of the main results obtained from c-fos expression in NAc neurons responding to early versus late learning, and activity of NAc D1- and D2-neurons during Pavlovian conditioning and fear conditioning..... 67

CHAPTER 1 – Introduction

1. Introduction

Daily, species learn and adjust their behavior according to their surroundings. Individuals use previously neutral environmental cues and attribute emotional/motivational value to them, if they are associated with a positive/rewarding or negative/aversive event (Cerri et al., 2014). These associations, often called Pavlovian conditioning, allow individuals to obtain desired outcomes and increase chance of survival and propagation (Soares-Cunha et al., 2020). A Pavlovian conditioning involves the association between a cue and an unconditioned stimulus (US) that possess inherently rewarding or aversive properties. This transforms the cue into a conditioned stimulus (CS), that after learning have the property of driving innate rewarding and aversive responses and contributes to learning (Pavlov (1927), 2010). Evidence shows that these processes are mediated by the brain reward circuit, and particularly by the nucleus accumbens (NAc) (Wise, 2002). In fact, impairment/dysfunction in this brain region has been associated with the development of neuropsychiatric disorders such as depression or substance abuse (reviewed in(Xu et al., 2020)). Thus, it is fundamental to understand how the NAc functions to understand the pathophysiological mechanisms of disease with altered rewarding/aversive responding (Cooper et al., 2017; Dichter et al., 2012).

Throughout the years, much attention has been given to the NAc in reward processing since it integrates both cortical (glutamatergic) and limbic (dopaminergic) signals to produce appropriate rewarded or aversive behaviors (Berridge & Kringelbach, 2015; Carlezon & Thomas, 2009; Roitman et al., 2005; Wise, 2002). These signals are decoded mainly by GABAergic medium spiny neurons (MSNs), which account for ~95% of the accumbal neurons, being divided into those that express dopamine receptor D1 (D1-MSNs) or D2 (D2-MSNs) (Gerfen et al., 1990). D1-MSNs project directly to basal ganglia effector brain regions, such as the ventral tegmental area (VTA), forming the direct pathway. D2-MSNs, together with a sub-population of D1-MSNs, project to the ventral pallidum (VP), which then projects to the VTA, forming the indirect pathway (Kupchik et al., 2015; Soares-Cunha et al., 2018).

MSNs were traditionally describe as having a dichotomous function in reward, with D1-MSNs mediating positive reinforcement/reward and D2-MSNs negative reinforcement/aversion (Hikida et al., 2010; Kravitz et al., 2012; Lobo et al., 2010; Volman et al., 2013). However, recent studies challenge this view (Cole et al., 2018; Natsubori et al., 2017; Soares-Cunha, Coimbra, David-Pereira, et al., 2016). Notably, optogenetic activation of either D1- or D2-MSNs in the NAc supports self-stimulation (Cole et al., 2018). In addition, other research, and particularly work from our team, has shown that both D1- and D2-MSNs can drive reward and aversion (Namvar et al., 2019; Natsubori et al., 2017; Soares-Cunha,

Coimbra, David-Pereira, et al., 2016; Soares-Cunha et al., 2018, 2020, 2022; Steinberg et al., 2014). Therefore, the prevailing notion of a functional dichotomy of MSN activity in the NAc was reconsidered.

Although it is known that NAc neurons are important for cue-reward learning, there is still controversial data around this topic. This emphasizes the need to investigate what is the anatomical and functional specificity of reward- and aversion-responsive ensembles. In this framework, we evaluated D1- and D2- neurons activity in the NAc during associative learning by performing fiber photometry during positive and aversive Pavlovian conditioning.

1.1. Brain reward circuit

In the early 1950s, James Olds and Peter Milner were the first to describe the brain's reward circuit (Haber & Knutson, 2010). Through a pioneering experiment, they realized that rats repeatedly press levers to receive electrical stimulation, especially when this stimulation was targeted to certain areas of the brain like the septum and the NAc (Kringelbach & Berridge, 2010; Olds & Milner, 1954). These results corroborated the idea of the existence of a reward circuit, therefore, in the subsequent years, many researchers have intensively studied this subject.

Reward is generally defined as any event, stimulus or object that motivates us, promoting pleasure or positive emotions, like food, sex, or social interactions (Hu, 2016; Pearce & Hall, 1980; Schultz, 1998, 2000). Reward is a central component involved in reinforcement learning since it increases the probability of a specific behavior in order to obtain the reward. The reward circuit is a complex neural network responsible for maintaining learned behavior, to mediate appropriate responses to stimuli, and to develop goal-directed behaviors for which individuals can evaluate reward value and risk accurately (Haber & Knutson, 2010; Lewis et al., 2021; Schultz, 2000; Soares-Cunha et al., 2020). Importantly, dysfunction of the reward circuit has been implicated in prominent neuropsychiatric disorders, including obsessive-compulsive disorder, depression, and drug addiction (Nicola, 2007; Sesack & Grace, 2010). Therefore, many studies are focused in understanding how this network works to better understand the pathophysiological mechanisms of patients with these disorders (Lewis et al., 2021; Soares-Cunha, Coimbra, Sousa, et al., 2016; Xu et al., 2020).

The reward circuit (**Figure 1**) links together a variety of brain structures, including the NAc, the VTA (Lammel et al., 2012; Nieh et al., 2013), medial prefrontal cortex (mPFC), central nucleus of the amygdala (CeA) (Balleine & Killcross, 2006; Šimić et al., 2021), basolateral amygdala (BLA) (Balleine & Killcross, 2006; Namburi et al., 2015; O'Neill et al., 2018), hippocampus (Swanson, 1982), laterodorsal tegmental nucleus (LDT) (Šimić et al., 2021) and VP (Mondoloni et al., 2022). Notably, the most important

and best characterized reward circuit node is the mesolimbic reward pathway, that comprise dopaminergic projections arising from the VTA to the NAc (Koob & Le Moal, 2008; G. Mogenson et al., 1980; Russo & Nestler, 2013). This VTA-NAc circuitry is critical for detecting environmental rewards and triggering their consumption; however, it is also critical for controlling responses to aversive stimuli (Russo & Nestler, 2013). Besides this dopaminergic projections to the NAc, VTA also innervates other regions, such as mPFC, CeA, BLA and hippocampus (Nieh et al., 2013; Oades & Halliday, 1987; Swanson, 1982). In addition, mPFC and hippocampus also modulate accumbal activity through glutamatergic innervations and, on the other hand, the NAc modulates VTA activity through GABAergic projections. Furthermore, VTA dopaminergic neurons receive glutamatergic inputs from the mPFC, LDT and LH resulting in increased dopamine release within the NAc, therefore, promoting reward. In turn, VTA GABAergic neurons receive glutamatergic inputs from the LHb which promote aversion. Finally, VTA and NAc receive direct cholinergic innervation from the LDT, that is predicted to induce positive reinforcement (Cooper et al., 2017; Russo & Nestler, 2013).

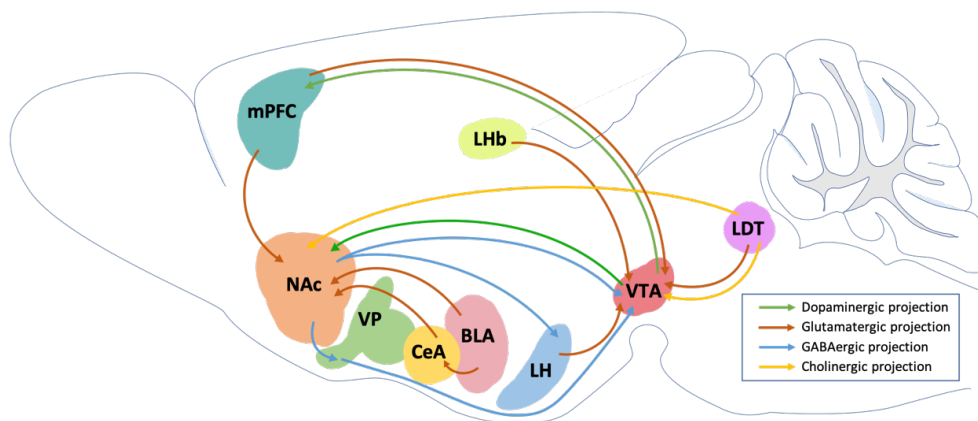


Figure 1- Brain reward circuit. Schematic sagittal representation of the main projections comprising the rodent brain reward circuit. The main reward circuit includes dopaminergic projections from the VTA to the NAc. In turn, NAc is able to modulate VTA through GABAergic projections (either direct or indirect through VP). In addition, NAc receives dense glutamatergic projections arising from the mPFC, BLA and CeA. The VTA receive such inputs from the mPFC, LDT and LH, promoting reward. On the other hand, receives glutamatergic projections from the Lhb, which act to promote aversion. Finally, VTA and NAc receive cholinergic projections from the LDT, which are thought to function on positive reinforcement. NAc - Nucleus Accumbens; VP - Ventral Pallidum; BLA - Basolateral Amygdala; CeA - Central Amygdala; LH - Lateral Hypothalamus; Lhb - Lateral Habenula; VTA - Ventral Tegmental Area; mPFC - medial prefrontal cortex; LDT - Laterodorsal tegmental nucleus.

1.2 Cue outcome associative learning

Every day, organisms have to learn about their environment and continually adapt their behavior to increase chance of survival and propagation (Day & Carelli, 2007; Soares-Cunha et al., 2020). Individuals use neutral environmental stimuli to perceive the availability of rewards and learn these

associations to attribute emotional value (Cerri et al., 2014). These associations, are classical cases of Pavlovian conditioning, in which a neutral cue is assigned to be positive/rewarding or negative/aversive (Day & Carelli, 2007; Hanley & Garland, 2019). Therefore, Pavlovian learning is the basis for both normal and maladaptive human behaviors. Thus, understanding reward-cue associative learning may help us better comprehend a range of human behaviors.

Cue-outcome associative learning (**Figure 2**) occurs every time an individual learns to associate two elements in the environment. There are two branches of cue-outcome associative learning, stimulus-outcome (classical or Pavlovian conditioning) and action-outcome (operant or instrumental conditioning).

Classical or Pavlovian conditioning was first described by Pavlov (1927), who showed that dogs could be conditioned to salivate at the sound of a bell if that sound was repeatedly presented at the same time that they were given food (Pavlov (1927), 2010).

Stimuli that evoke innate responses without requiring any type of learning are designated unconditioned stimuli (US) (Namburi et al., 2016; Pearce & Hall, 1980). For example, outcomes such as food, water or sexual stimuli are considered positive US since they elicit appetitive responses. On the other hand, outcomes like the presence of a predator or a foot shock, are considered a negative US (Day & Carelli, 2007; Pavlov (1927), 2010). When a neutral stimulus (cue), such as a sound, a light or an odor, predicts a positive or negative US, it is considered a conditioned stimulus (CS) (Galaj & Ranaldi, 2021; Namburi et al., 2016; Pearce & Hall, 1980). Therefore, Pavlovian conditioning involves the repeated pairing of a CS with a US, with learning taking place when the previously neutral stimulus gains predictive value for the upcoming reward (Day & Carelli, 2007; Flagel, Clark, et al., 2011; Namburi et al., 2016). Licking or nose poking in response to a tone (CS) followed by a sucrose reward (US) or freezing during the presentation of a tone (CS) that predicts foot shock (US) are examples of a positive and negative Pavlovian conditioning, respectively (Day & Carelli, 2007).

In operant or instrumental conditioning, animals learn associations between actions and a positive or negative outcome. Lever press, is an example of operant conditioning, in which the animal needs to performed an action (press the lever) in order to receive the outcome or avoid a negative outcome.

The ability to form and use cue-outcome associations is mediated by the cooperation of many brain regions that integrate sensory and motivational information and alter motor output. Specially, the NAc, which is consider the center of this network, has received much attention in this respect (Day & Carelli, 2007; Russo & Nestler, 2013). Emerging evidence indicates that NAc is critical to process information about unconditioned rewards and to learn Pavlovian associations between these rewards and

external stimuli. Intraoral administration of a sucrose solution reduces NAc neuronal activity (Roitman et al., 2005). This inhibition was also observed when animals performed operant responses for self-administration of sucrose (Nicola et al., 2004b) or water and food (Roitman et al., 2005). Nevertheless, when an aversive quinine solution was delivered intra-orally the opposite occurs (Roitman et al., 2005). Contrary to what happens in the NAc, VP neurons show an increase in activity during consumption of a rewarding sucrose solution (Tindell et al., 2006), indicating that other brain regions are involved in reward-related behaviors, such as consumption. In addition, repeatedly exposing animals to a CS followed by a sucrose reward resulted in the gradual development of selective conditioned approach responses towards the reward predictive cue but not towards the unpaired cue (Day et al., 2006a). Moreover, CS elicited a greater excitation response than the reward itself. As a result, it has been proposed that such excitations among NAc neurons are caused by glutamatergic inputs from cortical and limbic structures, competing for motor resources via striatal circuits (Pennartz et al., 1994).

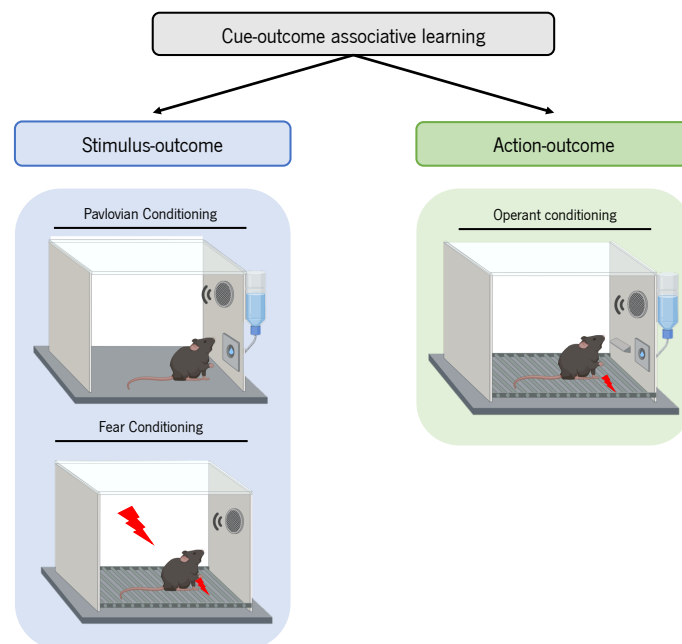


Figure 2- Cue-outcome associative learning. a) Schematic representation of the two branches of cue-outcome associative learning: Pavlovian conditioning and Fear conditioning behavior (on left, blue); Operant conditioning behavior (on right, green).

1.3. Nucleus Accumbens

1.3.1 Neuroanatomy and neuronal populations of the NAc

The NAc is a major component of the ventral striatum located ventrolaterally to the septal nuclei and ventromedial to the caudate-putamen (Setlow, 1997; Zahm & Brog, 1992; Zahm & Heimer, 1990). While, the NAc is the most prominent brain region for reward behavior, pioneering studies have revealed

that the NAc functions as a key hub of the brain reward circuit (Berridge & Kringelbach, 2015) receiving inputs from limbic and cortical areas (Heimer & Alheid, 1991; McGeorge & Faull, 1989; Sesack & Grace, 2010).

The NAc receives glutamatergic inputs (**Figure 3**) from the amygdala (Fuller et al., 1987; Heidbreder & Groenewegen, 2003; McDonald, 1991; Morgane et al., 2005; Phillipson & Griffiths, 1985; Stuber et al., 2011), thalamus (Heimer & Alheid, 1991; Lanciego et al., 2004; Phillipson & Griffiths, 1985), hippocampus, (Heidbreder & Groenewegen, 2003; Kelley & Domesick, 1982; Morgane et al., 2005), and prefrontal cortex (PFC) (Phillipson & Griffiths, 1985; Yin & Knowlton, 2006); cholinergic projections from the LDT (Dautan et al., 2014); and dopaminergic (Hnasko et al., 2012; Phillipson & Griffiths, 1985; Tritsch et al., 2012), glutamatergic (Qi et al., 2016) and GABAergic projections (Brown et al., 2012; Van Bockstaele & Pickel, 1995) from the VTA (Beier et al., 2015; Berrios et al., 2016; Tecuapetla et al., 2010; Tritsch et al., 2014). In turn, the NAc sends outputs to effector regions within the brainstem (Beier et al., 2015; Poulin et al., 2018), through GABAergic projections to the basal ganglia and some thalamic and cortical areas (Heimer & Alheid, 1991; Sesack & Grace, 2010), in particular, the VP (Groenewegen & Russchen, 1984; Lu et al., 1998), the VTA (Záborszky & Cullinan, 1992; Zhou et al., 2003), the thalamus and the lateral hypothalamus (Groenewegen & Russchen, 1984; G. J. Mogenson et al., 1983; Nauta et al., 1978; Williams et al., 1977). Furthermore, studies suggest that the NAc may also send efferent outputs to areas such as the amygdala, globus pallidus, *substantia nigra*, LHb, BNST, *substantia innominata* and septum (G. J. Mogenson et al., 1983; Williams et al., 1977; Zhou et al., 2003).

Indeed, the NAc modulates behavior to instruct individuals to gravitate their attention towards appetitive stimuli, such as food or sex (Hassani et al., 2001; Nicola, 2007). On the other spectrum of behavioral response, the NAc has also been highly implicated in aversive responses (Soares-Cunha et al., 2020).

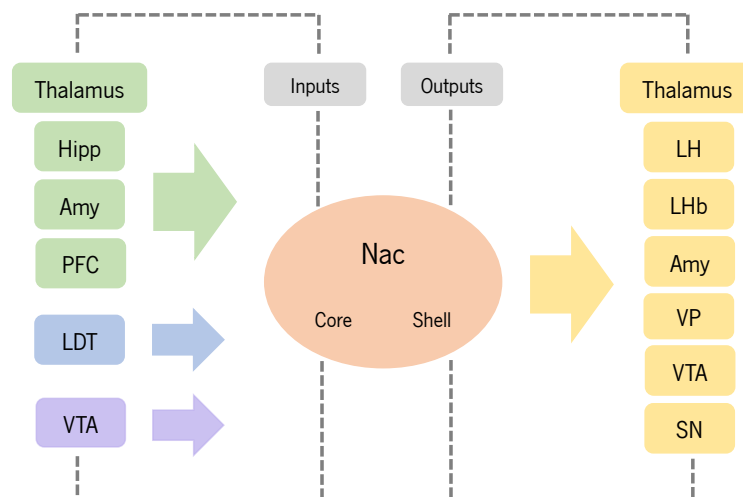


Figure 3 - Inputs and outputs of the nucleus accumbens. Schematic representation of NAc input and output regions. Inputs: glutamatergic projections from the amygdala, thalamus, hippocampus, prefrontal cortex (PFC) (left, green); cholinergic projections from the laterodorsal tegmentum (LDT (left, blue) and dopaminergic inputs from the ventral tegmental area (left, purple). Outputs: GABAergic projections to regions as the thalamus, lateral hypothalamus (LH), lateral habenula (LHb), amygdala (Amy), ventral pallidum (VP), ventral tegmental area (VTA) and substantia nigra (SN) (right, yellow).

1.3.1.1 NAc core vs shell

The NAc is divided into two anatomically and functionally distinct sub regions – core and shell (Ito & Hayden, 2011; Záborszky et al., 1985). At a molecular level, they differ in the distribution of neuroactive substances and receptors, specifically, molecules like substance P (Prensa et al., 2003), calretinin (Deutch & Cameron, 1992), dopamine (Deutch & Cameron, 1992), serotonin (Deutch & Cameron, 1992) and serotonin receptors (Patel et al., 1995) that are enriched in the NAc shell, and calbindin (Prensa et al., 2003; Voorn et al., 1989; Zahm & Heimer, 1990), enkephalin (Berendse & Groenewegen, 1990; Caboche et al., 1993; Rogard et al., 1993) and GABA_A receptors (Churchill et al., 1992) that are more prominently expressed in the core (Ito & Hayden, 2011). In addition, these two NAc sub-divisions receive different inputs and outputs that might contribute for different roles in behavior. Particularly, NAc core (NAcc) receives inputs from the prelimbic cortex, BLA and dopaminergic projections from the substantia nigra, therefore, it is more related with cue-conditioned motivated behaviors (McFarland et al., 2003; Robbins et al., 2008; Xia et al., 2020). On the other hand, NAc shell (NAcs) receives glutamatergic inputs from the infralimbic cortex (Quiroz et al., 2016), ventromedial PFC, hippocampus, and rostral and caudal basal amygdaloid complex as well as dopaminergic projections from the VTA, appearing to be important in reward processing (Ikemoto, 2007; Rodd-Henricks et al., 2002; Sellings & Clarke, 2003; Xia et al., 2020).

1.3.1.2 Neuronal population of the NAc - *direct and indirect pathway*

The NAc conveys positive and aversive reward information mainly through excitatory projections from the cortex that are differentially shaped through dopamine signals arising from the VTA (Fiorillo, 2013; Lammel et al., 2011, 2012; Roitman et al., 2005). The majority of these signals are decoded by GABAergic MSNs, which account for about 95% of the accumbal neurons, while the remaining cells (5%) are interneurons (Gangarossa et al., 2013; Graveland & DiFiglia, 1985; Heiman et al., 2008).

Traditionally, MSNs can be divided into two classes according to dopamine receptor expression: dopamine receptor D1 expressing neurons (D1-MSNs), projecting directly to basal ganglia effector brain regions such as the VTA (the direct pathway) or indirectly through the VP (the indirect pathway), while

dopamine receptor D2 expressing neurons (D2-MSNs) only project indirectly to effector regions of the brain such as the VTA through the VP (Berendse & Groenewegen, 1990; Churchill et al., 1992; Kupchik et al., 2015; Soares-Cunha et al., 2018). These two MSN populations present different neurochemical properties: D1-MSNs express substance P and dynorphin, while D2-MSNs express enkephalin and adenosine receptor 2a (A2aR) (Gerfen, 1992; Gertler et al., 2008; Kawaguchi, 1997; Lobo et al., 2006). In addition, both accumbal D1- and D2-MSNs appear to be distributed differently across the NAc. Both D1- and D2-MSNs are homogeneously distributed throughout the NAc core; however, D2-MSNs have been shown to exhibit a nonuniform distribution in the NAc shell, with higher expression in the medial and ventral NAc shell (Gangarossa et al., 2013).

Additionally, it has been hypothesized that 5-15% of MSNs co-express both *Drd1* and *Drd2* (Bertran-Gonzalez et al., 2008; Perreault et al., 2011; Valjent et al., 2009), which project to GPe, GPi, SNr and VTA (Deng et al., 2006; H. B. Wang et al., 2006; H.-B. Wang et al., 2007), however their exact role is still unknown (Soares-Cunha, Coimbra, Sousa, et al., 2016).

The remaining 5% of NAc neurons are local interneurons (Graveland & DiFiglia, 1985), that include large tonically active cholinergic interneurons (CINs) (Dautan et al., 2014), fast spiking (FS) GABAergic interneurons (Tepper & Bolam, 2004), low-threshold spiking (LTS) interneurons (Ibáñez-Sandoval et al., 2015; Kreitzer, 2009), and tyrosine hydroxylase and calretinin striatal interneurons, less explored subtypes (Soares-Cunha, Coimbra, Sousa, et al., 2016). Despite their low representation they play a crucial role in NAc activity and response to salient stimuli and modulate reward-dependent behaviors (Al-Hasani et al., 2021; Lee et al., 2020; Pakhotin & Bracci, 2007; Schall et al., 2021; Threlfell et al., 2012).

1.4. Role of D1- and D2-MSNs in reward and aversion

Classically, MSNs have been thought to have a dichotomous function in reward, with D1-MSNs being associated with reward and positive reinforcement and D2-MSNs being associated with negative reinforcement and aversion (Hikida et al., 2010; Kravitz et al., 2012; Lobo et al., 2010; Tai et al., 2012). For example, Kravitz et al. (2012) demonstrated that D1-MSN optogenetic stimulation induces persistent reinforcement, while D2-MSN stimulation induces transient punishment in the dorsomedial striatum (Kravitz et al., 2012). Similar to the previous study, activation of NAc D1-MSNs enhances cocaine-mediated conditioning, whereas activation of D2-MSNs induced the opposite effect (Airan et al., 2009; Cui et al., 2013; Vicente et al., 2016). However, recently new data has put this dichotomy into question. As a result, one might speculate that both D1- and D2-MSNs are able to distinctively and differently code

for the several events that encompass positive reward related responses (e.g. internal states, cue exposure, response after cue exposure, operant response, reward delivery and consumption), as well as aversive events (e.g. avoidance, fear) (Al-Hasani et al., 2015; Cole et al., 2018; Natsubori et al., 2017; Soares-Cunha, Coimbra, David-Pereira, et al., 2016; Soares-Cunha et al., 2018, 2020; Steinberg et al., 2014; Vicente et al., 2016).

In the following sections, we will discuss optogenetic, electrophysiology and calcium imaging studies in more detail to try to clarify the biological role of NAc D1- and D2-MSNs in associative learning and in rewarding and aversive behaviors.

1.4.1 Electrophysiology studies

It is well accepted that the NAc plays a key role in reward and aversion, and many electrophysiological studies have attempted to define this involvement since this technique enables temporal manipulation of neuronal activity during behavioral engagement.

Predictive cues paired with reward presentation - associative learning - are known to be processed by specific subsets of NAc neurons and the majority of these responses arise after learning the relationship between the cue (CS) and appetizing stimuli (US) (Setlow et al., 2003). Pioneering studies by Schultz and colleagues using electrophysiological recordings from primate ventral striatum have shown that MSNs reveal excitations in response to cues that predict reward, that strongly depend on the predictive value of the cue and the magnitude and temporal proximity of the reward (Apicella et al., 1992; Hollerman et al., 1998; Schultz, 1998). In line with that, other electrophysiological studies in primates have shown also an increase in activity in response to cue-reward associations (Bowman et al., 1996; Cromwell & Schultz, 2003; Hassani et al., 2001).

Another study describes that, in a Pavlovian-conditioned approach task, the majority of the recorded accumbal neurons (89%) exhibited significant responses during the conditioned stimulus (CS) and the reward (US) exposure (Wan & Peoples, 2006). Interestingly, when the sucrose (US) was presented in an unconditioned presentation context (innate response), the response was predominantly inhibitory (Nicola et al., 2004b; Roitman et al., 2005, 2010; Wheeler & Carelli, 2009). Likewise, the same response was verified using other rewards such as saccharin, which revealed that most neurons exhibited excitation following the second-order stimulus and inhibition to the primary reinforcer (Wheeler et al., 2008; Wilson & Bowman, 2004).

Furthermore, NAc MSNs increase phasically during cue presentations but decrease during reward delivery (Ambroggi et al., 2011; Day et al., 2011; Gale et al., 2014). Similarly, recordings during a

Pavlovian conditioning revealed that MSNs significantly increase their firing rate during the conditioned stimulus whereas the responses to reward were predominantly inhibitory (Day & Carelli, 2007; Wan & Peoples, 2006). In addition, evidences show that the NAc displays two subpopulations that can exhibit increase and/or decrease in firing rate during CS paired with a US. In contrast, when a CS is not paired with a US, the excitatory neurons shows a smaller increase in activity, while the inhibitory subpopulation exhibits no changes in firing (Day et al., 2006a). The same evidence was present in the NAc shell alone studies (Ghitza et al., 2003).

Concerning aversive stimuli, the delivery of quinine (unpleasant taste stimuli) without prior exposure, elicits an excitatory response (Roitman et al., 2005). In agreement, increase in NAc firing rates was also observed in response to other aversive stimuli like air puff (Yanagimoto & Maeda, 2003). Moreover, data show the existence of NAc neuronal subpopulations that seemed to respond to aversion-predictive cues. This response, like in reward, grows as learning progresses and associations between cue and the aversive stimuli (quinine) occur (Roitman et al., 2005; Setlow et al., 2003).

Furthermore, different neural populations appear to have distinctive phasic inhibition and excitation patterns related to different operant behavior stages, such as approaching the lever and reward consumption (water (Carelli et al., 2000; Carelli & Deadwyler, 1994; Carelli & Wondolowski, 2003); food (Carelli et al., 2000); sucrose (Kravitz et al., 2006; Nicola et al., 2004a)). During a decision-making task, in which distinct visual cues predicted high-value (low effort/immediate) and low-value (high effort/delayed) rewards, electrophysiology analysis revealed distinct subgroups of NAc neurons that exhibit phasic patterns of activity (excitation or inhibition) relative to all stages of the task, including cue presentation, operant responses and reward delivery. These findings provide evidence that NAc activity contributes to both cost- decision-making processes and actual consumption (Day et al., 2011). In line with that, NAc neurons display both excitations and inhibitions to reward consumption during a discriminative stimulus task. However, this response was smaller when the animals made an uncued entry in the reward receptacle. As a result, predictive cues are a key factor in almost all phasic firing pattern of NAc neurons, and these firing patterns during consummatory behavior are comparable to those during appetitive behavior (Nicola et al., 2004b). Additionally, reward-predictive cue elicited more frequent and larger magnitude responses in the NAcc than in the shell. Conversely, more NAc neurons selectively responded to unrewarded stimulus. This suggest that neurons with similar firing patterns in the core and shell may have different behavioral responses depending on their distinct projection targets (Ambroggi et al., 2011).

More recently, it was discovered that NAc D2-MSNs played a crucial role in the response to reward-predicting cues. Specifically, these neurons increased firing in response to cues that predicted lever availability for electrical stimulation of the VTA, while responses to lever pressing primarily involved D1-MSNs (Owesson-White et al., 2016). In agreement, our team's research also revealed that activity of D2-MSNs is necessary at cue presentation, but not so much at reward delivery (Soares-Cunha et al., 2022).

Although these results indicate relevance for MSNs in encoding cue reward/aversion-related value, they lack cell specificity, thus, not allowing extrapolation for the specific role of D1- or D2-MSNs.

1.4.2 Optogenetic studies

Optogenetics is a tool that allows to selectively manipulate specific neurons in a temporally controlled manner using light and genetic engineering. Therefore, this technique has been shown to be an excellent tool to help understand the role of NAc D1- and D2-MSNs in reward. Consistent with their reinforcing properties, activation of D1-MSNs in the dorsal striatum was sufficient to induce an operant behavior in order to receive optic stimulation of these neurons (Kravitz et al., 2010). Another study demonstrated that unilateral stimulation of D1-MSNs shifts reward responses towards the contralateral side of the stimulation (Tai et al., 2012). Additionally, optogenetic inhibition of D1-MSNs suppressed cocaine sensitization (Chandra et al., 2013). Conversely, optical stimulation of D1-MSNs would increase cocaine conditioning effects whereas optical activation of D2-MSNs would decrease it (Kupchik et al., 2015). Furthermore, optogenetic activation of dynorphin-expressing neurons (dyn; expressed in D1-MSNs) in the distinct subregions within the NAc drive opposing motivational behavioral states. Particularly, in dorsal NAc induced place preference, whereas in the ventral NAc it induced place aversion. These data show that manipulating genetically identical neuronal populations can have different, and even opposing, effects depending on their anatomical location (Al-Hasani et al., 2015).

Regarding the role of D2-MSNs, its inhibition enhances cocaine motivation while optical stimulation suppresses cocaine self-administration (Bock et al., 2013). In addition, activation of NAc D1-MSNs increased alcohol intake whereas inhibiting decreased it. On the contrary, inhibiting D2-MSNs increase alcohol intake (Strong et al., 2020). However, evidence show that this role of D2-MSNs is too simplistic once stimulation of NAc D2R-expressing neurons affected neither the acquisition nor the expression of cocaine-induced behavioral sensitization (Song et al., 2014).

Work from our team showed that brief optogenetic activation of either D1- or D2-MSNs within the NAc is sufficient to increased motivation to work towards the reward (reflected in a significant increase in

the breakpoint of the animals in a progressive ratio task). Conversely, inhibiting those neurons, a decrease in motivation was observed (Soares-Cunha, Coimbra, David-Pereira, et al., 2016). We also demonstrated that optogenetic modulation of D2-MSNs indirectly modulates VTA dopaminergic activity, contributing to increased motivation and that both *Drd1* and *Drd2* are required to produce this effect (Soares-Cunha et al., 2018). Interestingly, brief optogenetic activation of D1- and D2-MSNs induced positive reinforcement and increased cocaine conditioning, whereas prolonged optogenetic activation elicited negative reinforcement and decrease cocaine conditioning in the case of D2-MSN (Soares-Cunha et al., 2020). More recently, our team has also demonstrated that D2-MSN-VP projections are crucial for enhancing the value of a cue that predicts a future reward and increase effort to acquire the reward (Soares-Cunha et al., 2022). Moreover, optogenetic activation of these projections decreased preference for the lever that resulted in the delivery of the pellet and laser stimulation compared to the lever that resulted in the delivery of the pellet alone (Soares-Cunha et al., 2022).

Supporting our data, in the ventrolateral striatum, both D1- and D2-MSNs are activated at the trial start cue in the PR test. However, inhibiting either MSNs population immediately after the trial start cue resulted in a reduction of goal-directed behavior (Natsubori et al., 2017). In addition, only D1-MSN selective inhibition immediately following the initial lever press reduced behavior, showing D1-MSN-specific coding at that precise moment (Natsubori et al., 2017). In line with previous studies, optogenetic activation of either D1- or D2-MSNs in the NAc supports self-stimulation, but only D1-MSN activation would induce place preference for a location associated with optical stimulation (Cole et al., 2018). In agreement activation of both D1- and D2-MSNs are required to drive intra cranial self-stimulation (ICSS) behavior, thus contributing for positive reinforcement (Steinberg et al., 2014).

All these results confirm that excitation of both D1- and D2-MSNs support incentive motivation, either this being to obtain a specific reward or to self-stimulate.

Despite a lot of attention has been given to D1- and D2-MSNs in relation to rewarded responses, one has to consider its role in aversion. In a recent study, we showed that both D1- and D2-MSNs can drive reward and aversion (Soares-Cunha et al., 2020). Interestingly, brief stimulation of D1-MSNs (1 second pulsed stimulation at 40Hz) caused place preference in a classical conditioned place preference (CPP) task. This effect was through direct inhibition of GABAergic activity within the VTA, and indirect disinhibition of dopaminergic activity within the same brain region. In the case of D2-MSNs, brief activation also caused place preference, but in this case, it was due to loss of inhibitory activity of VP neurons over dopaminergic neurons of the VTA. On the opposite spectrum, prolonged, high frequency-like stimulation (sixty seconds of pulsed 40Hz stimulation) of both accumbal D1- and D2-MSNs caused aversive

responses (Soares-Cunha et al., 2020). Importantly, deeper investigation on the mechanism behind these results revealed a relevant role of the opioid system, since both D1- and D2-MSNs are capable of co-releasing opioids (dynorphin and enkephalin, respectively) in the VTA and VP. Interestingly, blocking kappa opioid receptors at VTA or delta opioid receptors at VP blocked the prolonged stimulation-induced aversion (Soares-Cunha et al., 2020). Another recent study also reported that high frequency stimulation of D1-MSNs induces co-release of the excitatory neurotransmitter substance P within the NAc (Francis et al., 2019). These studies show that D1- and D2-MSNs may co-release GABA and opioids, that can have counteracting effects in behavior, thus contributing to explain contradictory results in the field.

Despite these data showing evident involvement of accumbal D1- and D2-MSNs in cue-related motivated behaviors, they do not directly show an involvement of these neurons in classical Pavlovian conditioning, indicating that further investigation is needed.

1.4.3 Calcium imaging studies- Fiber Photometry and miniaturized microscopes

Calcium is a second messenger that is involved in almost every cellular function. In neurons, it is critical for action potential firing and synaptic input, causing a rapid change of intracellular free Ca^{2+} . Therefore, tracking calcium transients offers an opportunity to monitor neuronal activity (Burgoyne, 2007).

Indeed, there are new cutting-edge techniques such as calcium imaging with miniaturized microscopes or fiber photometry that can detect calcium transients in neurons, which could be used to help clarify the role of NAc D1- and D2-MSNs. Calcium imaging is a tool that enables to visualize the activity of neurons simultaneously by taking advantage of genetically encoded calcium indicators (GECI) (T.-W. Chen et al., 2013; Kim & Schnitzer, 2022). The most widely used GECI, GCaMP6, is a protein composed by a calmodulin domain fused with a green fluorescent protein. As a result, when Ca^{2+} binds to the calmodulin domain, the protein changes conformation, switching from a weakly fluorescent to a strongly fluorescent state. Therefore, when GECI is expressed in neurons, it exhibits increased fluorescence in response to influx of calcium ions that accompanies action potentials, and this change in fluorescence can be recorded and used as a proxy for neuronal activity (Grienberger & Konnerth, 2012; Jacob et al., 2018a; Russell, 2011). Calcium imaging with miniaturized microscopes and fiber photometry are two examples of such system. In particular, fiber photometry allows optical imaging of bulk neural activity but does not provide cellular resolution, thus providing much less detailed behaviorally relevant information (Li et al., 2019; Resendez & Stuber, 2015). This system applies a specific wavelength of excitation light to a calcium (i.g. GCaMP) or neurotransmitter indicator, which is then transmitted through an optic fiber implanted in the brain region of interest. Subsequently, this light excites the calcium

indicator, which is expressed in a cell-type specific manner, and it emits its own signal, which travels back through the same fiber. A dichroic mirror separates the emission signals spectrally before reaching a sensitive photodetector that converts the information about fluorescence intensity into an analog signal. As a result, the signal detected corresponds to calcium transients (fluorescence variation, $\Delta F/F$) (Li et al., 2019). Miniaturized microscopes allow to simultaneously record hundreds of neurons from deep brain regions in freely behaving animals. It enables the longitudinal recording of neuronal activity from a specific, genetically-defined population of neurons at single-cell resolution (L. Zhang et al., 2019). This system consists of gradient index (GRIN) lenses implanted above the brain region to be imaged, as well as the genetically encoded calcium indicator GCAMP6. In addition, a miniaturized microscope, which sits above the skull and collects images from the tissue through the implanted GRIN lens. This microscope includes an excitation light and a detector which captures emitted fluorescence (Jacob et al., 2018b).

These two techniques provide the ability to track the activity of neurons over time and investigate how networks grow or change during learning. Fiber photometry is easier to implement; however, it does not allow tracking single cell activity, but the overall fluorescence emitted by a specific cell type (bulk activity).

More and more studies have been trying to elucidate the role of NAc in positive and aversive learning using calcium imaging to track the activity of neuronal subpopulations or the involvement of dopamine in this brain region. Recent fiber photometry recordings of dopamine transients by Patriarchi and colleagues (2018) during associative learning in NAc revealed an increase dopamine signal to the US at the first session, as well as a significant increase in amplitude of CS response upon repeated cue-reward pairings. On the other hand, upon US responses, a linear decrease across learning sessions was observed. Along with these data, it seems that accumbal dopamine response gradually shifted from US to CS as animals learn cue-reward association (Patriarchi et al., 2018a). In agreement, NAc dopamine responses to the auditory discriminative cue increased over training, whereas dopamine responses during sucrose retrieval (positive reward) decreased (Kutlu, Zachry, Melugin, Cajigas, Chevee, Kelley, et al., 2021). On the contrary, dopamine responses to the auditory cue for a negative outcome did not change over training. Moreover, as learning progressed, dopamine response to aversive footshocks increased (Kutlu, Zachry, Melugin, Cajigas, Chevee, Kelley, et al., 2021).

Additionally, other studies have been shown that dopamine signaling in different NAc subnuclei can have different effects on aversive and rewarding conditioning tasks. Specifically, ventral NAc medial shell (vNAcMed) exhibit an increase in dopamine signaling to unexpected aversive US and aversion predictive CS, whereas other NAc subregions, such as the lateral portion of the NAc shell (NAcLat), have

decreased this response. Unlike aversive conditioning tasks, dopamine responses in the NAcLat showed a significant increase to reward delivery and to reward predictive CS, while this response to the reward predictive cue is largely absent in the in vNAcMed. These findings suggest a remarkable topographic organization of aversive and reward dopamine signaling in the NAc (de Jong et al., 2019). In line with that, dopamine signaling was increased during rewarding events and decreased during aversive events in the dorsomedial NAc and dorsolateral NAc. In contrast, both rewarding and aversive stimuli evoke an increase in the release of dopamine in the ventromedial NAc. These also recapitulate the distinct role of the mesolimbic DA system in different subregions of NAc in encoding value and salience (Yuan et al., 2019). Although highly relevant, these studies are focused on dopamine and still do not tackle the involvement of MSN activity in reward and aversion.

There are not so many studies evaluating D1- and D2-neurons in associative learning using fiber photometry. In a heroin CPP procedure, fiber photometry recordings revealed that entering a heroin-paired context was driven by activation of dMSN (direct pathway), whereas exiting a heroin-paired context was driven by activation of iMSN (indirect pathway) (O'Neal et al., 2022). Furthermore, D1-MSNs showed increased activity in response to light transitions (CS) that signaled availability of reward and to lever extensions that occurred when food was available, suggesting that this cell population may encode cues that signal the presence of rewards in the environment. In contrast, transient event-related changes in D2-MSN activity did not differ significantly between reward availability conditions (Lafferty et al., 2020).

A recent study using Ca^{2+} fiber photometry demonstrated that acute cocaine administration enhances D1- and suppresses D2-MSN activity, and that cocaine-induced facilitation of D1-MSN activity is required for the formation of cocaine-context associations (Calipari et al., 2016). Accordingly, D1- and D2-MSNs showed distinct temporal activity during a cocaine CPP protocol choice session: increased D1-MSN activity immediately preceded entry into the drug-paired context, whereas D2-MSN activity was suppressed only after entry into the compartment (Calipari et al., 2016). On the contrary, other study in ventral striatum has shown, using event-related concurrent Ca^{2+} , activity in D1- and D2-MSNs at cue presentation in a motivation lever-pressing task (Natsubori et al., 2017). Thus, these results indicate that both D1- and D2-MSN subpopulations in the NAc positively encode food-incentive behavior and do not support the opposing functional roles of D1- versus D2-MSNs (Natsubori et al., 2017). Miniaturized microscope calcium imaging recordings during voluntary sucrose intake showed that enkephalin-positive (D2-MSNs) medial NAc neurons did not respond uniformly to sucrose consumption. Instead, different subpopulations with distinct response patterns were identified and classified into four clusters: onset activated (2%); pre-onset activated (7%); onset inhibited (15%) and non-responsive (76%). These suggest

that local this neuronal population is selectively recruited to improve consumptive behavior (Castro et al., 2021).

Importantly, recent preliminary data from our team, using calcium transient recordings with miniaturized microscopes, indicate that distinct D2-MSN sub-populations respond differently to the same behavioral events (e.g.: lever pressing; reward consumption), in a reinforced task, with some D2-MSNs increasing activity, while others decreased (and others did not change) (unpublished observations).

Altogether, these findings show that, so far, there is still a lack of information about studies involving cue-reward associative learning or Pavlovian conditioning, as well as a clear picture about the temporal involvement of D1- and D2-MSNs in both positive and negative CS-US associative learning.

CHAPTER 2 – Objectives

2. Objectives

In a challenging environment, species perceive and learn about their surroundings and adjust their behavior to increase chance of survival and propagation. Organisms use environmental cues (CSs) to perceive availability of rewards or threats (USs) and learn these associations – Pavlovian conditioning – to optimize behavior and obtain desired outcomes or escape danger. These processes are mediated by the NAc; however, the anatomical distribution and functional relevance of NAc CS-US responsive neurons is still poorly characterized.

We hypothesize that distinct patterns of D1- and D2-neurons activity are necessary to guide CS-US associative learning. To test our hypothesis, we will determine which are the neuronal ensembles responsive to Pavlovian associations and what is their role in CS-US associative learning. Specifically, we aim to:

- 1) Identify the anatomical distribution of NAc neuronal ensembles that represent early *versus* late learning associations using Pavlovian conditioning, by examining the pattern of expression of a marker of neuronal activity (endogenous c-fos).
- 2) Determine the functional relevance of accumbal D1- or D2-neurons for the acquisition of CS-US (for both reward and punishment) associative learning, using a calcium indicator with fiber photometry.

CHAPTER 3 – Materials and Methods

3. Materials and Methods

3.1 Animals

Male and female wild-type C57BL/6J mice (2-3 months of age; Charles River Laboratories, Barcelona, Spain) and heterozygous D1-cre, D2-cre transgenic mouse lines (2-3 months of age) were used. All animals were maintained under standard laboratory conditions: an artificial 12h light/dark cycle with lights on from 8am to 8pm; with an ambient temperature of $21\pm 1^{\circ}\text{C}$ and a relative humidity of 50-60%. Mice were housed in type 2L home cage with a maximum of 6 mice per cage, with food and water *ad libitum*, unless stated otherwise.

D1-cre allows to selectively tag D1-MSNs but D2-cre lines label both D2-MSNs and cholinergic interneurons (80% express D2), so we will use the terminology D1-neurons and D2-neurons in this thesis to be more accurate (instead of D1- and D2-MSNs).

Behavior experiments were performed during the light period of the light/dark cycle (between 8:00am and 4:00pm). All animals were kept divided according to gender and mouse strain from the postnatal day 21. 5-10 min handling was performed one week before behavioral experiments began to avoid anxiety and stress responses. Animals were also habituated to all behavior apparatus for 3 consecutive days for 15 min before starting the behavior tasks.

All procedures involving mice were performed according to the guidelines for the welfare of laboratory mice as described in the European Union Directive 2010/63/EU. All protocols were approved by the Ethics Committee of the Life and Health Sciences Research Institute (ICVS) and by the national authority for animal experimentation, Direção-Geral de Alimentação e Veterinária (DGAV) (approval reference #8332, dated of 2021-05-08). Health monitoring was carried out according to FELASA guidelines and all experimenters and animal facilities were accredited by DGAV.

3.2 D1 and D2-cre line: mating and genotyping

D1-cre and D2-cre mice express Cre recombinase under the control of the mouse *Drd1a* (dopamine receptor D1) or *Drd2* (dopamine receptor D2) promoter. The following heterozygous mouse lines were used: D1-cre (*Drd1a-cre*, 262, Gensat), and D2-cre (*Drd2-cre*, ER44, Gensat). The progeny produced by mating a D1-cre or D2-cre heterozygous transgenic male mouse with a wild-type C57/B16 female was genotyped at weaning by PCR.

DNA was isolated from tail biopsy using the Citogene DNA isolation kit (Citomed, Lisbon, Portugal). In a single PCR genotyping tube, the primers *Drd1a* F1 (5'- GCTATGGAGATGCTCCTGATGGAA-3') and CreGS R1 (5'- CGGCAAACGGACAGAAGCATT-3') were used to amplify the D1-cre transgene (340

bp), the primers Drd2 (32108) F1 (5'-GTGCGTCAGCATTTGGAGCA-3') and CreGS R1 (5'-CGGCAAACGGACAGAAGCAT-3') to amplify the D2-cre transgene (700 bp). An internal control gene (lipocalin 2, 500 bp) was used in the PCR (LCN_1 (5'- GTCCTTCTCACTTTGACAGAAGTCAGG-3') and LCN_2 (5'- CACATCTCATGCTGCTCAGATAGCCAC-3'). Heterozygous mice were discriminated from the wild-type mice by the presence of two amplified DNA products corresponding to the transgene and the internal control gene. Gels were visualized with GEL DOC EZ imager (Bio-Rad, Hercules, CA, USA) and analyzed with the Image Lab 4.1 (Bio-Rad, Hercules, CA, USA).

3.3 Surgery and optical fiber implantation

D1- and D2-cre mice (2-4 months old) were anaesthetized with 75mg kg⁻¹ ketamine (Imalgene, Merial, Lyon, France), and 1mg kg⁻¹ medetomidine (Dorbene, Cymedica, Horovice, Czech Republic), for stereotaxic surgeries. The animals were injected with a Cre-inducible AAV5-hSYN-FLEX-GCAMP6f-WPRE-SV40 (300nl, Addgene, Watertown, MA, USA) and AAV1-hSYN-FLEX-tdTomato (300nl (1:10 dilution), Addgene, Watertown, MA, USA) virus in the NAc (stereotaxic coordinates from bregma (Paxinos & Franklin, 2001): +1.3mm anteroposterior (AP), 0.9mm mediolateral (ML), and -4.5mm dorsoventral (DV)), using an 30-gauge needle Hamilton syringe (Hamilton Company, Reno, NV, USA), at a rate of 100nl min⁻¹. After injection, the syringe was left in place for 5min to allow viral diffusion.

After viral delivery, fiber optic cannula (400 μm, 0.50NA; 5mm in length; Doric Lenses, Quebec, Canada) were implanted in the NAc using the injection coordinates (except of DV: -4.4) (Paxinos & Franklin, 2001) and were then secured to the skull with dental cement (C&B kit, Sun Medical, Shiga, Japan). At the end of the surgical procedures, mice were removed from the stereotaxic frame and injected with anaesthesia reversal (1mg kg⁻¹ atipamezole; Antisedan). Postoperative care was carried out by administering analgesia (0.05mg kg⁻¹ buprenorphine; Bupaq, Richter Pharma, Austria) 6h post-procedure, as well as once every 24h during three successive days. A multivitamin supplement and saline were also administered post-procedure when necessary.

3.4 Behavioral experiments

3.4.1 Subjects

Both males and females were used for the D1-cre and D2-cre mice fiber photometry experiments, and the following number of animals was used: $n_{D1-cre} = 9$, $n_{D2-cre} = 7$.

3.4.2 Pavlovian Conditioning

Apparatus

Behavioral sessions were performed in a custom-made operant chamber using pyControl (17.8cm length x 19cm width x 23cm height) within a sound-attenuating box. The chamber is composed by a central magazine, to provide access to 20ul of sucrose solution (20% wt/vol in water) delivered by a solenoid (for liquid dispenser), a cue-sound (70dB 5kHz), a house-light (100mA, 2.8W) installed on the top, and metallic floor. A computer was used to control the equipment and record the data, and a webcam (CMOS OV2710, ELP, Shenzhen, China) was used to acquire video.

Sucrose consumption

Mice were first habituated to the behavior apparatus (3 days) with the fiber placed, in which they were introduced to a chamber and allowed to freely explore for about 15min. At the end of the second day of the habituation period, animals receive a bottle of 20% sucrose in their home cage (that stayed for 16hours) to avoid neuronal activation due to the novelty of the sucrose flavor. 48h before the initiation of the task, mice were food restricted to 2g per day of standard laboratory chow and maintained at 85-90% of their initial body weight. Following that, mice were put on the behavior apparatus and were allowed to freely explore while 20ul of 20% sucrose was delivered every 30 seconds during a 30min session (60 deliveries) so that animals could learn the position of the sucrose receptacle. This habituation session was repeated for each mouse until they showed a robust nose poke activity (all animals received 1-3 sessions).

Cue-reward associative learning (Pavlovian conditioning)

After sucrose consumption, mice started the Pavlovian Conditioning (schematic representation of the Pavlovian conditioning task is illustrated in the results section in **Figure 7B**) in which a conditioned stimulus (CS) consisting of a 70dB 5kHz tone and a house-light (100mA, 2.8W) were turned on for 10 seconds with a variable inter-trial interval (ITI) of 20-35 seconds (randomly assigned). Unconditioned stimulus (US) was 20ul of 20% sucrose solution, available at the 7th second after each CS onset. CS-US pairings were repeated 35 times per session (± 25 min for each session). Mice underwent a total of 12 sessions of Pavlovian Conditioning. The behavior apparatus and the sucrose receptacle were disinfected with 10% ethanol between animals to remove any odor. For all sessions nose poke data and photometry recordings were simultaneously obtained. To quantify CS-triggered behavior, number of nose pokes were

recorded during the CS presentation; nose pokes were also registered during the ITI period (Protocol adapted from (Patriarchi et al., 2018a)).

3.4.3 Pavlovian aversive conditioning

Behavioral sessions were performed in an operant chamber (same size of the Pavlovian Conditioning one) within a sound-attenuating box. The chamber contained a house-light (100mA, 2.8W) installed on the top of the chamber, a cue-sound (80dB 3kHz) and a cue-light installed in one side of the walls, a shocker and a grid floor. A computer was used to control the equipment and record the data, and webcams (CMOS OV2710, ELP, Shenzhen, China) were used to acquire video to analyze freezing behavior.

Mice were first familiarized to the behavior apparatus (3 days) with the fiber connected, in which they were introduced to the chamber and allowed to freely explore for about 15min. Following, mice started a Pavlovian aversive conditioning (schematic representation of the Pavlovian aversive conditioning task is illustrated in the results section in **Figure 17A**) protocol of 3 days. Three sessions were performed across three days. All sessions started with 60s of habituation period, with house light on and a 30s extra period with the house light off. Conditioned stimuli (CS) consisted of an 80dB, 3kHz tone plus a cue-light. Unconditioned stimuli (US) was a mild foot shock (0.5mA, over 1s). During the first conditioning session, mice were exposed to 10 CS-US pairings. Each trial consisted of a random ITI (45-50 sec) followed by a 10s tone, which was immediately followed by electric foot shock delivered through the stainless-steel grid floor. On the second day, mice performed 30 trials, in order to further examine the effects of shock omission: 10 out of 30 tones (randomly assigned) were not followed by an electric foot shock. On the third day animals received a US extinction session, in which they received 30 trials with only CS exposure, but without US delivery (protocol adapted from (de Jong et al., 2019)). All sessions were recorded with webcams and photometry recordings were simultaneously obtained. To assess CS-triggered aversion, we measured freezing during the CS period from all sessions. The freezing response was defined as the time (seconds) that mice spent immobile (lack of any movement including sniffing) except respiration during the tone period and calculated as percentage of total cue time ($(\text{freezing time} \times 100) / \text{cue duration}$).

This behavior was performed after all other experiments, since such aversive stimuli can induce sustained fear and anxiety to the context.

3.4.4. Locomotor behavior

Briefly, mice were placed in the center of an open field arena for 10 min and fiber photometry recordings were performed simultaneously. This allows to track basal neural activity that is related with locomotion and exploration.

3.5 Fiber Photometry recordings

After four weeks of viral expression, we start to record NAc D1- and D2-neurons activity during positive Pavlovian and Pavlovian aversive conditioning, using an open-source Python-based hardware and software for fiber photometry data acquisition (Akam & Walton, 2019). Fiber optic cables (1m long; 400 μm core; 0.50 NA; Doric Lenses, Quebec, Canada) were coupled to implanted optic fibers with zirconia sleeves. Black heat shrink material was placed around the fiber coupling to prevent external sources of light from interfering with recordings. The system used two LEDs (CLED_465; CLED_560; Doric Lenses, Quebec, Canada) via an LED driver circuit built into the system (with an adjustable 0-100 mA output). Excitation light with two different wavelengths of 465nm for GCaMP6 (green) and 560nm for tdTomato (red), and an emission light were passed through a minicube (FMC5_E1(450–490) _F1(500–540) E2(550-580)_F2(600-680)_S; Doric Lenses, Quebec, Canada). GCaMP signal and a movement control signal from co-expressed tdTomato were recorded using the *'2 colour time-division'* acquisition. Light emitted by the indicators is transmitted back through the same optic fiber, separated from the illumination light and fluorescence from other indicators by optical filters, and converted to electrical signals by two separate high sensitivity photoreceivers (Newport 2151 with lensed FC adapter; Doric Lenses, Quebec, Canada). Next a Micropython Pyboard, with two analog and two digital inputs receives the fluorescence signals as analog voltage signals at 130Hz (time division), which are then convert to digital signal via an RC lowpass filter. The digital inputs are read at the same sampling rate as the analog signals to enable post hoc synchronization of the photometry data with the behavioral hardware. The system uses one digital input to receive synchronization pulses from the behavioral hardware and the other to receive a TTL each time a behavioral event of interest (reward delivery of foot shock) occurs. The average response to the event of interest can be visualized online, and the response to other behavioral events are calculated offline by using the sync pulse times to align behavioral and photometry data. Data were saved as .csv files (Akam & Walton, 2019).

3.6 Fiber photometry data analysis

Initial analysis was performed in GuPPy, Guided Photometry Analysis in Python, a free and open-source package (Sherathiya et al., 2021). First step was to remove artifacts, to allow to select portions of the recordings to include and exclude from the analysis. GuPPy uses a control channel (red) that includes smaller movement artifacts and photobleaching artifacts that are subtracted from the signal and used to normalize the data to determine changes from baseline fluorescence ($\Delta F/F$). After established a control channel, a fitted control channel is used to calculate $\Delta F/F$ by subtracting the fitted control channel from the signal channel, and dividing by the fitted control channel:

$$\frac{\Delta F}{F} = \frac{\text{Signal} - \text{Fitted control}}{\text{Fitted Control}}$$

A standard z-score was calculated for the entire data stream by subtracting the mean value from each data point and dividing by the standard deviation.

$$z - score = \frac{\Delta F/F - (\text{mean of } \Delta F/F)}{\text{Standard deviation of } \Delta F/F}$$

For peak detections, the average amplitude and frequency of transients in the z-score trace were calculated for the whole session. High amplitude events, defined as those with amplitudes greater than three times the median absolute deviation (MAD) above the median of the moving window, are filtered out and the median of the resulting trace is calculated. Transients are defined as peaks with amplitudes greater than three MADs of the resultant trace. After baseline correction, post-stimulus histogram (PSTH) is then calculated based on a user-defined window set around each event timestamp (Sherathiya et al., 2021). The PSTH's area under the curve (AUC), mean fluorescence activity (average of the fluorescence signal) and peak amplitude (X. Zhang & Li, 2018) in specific periods of time were then calculated and plotted by a custom-made script. The intervals used for this analysis were: for Pavlovian conditioning data: pre-CS period (-10, -7); CS period: (-7, -4); pre-US period (-3, 0); US period: (0, 3); and for Pavlovian aversive conditioning data: pre-CS period (-13, -10); CS period: (-10, -7); pre-US period (-3, 0); US period: (0, 3). Next, to determine group differences, a group analysis was performed to average together results from multiple animals or multiple recording sessions (analysis adapted from (Sherathiya et al., 2021)). Additionally, to determine whether a neuron is significantly ($p < 0.05$) excited or inhibited by a stimulus, and thus be classified as “responsive” to the stimulus, the Wilcoxon signed-rank test was used to compare

the mean $\Delta F/F$ values in the 3 s immediately after stimulus onset with those in the 3 s immediately before stimulus onset, using the same intervals as describe above (X. Zhang & Li, 2018).

3.7 Histology

3.7.1. Sacrifice and brain sectioning

At the end of all behavior procedures, mice were deeply anesthetized by a mixture of ketamine/medetomidine. Animals were then transcardially perfused with 0.9% saline, followed by 4% paraformaldehyde (PFA) solution. Brains were carefully removed and immersed for 24h in 4% PFA for fixation, and then rinsed and stored in 30% sucrose at 4°C until sectioning. In the case of fiber implanted mice, after transcardial perfusion, whole heads were immersed for 48h in 4% PFA so that the fiber track is clearly visible for histological analysis. Sectioning was performed coronally, in 40 μ m slices, on a vibrating microtome (VT1000S, Leica, Germany) and slices were stored at 4°C on 12-well plates (or long-term storage in cryoprotectant solution at -20°C) until use. Slices from the area of interest (NAc) were selected using the Mouse Brain Atlas (Paxinos & Franklin, 2001).

3.7.2. Immunostaining

IHC for c-fos

In order to identify neuronal ensembles responding to early *versus* late learning, we examined the pattern of expression of endogenous c-fos, an immediate early gene and marker of neuronal activity (Krukoff, 1999) in B6 wild-type mice, after the Pavlovian conditioning test. At early learning, the animals were subjected to two days of Pavlovian conditioning and were sacrificed at the end in order to detect cells that respond to early cue-reward associative learning (Early learning; n = 5; no Early learning as control, n=5). For the cells that respond to late cue-reward associative learning, animals were subjected to 12 days of Pavlovian conditioning and were also sacrificed at the end (Late learning; n = 6; no Late learning as control, n=5). The corresponding control groups did not perform the Pavlovian conditioning task. All animals were sacrificed 90 min (peak of expression 60-90 min after neuronal activation) after the beginning of the task for assessment of endogenous c-fos expression.

Brain slices containing all NAc were washed first with phosphate buffered saline (PBS), and then permeabilized with PBS/Triton-X100 (0.3%) (PBS-T). Blocking, to avoid unspecific binding, was executed for 1h using 5% fetal bovine serum (FBS; Invitrogen, MA, USA) in PBS-T at room temperature (RT). The primary antibody anti-c-fos, was incubated overnight at RT with agitation (1:750; rabbit anti-c-fos; Merck Millipore, Burlington, MA, USA, ABE457), followed by PBS-T washes and subsequent incubation with the secondary fluorescent antibody Alexa Fluor® 488 donkey anti-rabbit (1:500;

Invitrogen, Carlsbad, CA, USA, A21206). All antibodies were diluted in PBS-T with 2% FBS. Slices were washed with PBS-T, incubated with 4',6-diamidino-2-phenylindole (DAPI; 1:1000; Thermo Scientific™, 62248), washed with PBS and mounted using Permafluor (mounting media; Invitrogen, MA, USA). Slides were stored at 4°C and kept protected from light.

Immunofluorescence for GFP

To assess GCaMP6 expression in D1-cre and D2-cre mice, brain slices containing NAc sections with fiber tracks were washed with PBS, and then permeabilized with PBS-T (0.3%). Blocking was performed for 1h using 5% FBS (Invitrogen, MA, USA) in PBS-T at RT. The primary antibody goat anti-GFP, was incubated overnight at 4°C with agitation (1:750; ABCAM, Cambridge, UK, ab6673), followed by PBS-T washes and subsequent incubation with the secondary fluorescent antibody Alexa Fluor® 488 donkey anti-goat (1:500; Invitrogen, Carlsbad, CA, USA, A11055). All antibodies were diluted in PBS-T with 2% FBS. Slices were washed with PBS-T, incubated with DAPI (1:1000; Thermo Scientific™, 62248), washed with PBS and mounted using Permafluor (mounting media; Invitrogen, MA, USA). Slides were stored at 4°C and kept protected from light.

3.7.3 Image acquisition and analysis

Images from the brain regions of interest (NAc) of WT animals were collected and analysed by confocal microscopy (Olympus FluoViewTMFV1000). About 10-12 slices per animals were used for each analysis. Slices were classified in terms of stereotaxic coordinates using the Mouse Brain Atlas (Paxinos & Franklin, 2001) and the evaluated regions (*i.e.* NAc subregions, core and shell) were drawn and measured in terms of area (mm²) using Fiji (ImageJ) software (Schindelin et al., 2012).

Quantification of neuronal activation (c-fos⁺ cell density) was performed using the Cell Counter plugin in the Fiji (ImageJ) software (Schindelin et al., 2012). Cell densities were presented as cells per mm². For the c-fos⁺ cell counting the Nac was divided into 3 subregions: NAc core (NAcc), Nac medial shell (NAcsMed) and Nac lateral shell (NAcsLat) according to (Paxinos & Franklin, 2001).

Images from the NAc of D1-cre, D2-cre and A2A-cre mice were collected in inverted fluorescence microscopy (Olympus Widefield Inverted Microscope IX81). About 10-12 slices per animals were used for each analysis. Optic fiber placement was assessed to confirm if the activity detected was from the intended NAc region. For that, slices where the optic fiber was detected were classified according to (Paxinos & Franklin, 2001) to estimate the stereotaxic coordinates.

3.8. Statistical analysis

Statistical analysis was performed in GraphPad Prism 8.0 (GraphPad Software, Inc., La Jolla, CA, USA). Normality was assessed in all data analysed by using the Shapiro–Wilk test and outliers were removed when applicable (Grubbs' test; a standard test in univariate data sets) (data not shown). If normality assumptions were not met, Non-parametric analysis (Mann-Whitney or Wilcoxon test) was performed. Statistical analysis between two groups was made using *Student's t-test*. In particular, a paired *Student's t-test* was used for fiber photometry analysis to compare mean activity, area under the curve (AUC) and peak activity between baseline period and CS or US period, and between day 1 and day 12 or day 3; and for freezing analysis, to compare % of freezing in first and last trials on day 1 and 3; an unpaired *Student's t-test* was used to assess the effect of c-fos expression in early and late learning. To assess learning in Wild-type, and in D1- and D2-cre mice, a Repeated measures ANOVA was performed. If statistically significant differences were found, Bonferroni's *post hoc* multiple comparison test was used for group differences determination. Additionally, a linear regression was also performed to see the correlation between number of nose pokes and days of training. To determine if a neuron was significantly "responsive" to a stimulus, a Wilcoxon signed-rank test was used (analyses performed with Matlab (MathWorks, Natick, MA)). All data analyses are presented as mean \pm standard error of mean (SEM). Individual points are shown in the graphs. Statistical significance was accepted for $p \leq 0.05$. All statistical comparisons are presented in the results section.

CHAPTER 4 – Results

4. Results

The nucleus accumbens has been shown to play an important role in rewarding and aversive events, and particularly in mediating Pavlovian conditioning associations. Although *in vivo* electrophysiological recordings in the NAc have shown the involvement of MSNs in encoding cue-outcome associations (Roitman et al., 2005), this approach did not allow the distinction between D1- and D2-MSN activity. Thus, it remains unclear the anatomical distribution and functional role of D1- and D2-MSNs in cue-reward/aversive (Pavlovian) associative learning.

To identify the anatomical distribution of NAc neuronal ensembles that represent early *versus* late learning cue-reward associations in Pavlovian conditioning, we examined the pattern of expression of endogenous c-fos protein, encoded by an immediate early gene that is considered a marker of neuronal activity.

To determine the functional relevance of accumbal D1- and D2-neurons in cue-outcome associations, we imaged the neuronal activity of NAc neurons responsive to CSs, positive outcome (sucrose) and to negative outcome (shock) during cue-reward/aversion associative learning using calcium imaging with fiber photometry.

4.1 NAc neuronal ensembles responding to early *versus* late associative learning

In order to identify NAc neuronal ensembles responding to early *versus* late cue-reward associative learning (or Pavlovian conditioning), C57/Bl6J wild-type mice were submitted to a Pavlovian conditioning test in which a CS (tone and a house-light) turned on for 10 seconds was paired with a US (delivery of 20 μ l of 20% sucrose solution). The US was available at the 7th second after CS onset, with a total of 30 CS-US pairings in one single session (**Figure 4A**). To evaluate endogenous c-fos expression at early learning, animals performed two days of Pavlovian conditioning and were euthanized 90 min after the beginning of the second session (Pav_d2 group). To evaluate endogenous c-fos expression at late learning, animals were subjected to 12 days of Pavlovian conditioning and were euthanized 90 min after the beginning of the last session (Pav_d12 group) (**Figure 4B**). The corresponding control groups (noPav_d2, noPav_d12) were placed in the operant box for the same amount of time per day as the test groups, but no CS-US pairings were presented. These groups were also euthanized 90 min after the beginning of the 2nd or the 12th session, respectively.

To confirm that animals acquired behavioral conditioning to the CS-US pairings, the number of nose pokes in the sucrose receptacle performed during CS presentation and during inter-trial interval (ITI) period were recorded. All statistical data are summarized in **Table S1**.

Animals that performed two sessions of conditioning (Pav_d2 group), present a statistically significant difference between number of nose pokes/min during CS presentation and ITI period on day 1 (**Figure 4C**; *post hoc* analysis, $p = 0.0155$). However, there is no significant correlation between the total number of nose pokes performed during CS and day of training (**Figure 4D**).

After 12 days of the Pavlovian conditioning, animals successfully learned to associate the CS with the US, as shown by the significant increase in the number of nose pokes/min during the CS presentation compared with the ITI period (**Figure 4C**; $F_{(1,5)} = 8.687$, $p = 0.0320$). A statistically significant difference is present from the 6th day on of Pavlovian Conditioning (**Figure 4C**; day 6: $p = 0.0087$; day 7: $p = 0.0026$; day 8: $p = 0.0074$, day 9: $p = 0,0019$, day 10: $p < 0.0001$, day 11: $p < 0.0001$, day 12: $p < 0.0001$). In addition, there is a significant positive correlation between number of pokes during the CS period and day of training (**Figure 4D**; $r^2 = 0.1892$, $s = 190$, $p = 0.0002$). No correlation was observed between number of nose pokes during the ITI and day of training (data not shown; $r^2 = 0.001206$, $s = 254.1$, $p = 0.3655$).

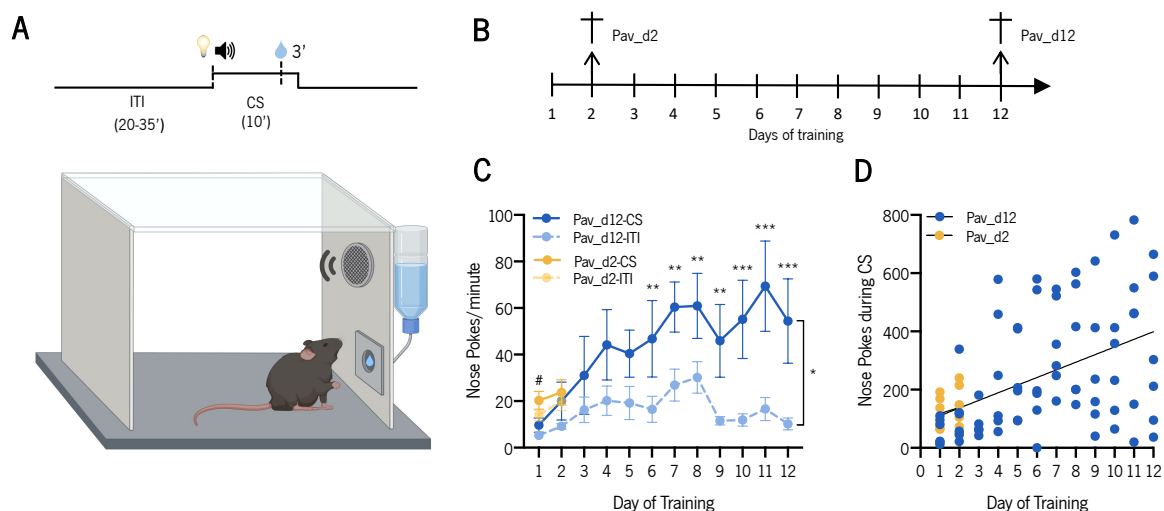


Figure 4 – Animals learn the association between cue and reward throughout training. A) Schematic representation of the Pavlovian conditioning task in which animals learn to associate a CS (70dB 5kHz tone and house-light) with a US (20µl of 20% sucrose). **B)** Experimental design. Mice went through a Pavlovian conditioning test. In the early learning group (Pav_d2, $n = 5$), mice were euthanized 90 min after the beginning of the second session, and in the late learning group (Pav_d12, $n = 6$) animals were euthanized 90 min after the beginning of the 12th session. Control groups did not receive CS-US pairings, and were euthanized 90 min after the beginning of the 2nd or the 12th session. **C)** Number of nose pokes/min across days during CS and ITI period for the early learning group (yellow) and for the late learning group (blue). **D)** Number of nose pokes during CS presentation across the 12 days of training. Data are represented as mean \pm SEM #* $p \leq 0.05$, ** $p \leq 0.01$, *** $p \leq 0.001$.

We then calculated the c-fos⁺ cell density in the NAc core (NAcc), Nac medial shell (NAcsMed) and Nac lateral shell (NAcsLat) (Paxinos & Franklin, 2001) in the early learning (Pav_d2 group) and late learning (Pav_d12 group) animals. All statistical data are summarized in **Table S2**. As it can be seen by the c-fos⁺ cell density, at early learning there is no significant difference in neuronal activation between Pav_d2 group and the control group (noPav_d2) neither in the NAcc (**Figure 5C**) nor the NAcsLat (**Figure 5G**); a trend for an increase was observed in NAcsMed (**Figure 5E**; $t_{(6)} = 2.133$, $p = 0.0769$; noPav_d2: 18.00 ± 3.592 cells/mm²; Pav_d2: 44.67 ± 15.81 cells/mm²). In addition, NAcc (**Figure 5D**, $F_{(5,17)} = 3.518$, $p = 0.0230$), NAcsMed (**Figure 5F**, $F_{(4,10)} = 11.15$, $p = 0.0010$) and NAcsLat (**Figure 5H**, $F_{(4,11)} = 4.936$, $p = 0.0159$) exhibit a heterogeneous distribution among anterior-posterior axis of the coordinates from Bregma. No statistical differences were found for c-fos⁺ cell density between groups; however, a trend was observed in NAcc in the coordinate (1-0.9) (*post hoc* analysis, $p = 0.0765$); and a statistically significant difference is present in NAcsMed in (1-0.9) (*post hoc* analysis, $p = 0.0430$) and in NAcsLat in (1.7-1.5) (*post hoc* analysis, $p = 0.0181$).

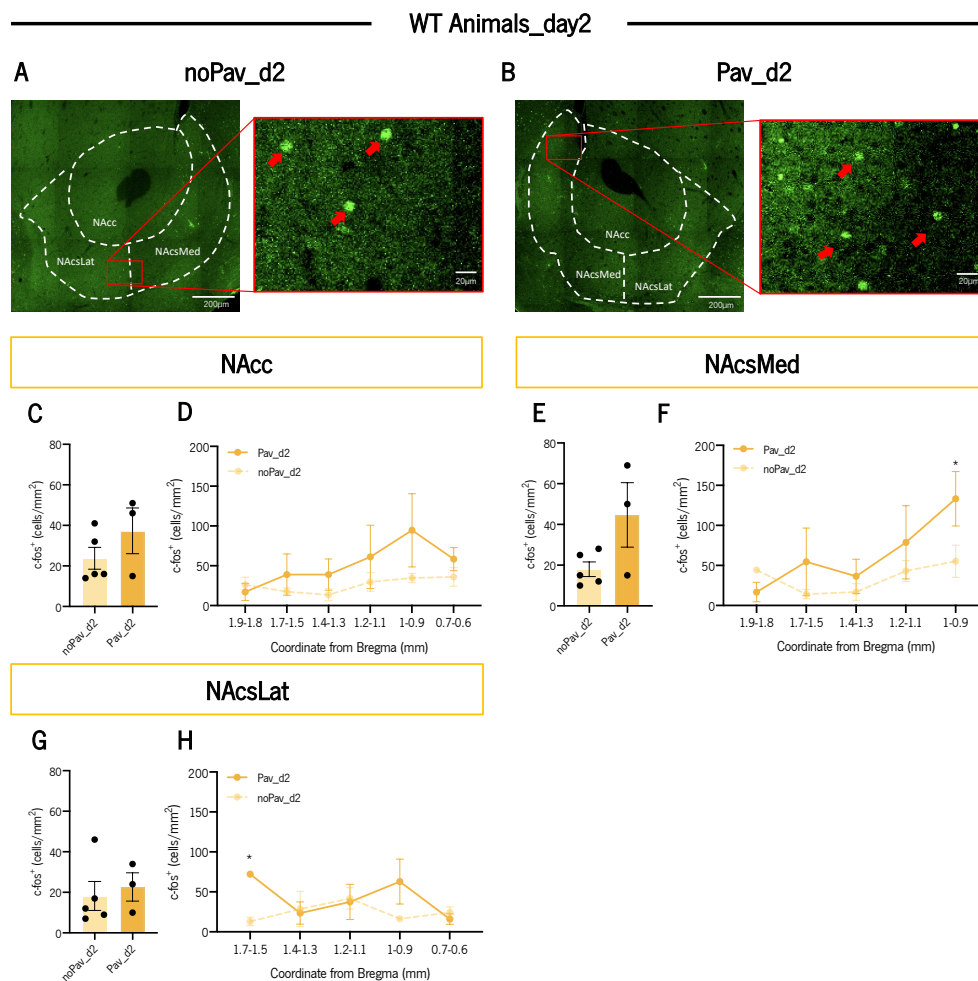


Figure 5 – Quantification of c-fos⁺ cell density in the NAc of mice at early learning (day 2). Representative c-fos immunofluorescence image showing endogenous c-fos expression in the NAc of **A**) control group (noPav_d2) and **B**) in the

Pavlovian conditioning group (Pav_d2); (20x mosaic - left; 40x - right). Arrows point to a few examples of c-fos⁺ cells; Scale bar: 200µm – left; 20 µm - right. c-Fos⁺ cell density (cells/mm²) in the **C**) NAcc, **E**) NAcMed and **G**) NAcLat (noPav_d2, n = 5; Pav_d2, n = 3). c-Fos⁺ cell density along the anterior-posterior coordinate from the Bregma in the **D**) NAcc, **F**) NAcMed and **H**) NAcLat. Data are represented as mean ± SEM *p≤0.05.

All statistical data are summarized in **Table S3**. At late learning, no significant differences were found in c-fos⁺ cell density for the Pav_d12 group in the NAcc (**Figure 6C**), the NAcMed (**Figure 6E**) and the NAcLat (**Figure 6G**). Additionally, no differences were found in the c-fos⁺ cell density between noPav_d12 and Pav_d12 groups, however there is a heterogeneous distribution among anterior-posterior axis of the coordinates from Bregma in NAcc (**Figure 6D**, $F_{(5,25)} = 2.947$, $p = 0.0317$), and in NAcMed (**Figure 6F**, $F_{(4,20)} = 3.489$, $p = 0.0257$).

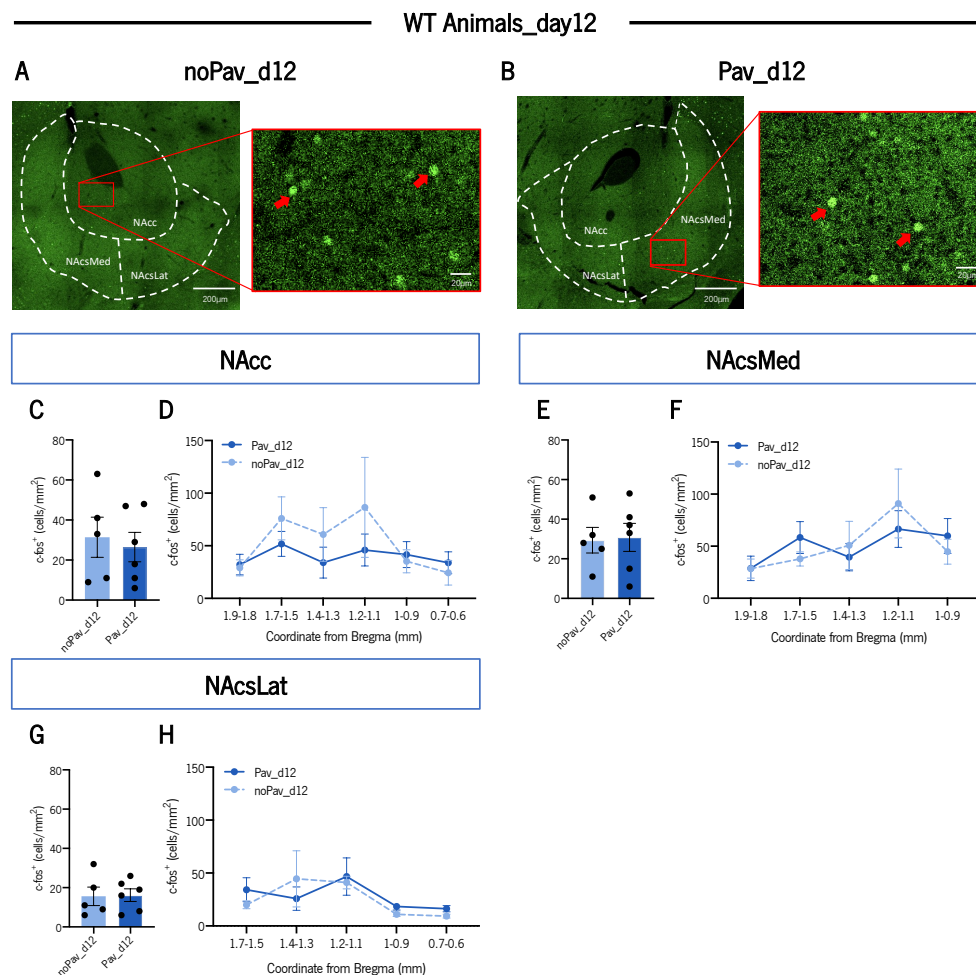


Figure 6 - Quantification of c-fos⁺ cell density in the NAc of mice at late learning (day 12). **A**) Representative c-fos immunofluorescence images showing endogenous c-fos expression in the NAc of **A**) control group (noPav_d12) and **B**) in the Pavlovian conditioning group (Pav_d12); (20x mosaic - left; 40x - right). Arrows point to a few examples of c-fos cells. Scale bar: 200µm - left; 20 µm - right. c-Fos⁺ cell density (cells/mm²) in the **C**) NAcc, **E**) NAcMed and **G**) NAcLat (noPav_d12, n

= 5; Pav_d12, n = 6). c-Fos⁺ cell density along the anterior-posterior coordinate from the bregma in the **D)** NAcc, **F)** NAcMed and **H)** NAcLat. Data are represented as mean \pm SEM.

4.2 Distinct patterns of activity of D1- and D2-neurons in associative learning

We next aimed to evaluate the neuronal activity of NAc D1- and D2-neurons during the acquisition of reward or aversive associative learning. To do so, we used fiber photometry to register calcium transients in either MSN subtype in response to CSs and USs. We injected an adeno-associated virus expressing the cre-dependent genetically-encoded calcium indicator (GECI) GCaMP6f in the NAc of D1-cre or D2-cre mice, in combination with an AAV carrying expression of a fluorescent tag, tdTomato that was used for motion correction. After viral delivery, an optic fiber was implanted in the NAc. Animals without expression or whose fiber placement was outside the brain region of interest (NAc) were excluded from the analysis.

4.2.1 D1-neurons respond to positive Pavlovian conditioning

D1-cre animals were injected in the NAc with AAV5-hSYN-FLEX-GCaMP6f-WPRE-SV40 and AAV1-hSYN-FLEX-tdTomato for motion correction (**Figure 7A**). GCaMP6f expression was assessed by GFP immunostaining and fiber placement was checked for all animals in all the groups. Two animals were excluded from the analysis due to fiber misplacement. Four weeks after surgery, animals were subjected to the Pavlovian conditioning test, which involves 35 pairings of a CS (10s tone and house-light) with a US (delivery of 20 μ l of 20% sucrose solution). At the 7th second of CS, the US was delivered. After reward delivery, trial entered on a variable ITI period (20-35 seconds, randomly assigned) (protocol adapted from (Patriarchi et al., 2018a)) (**Figure 7B**). The number of nose pokes during CS presentation and during ITI period were quantified. All statistical data are summarized in **Table S4**.

Mice successfully learned to associate CS to the US, as shown by the increased number of nose pokes/min during CS presentation compared with the ITI period (**Figure 7C**; $F_{(1,8)} = 4.633$, $p = 0.0635$). We observed a significant difference from the 7th day of the Pavlovian Conditioning task (**Figure 7C**; day 7: $p = 0.0045$; day 8: $p = 0.0430$; day 9: $p = 0.0001$; day 10: $p < 0.0001$; day 11: $p = 0.0005$; day 12: $p < 0.0001$). No significant correlation regarding the number of nose pokes during the CS presentation across days of training was found (**Figure 7D**).

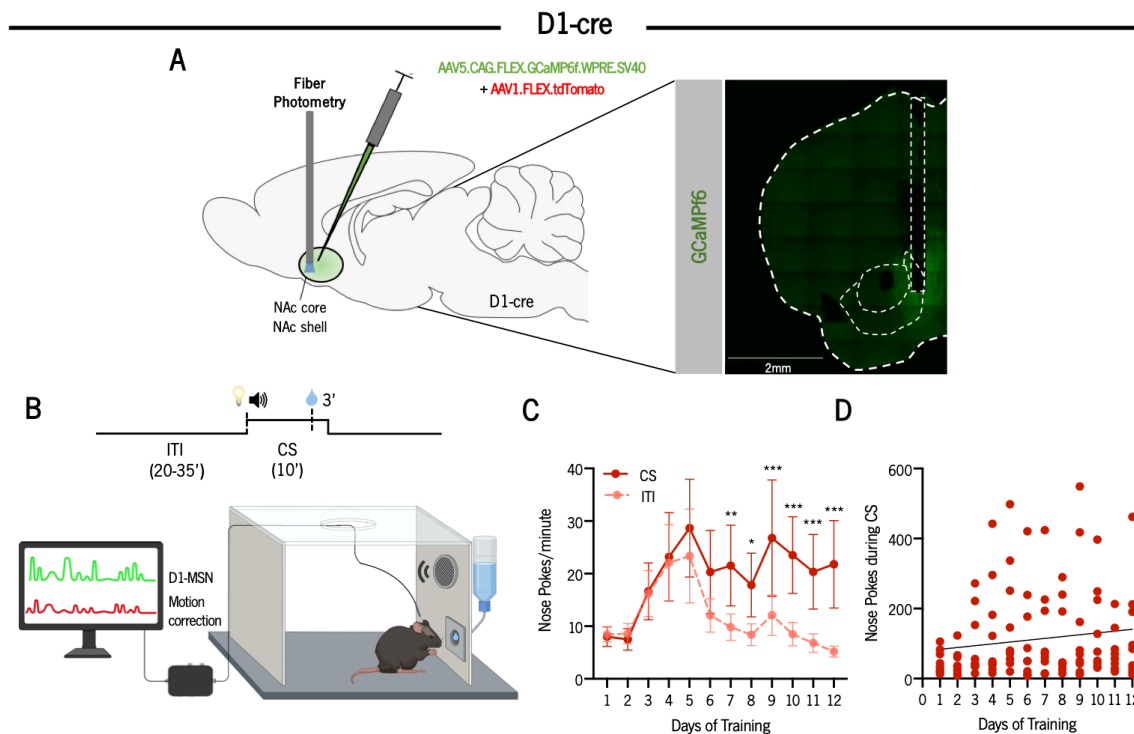


Figure 7 – Behavior of D1-cre mice injected with GCaMP6f during positive Pavlovian conditioning. A) Injection of AAV5-hSYN-FLEX-GCaMP6f-WPRE-SV40 and AAV1-hSYN-FLEX-tdTomato in the NAc of D1-cre mice ($n = 7$). Representative image of GFP immunostaining showing expression of GCaMP6f and fiber placement; Scale bar = 2mm. **B)** Schematic representation of the Pavlovian conditioning test. The CS (70dB 5kHz tone and house-light) was turned on for 10s and paired with a US (20 μ l of 20% sucrose solution) that was available 7 seconds after CS onset, followed by a random ITI period (20-35s). **C)** Number of nose pokes/minute across the 12 days of training during CS and ITI periods, showing that animals learn to associate the CS with US throughout training. **D)** Number of nose pokes during CS presentation across the 12 days of training. Data are represented as mean \pm SEM * $p \leq 0.05$, ** $p \leq 0.01$, *** $p \leq 0.001$.

During behavior, fiber photometry recordings in the NAc of D1-cre mice was done in all days of Pavlovian conditioning. Because the first trials within a session may be different from the last trials, we present the average activity of the first 5 trials, last 5 trials, and all trials.

We compared the activity during the first 3 seconds of the CS period [from -7 to -4s; considering reward delivery at 0s] with the 3 seconds of baseline activity immediately before the CS onset [-10 to -7s]. For simplification, we only present data from days 1, 6 and 12 of Pavlovian conditioning. All statistical data are summarized in **Table S5**.

On day 1, the activity of D1-neurons during CS period is increased comparatively to the baseline, considering the average of all trials (**Figure 8A-B**; all trials: $W = 0$, $p < 0.0001$). Interestingly, there are differences in the pattern of bulk activity between the first and last 5 trials.

On days 6 and 12 the activity of D1-neurons during CS decreases compared to the baseline period, when considering all trials (**Figure 8C-D**; day 6 all trials: $W = 58$, $p < 0.0001$; **Figure 8E-F**; day 12 all trials: $W = 17445$, $p < 0.0001$).

Next, we compared the reward (US) period [0 to 3s] with the activity immediately before the reward delivery [-3 to 0s] (baseline before US). During days 1 and 12, the average activity of D1-neurons during US decreased when compared to the baseline before US period (**Figure 8A-B**; day 1 all trials: $W = 0$, $p < 0.0001$; **Figure 8E-F**; day 12 all trials: $W = 799$, $p < 0.0001$). However, on day 6, the average activity during US increases compared to the baseline before US period (**Figure 8C-D**; all trials: $W = 22779$, $p < 0.0001$).

In summary, the activity of D1-neurons during CS presentation increases at early stages of learning and then it decreases as learning is consolidated. Additionally, the activity of D1-neurons in response to reward fluctuates across learning days (decrease – increase – decrease).

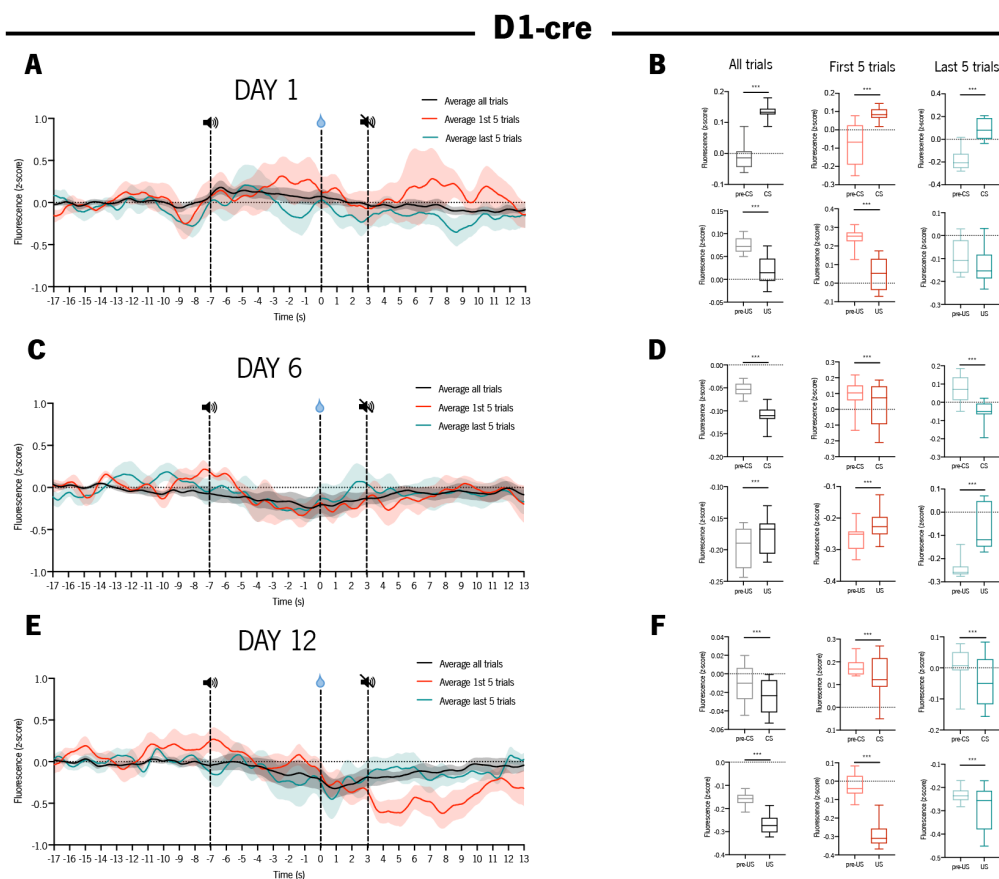





Figure 8 – Activity of D1-neurons during Pavlovian conditioning. Normalized activity (z-score) of D1-neurons evaluated by measuring GCaMP6f signals with fiber photometry. The activity of the first 5 trials is shown in red, the last 5 trials in blue, and average of all 35 trials in black. **A**) Normalized activity of day 1; **B**) Boxplot showing the normalized activity between the period before CS (pre-CS) [-10, -7] and during CS period (CS) [-7, -4] and between the period before US (pre-US) [-3 to 0s] and US period (US) [0 to 3s] during day 1; **C**) Same as in A) for day 6; **D**) Same as in B) for day 6; **E**) Same as in

A) for day 12; **F)** Same as in B) for day 12. Data are represented as mean \pm SEM for A), C) and E); Data are represented as median \pm Min to Max for B), D) and F) *** $p \leq 0.0001$.  - Sucrose delivery;  - Cue start;  - Cue stopped.

Next, we performed complimentary analysis of the photometry data, namely we calculated the mean activity, area under the curve (AUC) and Peak fluorescence activity. This allowed us to compare side by side the activity of D1-neurons in response to the CS or US (same periods in the analysis as describe above). All statistical data are summarized in **Table S6**.

The mean activity of D1-neurons during CS presentation is higher in the first days of training, but it decreases as the learning process is consolidated, as shown by the significant negative correlation of the mean activity (**Figure 9A**; $r^2 = 0.07561$, $s = 0.2134$, $p = 0.0124$). No statistical differences were observed comparing the mean activity of baseline and CS periods (**Figure 9B**; Day1: $t_{(6)} = 1.874$, $p = 0.1101$; Day6: $t_{(6)} = 1.672$, $p = 0.1456$; Day12: $t_{(6)} = 1.089$, $p = 0.3259$).

Similarly, the AUC also presents a significant negative correlation with days of training (**Figure 9C**; $r^2 = 0.07561$, $s = 0.6386$, $p = 0.0124$). No significant differences between baseline period and CS period are observed for days 1, 6 and 12 of Pavlovian conditioning (**Figure 9D**).

Regarding Peak fluorescence activity, there is no correlation across days of training (**Figure 9E**). Similarly, no significant differences are observed between baseline and CS period on days 1, 6 and 12 of Pavlovian conditioning (**Figure 9F**).

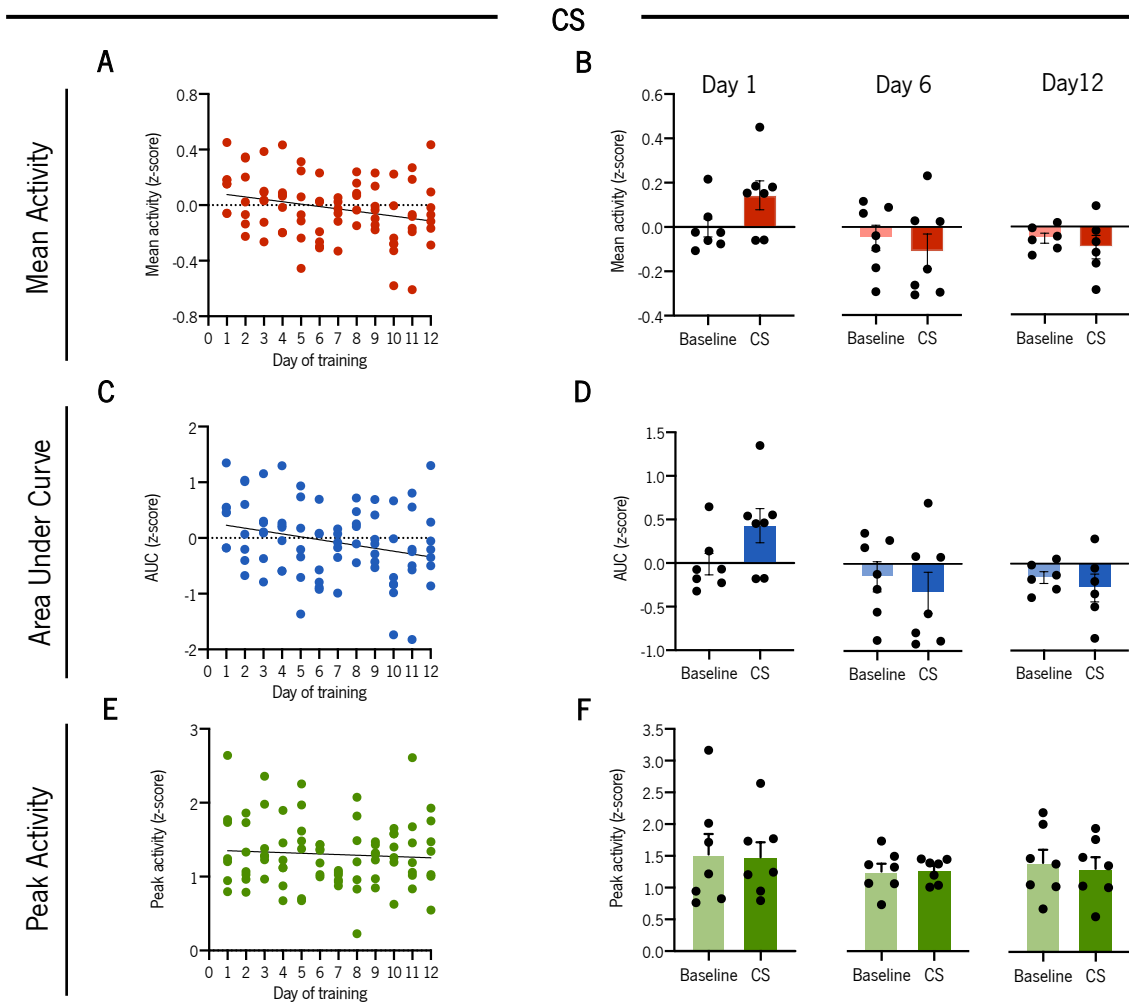


Figure 9 – Activity of D1-neurons decreases in response to the CS across days of training in the Pavlovian conditioning. **A)** Negative correlation between mean activity during CS period and days of training. **B)** Mean activity between baseline period [-10, -7] and CS period [-7, -4] during day 1, day 6, and day 12 of training. **C)** Negative correlation between AUC during CS period and days of training. **D)** Same as in B) for AUC. **E)** Correlation between peak activity during CS period and days of training. **F)** same as in B) for peak activity. Data are represented as mean \pm SEM.

Next, we compared the activity of D1-neurons in response to the US. All statistical data are summarized in **Table S7**. The mean activity during US delivery is higher on the first days of training, but it decreases as the learning process is consolidated, as shown by the significant negative correlation (**Figure 10A**; $r^2 = 0.1186$, $s = 0.2495$, $p = 0.0016$).

No significant differences were found on days 1, 6 and 12 for mean activity during US period, though there is a trend for a decrease in the last day of training (**Figure 10B**; Day1: $t_{(6)} = 1.045$, $p = 0.3364$; Day6: $t_{(6)} = 0.279$, $p = 0.7897$; Day12: $t_{(6)} = 2.038$, $p = 0.0877$).

Similarly, the AUC also presents a significant negative correlation with days of training (**Figure 10C**; $r^2 = 0.1185$, $s = 0.7464$, $p = 0.0017$). No significant differences between baseline period and US period for days 1, 6 and 12 of Pavlovian conditioning are observed (**Figure 10D**).

Regarding the Peak activity, we found no differences in the correlation across days of training (**Figure 10E**); and no significant differences between baseline period and US period (**Figure 10F**).

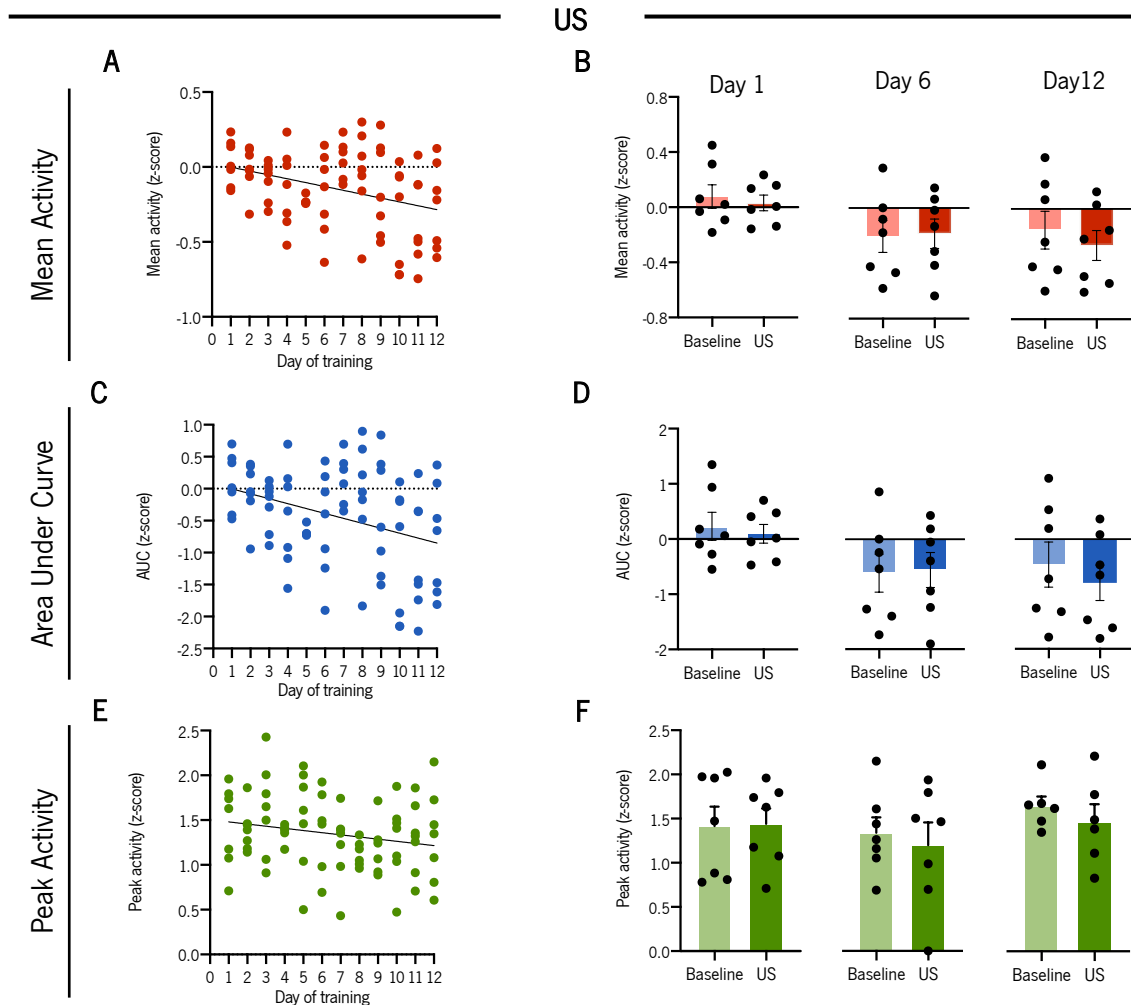


Figure 10 - Activity of D1-neurons decreases in response to the US across days of training in the Pavlovian conditioning. **A)** Negative correlation between mean activity during US period across days of training. **B)** Mean activity between baseline period [-3, 0] and US period [0, 3] during days 1, 6 and 12 of Pavlovian conditioning. **C)** Negative correlation between AUC during US period and days of training. **D)** same as in B) for AUC. **E)** Correlation between peak activity during US period and days of training. **F)** same as in B) for peak activity. Data are represented as mean \pm SEM.

Finally, to understand the evolution of D1-neurons activity throughout training, we compared the average activity during CS period and US period between days 1 and 12. All statistical data are summarized in **Table S8**. As shown in Figure 11A, on day 1 the activity increases immediately after the CS onset and then begins to decrease until the reward is delivered. On the contrary, on day 12 the activity

is decreased from the beginning of the CS onset and continues to decrease until the reward is delivered. Overall, the activity of D1-neurons significantly decreases from day 1 to day 12 in response to CS (**Figure 11A**; $W=100$, $p < 0.0001$).

In agreement, comparison of mean activity and AUC between day 1 and day 12 revealed that the activity of D1-neurons significantly decreases in response to the CS (**Figure 11B**; $t_{(6)} = 2.370$; $p = 0.0500$; **Figure 11C**; $t_{(6)} = 2.370$; $p = 0.0500$). However, peak activity shows no significant difference between day 1 and day 12 (**Figure 11D**).

Furthermore, there is a substantial decrease in mean activity and AUC of D1-neurons in response to the US from day 1 to day 12 (**Figure 11E**; $t_{(6)} = 2.573$; $p = 0.0422$; **Figure 11F**; $t_{(6)} = 2.572$, $p = 0.0422$). Peak activity shows no significant difference between day 1 and day 12 (**Figure 11G**).

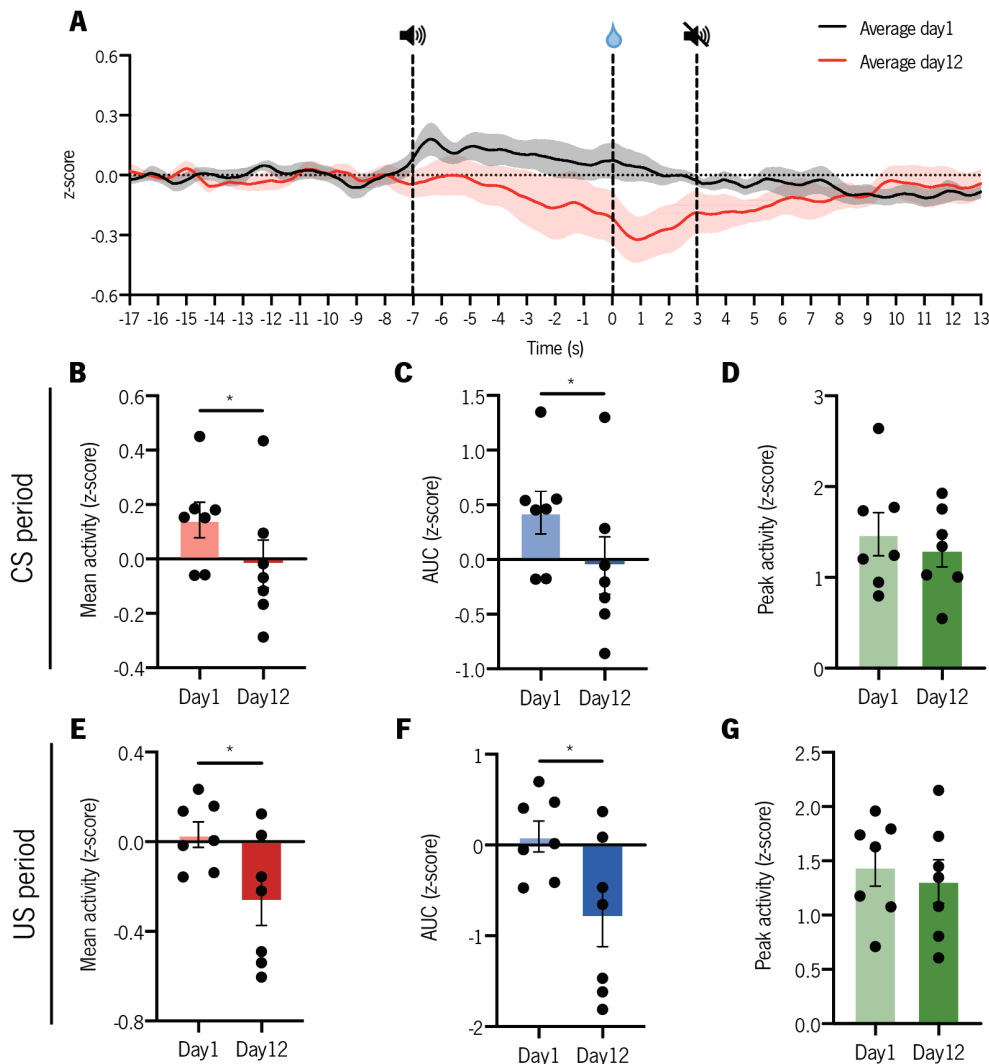


Figure 11 –D1-neurons activity decreases in response to CS and US from day 1 to day 12 of Pavlovian conditioning. A) Average of fluorescence during day 1 (black) and day 12 (red) of Pavlovian conditioning. **B)** Mean activity between day 1 and day 12 during CS period. **C)** same as in B) for AUC and **D)** peak activity. **E)** Mean activity between day 1

and day 12 in during US period. **F)** same as in E) for AUC and **G)** peak activity. Data are represented as mean \pm SEM * $p \leq 0.05$, ** $p \leq 0.01$, *** $p \leq 0.001$.

In sum, the activity of D1-neurons during CS presentation is increased at the early stages of learning and then decreases as learning is consolidated. In response to reward delivery, D1-neurons activity is decreased, but this decrease becomes even more pronounced at late stages of learning.

4.2.2 D2-neurons respond to positive Pavlovian conditioning

Next, we evaluated the neuronal activation pattern of D2-neurons in response to CS and US in a Pavlovian conditioning task. Viral injection and optic fiber implantation were done similarly to what is describe above but using D2-cre mice. GCaMP6f expression was assessed by GFP immunostaining and fiber placement was checked for all animals (**Figure 12A**). No animals were excluded.

D2-cre mice were subjected to the Pavlovian conditioning test, as described before (**Figure 12B**). All statistical data are summarized in **Table S9**. Mice successfully learned to associate CS to the US, as shown by the increased number of nose pokes/minute during CS presentation compared with the ITI period (**Figure 12C**; $F_{(1,9)} = 2.584$, $p = 0.1591$). Particularly, the association is evident from the 10th day of training (**Figure 12C**; Day 10: $p = 0.0147$; Day 11: $p = 0.0017$; Day 12: $p = 0.0012$). In addition, this is also shown by the positive correlation between the number of nose pokes during the CS presentation and days of training (**Figure 12D**; $r^2 = 0.07348$, $s = 94.27$, $p = 0.0132$).

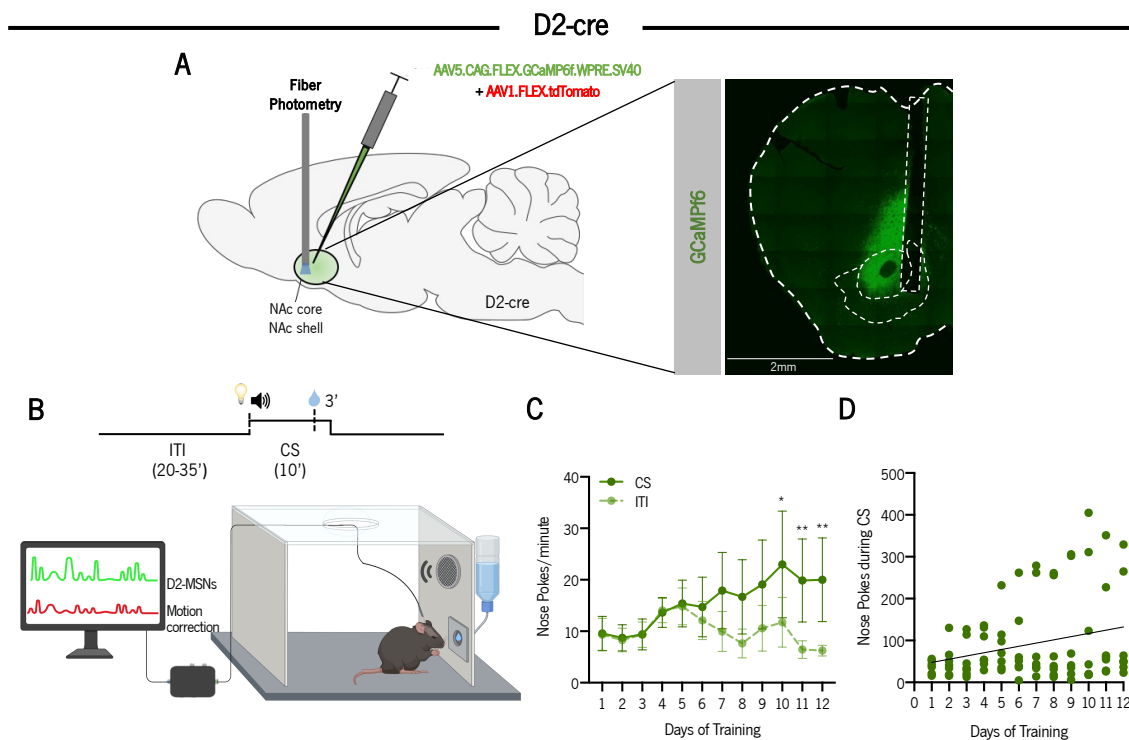


Figure 12 – Behavior of D2-cre injected with GCaMP6f during positive Pavlovian conditioning. **A)** Injection of AAV5-hSYN-FLEX-GCaMP6f-WPRE-SV40 and AAV1-hSYN-FLEX-tdTomato in the NAc of D2-cre mice (n = 7). Representative image of GFP immunostaining showing expression of GCaMP6f and fiber placement; Scale bar = 2mm. **B)** Schematic representation of the Pavlovian conditioning test. The CS (70dB 5kHz tone and house-light) was turned on for 10s and paired with a US (20 μ l of 20% sucrose solution) that was available 7 seconds after CS onset, followed by a random ITI period (20-35s). **C)** Number of nose pokes/min across the 12 days of training during CS and ITI period, showing that animals learn to associate the CS with US throughout training. **D)** Number of nose pokes during CS presentation across the 12 days of training. Data are represented as mean \pm SEM * $p \leq 0.05$, ** $p \leq 0.01$.

Next, we performed fiber photometry recordings of calcium transients of D2-neurons in the NAc. Analysis was done exactly the same as for D1-neurons. All statistical data are summarized in **Table S10**.

During days 1, 6 and 12, the activity of D2-neurons in response to the CS decreases comparatively to the baseline period (**Figure 13A-B**; day 1 all trials: $W = 0$, $p < 0.0001$; **Figure 13C-D**; day 6 all trials: $W = 0$, $p < 0.0001$; **Figure 13E-F**; day 12 all trials: $W = 0$, $p < 0.0001$), except for the last 5 trials on day 12, where the activity was increased (last 5 trials: $W = 28294$, $p < 0.0001$).

The activity of D2-neurons was decreased in response to reward delivery in comparison to the baseline period during days 1, 6 and 12 (**Figure 13A-B**; day 1 all trials: $W = 0$, $p < 0.0001$; **Figure 13C-D**; day 6 all trials: $W = 0$, $p < 0.0001$; **Figure 13E-F**; day 12 all trials: $W = 7040$, $p < 0.0001$).

Overall, the activity of D2-neurons during CS presentation and reward delivery decreases during Pavlovian conditioning acquisition.

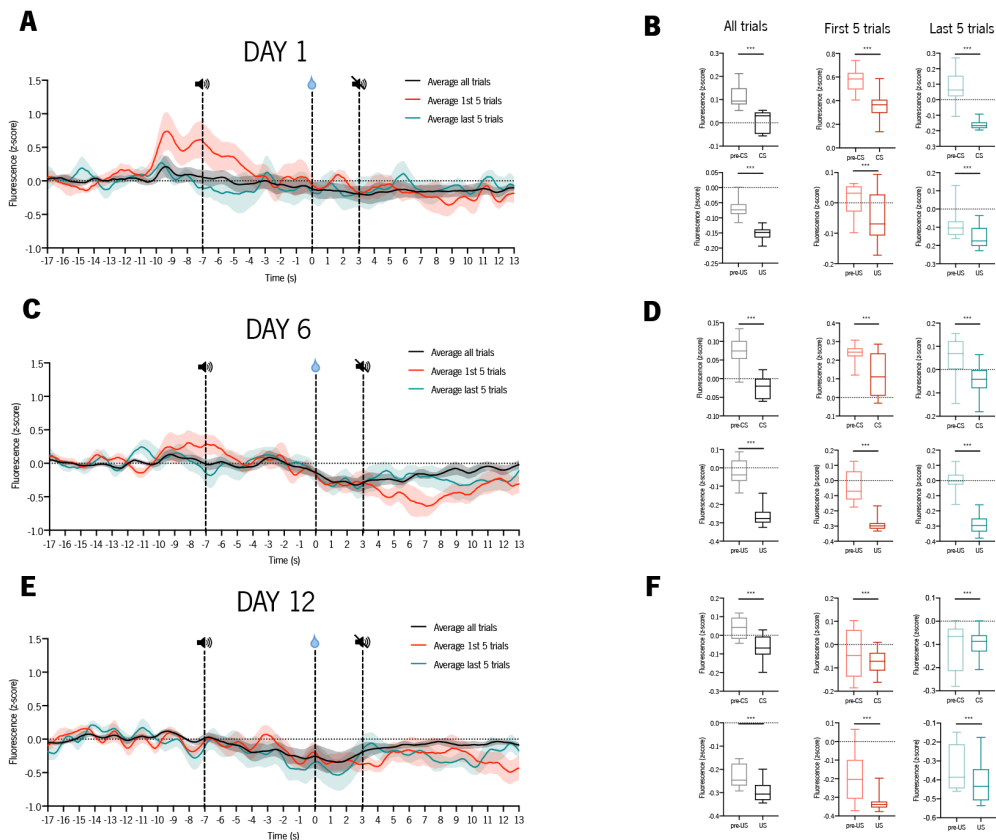


Figure 13 – Activity of D2-neurons during Pavlovian conditioning. Normalized activity (z-score) of D2-neurons evaluated by measuring GCaMP6f signals with fiber photometry. The activity of the first 5 trials is shown in red, the last 5 trials in blue, and average of all 35 trials in black. **A)** Normalized activity of day 1; **B)** Boxplot showing the normalized activity between the period before CS (pre-CS) [-10, -7] and during CS period (CS) [-7, -4], and between the period before US (pre-US) [-3 to 0s] and US period (US) [0 to 3s] during day 1; **C)** Same as in A) for day 6; **D)** Same as in B) for day 6; **E)** Same as in A) for day 12; **F)** Same as in B) for day 12. Data are represented as mean \pm SEM for A), C) and E); Data are represented as median \pm Min to Max for B), D) and F) *** $p \leq 0.0001$. - Sucrose delivery; - Cue start; - Cue stopped.

Next, we compared the mean activity, AUC and peak activity of D2-neurons in response to the CS. All statistical data are summarized in **Table S11**. The mean activity of D2-neurons in response to the CS is higher on the first days of training, but it decreases as the learning process is consolidated, as shown by the significant negative correlation with days of training (**Figure 14A**; $r^2 = 0.06563$, $s = 0.1934$, $p = 0.0218$). In addition, on day 1 of training, the mean activity during CS period is significantly lower than baseline activity (**Figure 14B**; $t_{(5)} = 2.959$, $p = 0.0315$). On day 6, the mean activity during CS presentation presents a trend for a decrease relative to the baseline (**Figure 14B**; $t_{(6)} = 2.212$, $p = 0.0689$). On day 12, no differences were found (**Figure 14B**).

No correlation was found between AUC and days of training (**Figure 14C**). Additionally, on days 1 and 6 of Pavlovian conditioning there is a significant decrease in the AUC during CS period relative to

baseline period. On day 12 no significant differences were found (**Figure 14D**; Day1: $t_{(5)} = 2.962$, $p = 0.0314$; Day6: $t_{(5)} = 3.034$, $p = 0.0289$; Day12: $W = -11$, $p = 0.3125$).

Regarding fluorescence peak activity, there is no statistically significant difference across days of training (**Figure 14E**), and no significant differences between baseline and CS period on days 1, 6 and 12 of Pavlovian conditioning were found (**Figure 14F**).

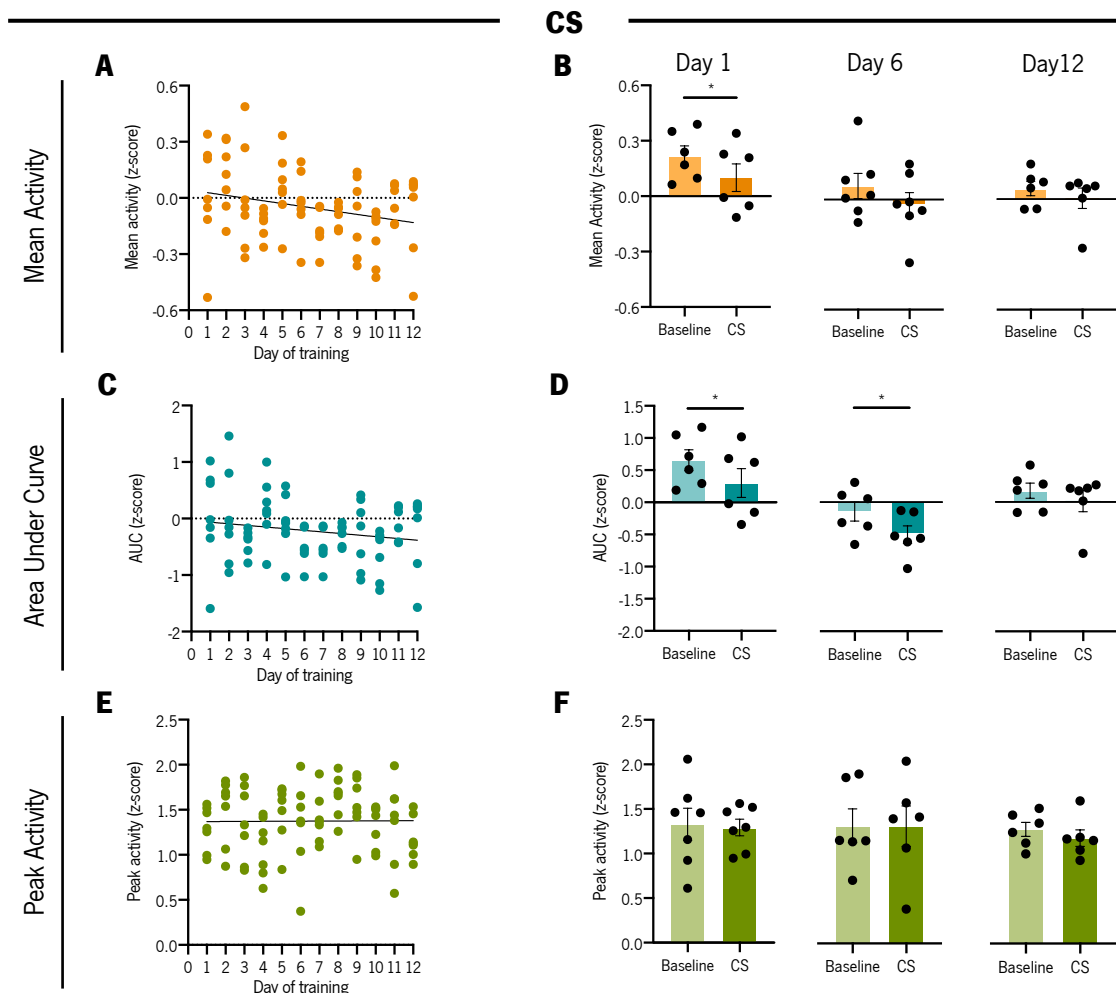


Figure 14 – Activity of D2-neurons decreases in response to the CS across days of training in the Pavlovian conditioning. **A**) Negative correlation between mean activity during CS period and days of training. **B**) Mean activity between baseline period [-10, -7] and CS period [-7, -4] during day 1, day 6, and day 12 of training. **C**) Negative correlation between AUC during CS period and days of training. **D**) same as in B) for AUC. **E**) Correlation between peak activity during CS period and days of training. **F**) same as in B) for peak activity. Data are represented as mean \pm SEM * $p \leq 0.05$.

Afterwards, we compared the mean activity, AUC and peak activity of D2-neurons in response to the US. All statistical data are summarized in **Table S12**. The mean activity of D2-neurons in response to the US appears to be decreased as learning process is consolidated, as reflected by a trend for a negative correlation (**Figure 15A**; $r^2 = 0.03835$, $s = 0.2528$, $p = 0.0778$). In addition, no significant differences were found on days 1, 6 and 12 for mean activity during US period (**Figure 15B**).

No correlation between AUC of CS period and days of training (**Figure 15C**), and no significant differences between baseline and US period for days 1, 6 and 12 of Pavlovian conditioning were found (**Figure 15D**).

Regarding peak activity, there are no differences across days of training (**Figure 15E**), and no significant differences between baseline and US period on days 1, 6 and 12 (**Figure 15F**).

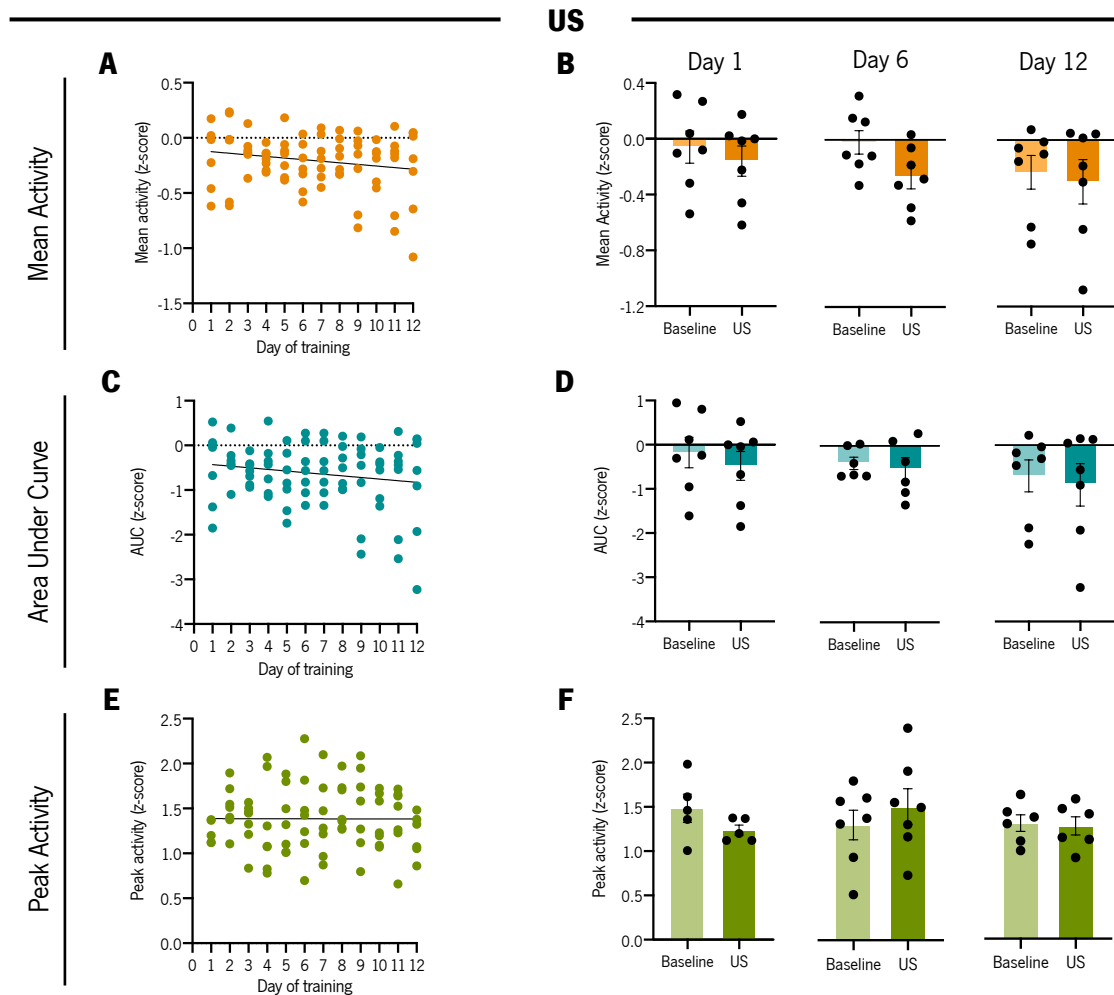


Figure 15 - Activity of D2-neurons decreases in response to the US across days of training in the Pavlovian conditioning. **A)** Negative correlation between mean activity during US period and days of training. **B)** Mean activity between baseline period [-3, 0] and US period [0, 3] during day 1, day 6 and day 12 of Pavlovian conditioning. **C)** Negative correlation between AUC during US period and days of training. **D)** same as in B) for AUC. **E)** Correlation between peak activity during US period and days of training. **F)** same as in B) for peak activity. Data are represented as mean \pm SEM.

Finally, we compared the average activity of D2-neurons during CS and US periods between day 1 and day 12 of training. All statistical data are summarized in **Table S13**. As shown in figure 16A, the activity on both days decreases in response to the CS and to reward delivery. A statistically significant difference between the two days appears for both CS and US periods (**Figure 16A**; $W = 150$, $p < 0.0001$).

Comparison between day 1 and day 12 regarding mean activity, AUC, and peak activity revealed no significant difference in response to the CS (**Figure 16B-D**).

Furthermore, the activity of D2-neurons in response to the US is similar when comparing the mean activity, AUC and peak activity of day 1 with day 12 (**Figure 16E-G**).

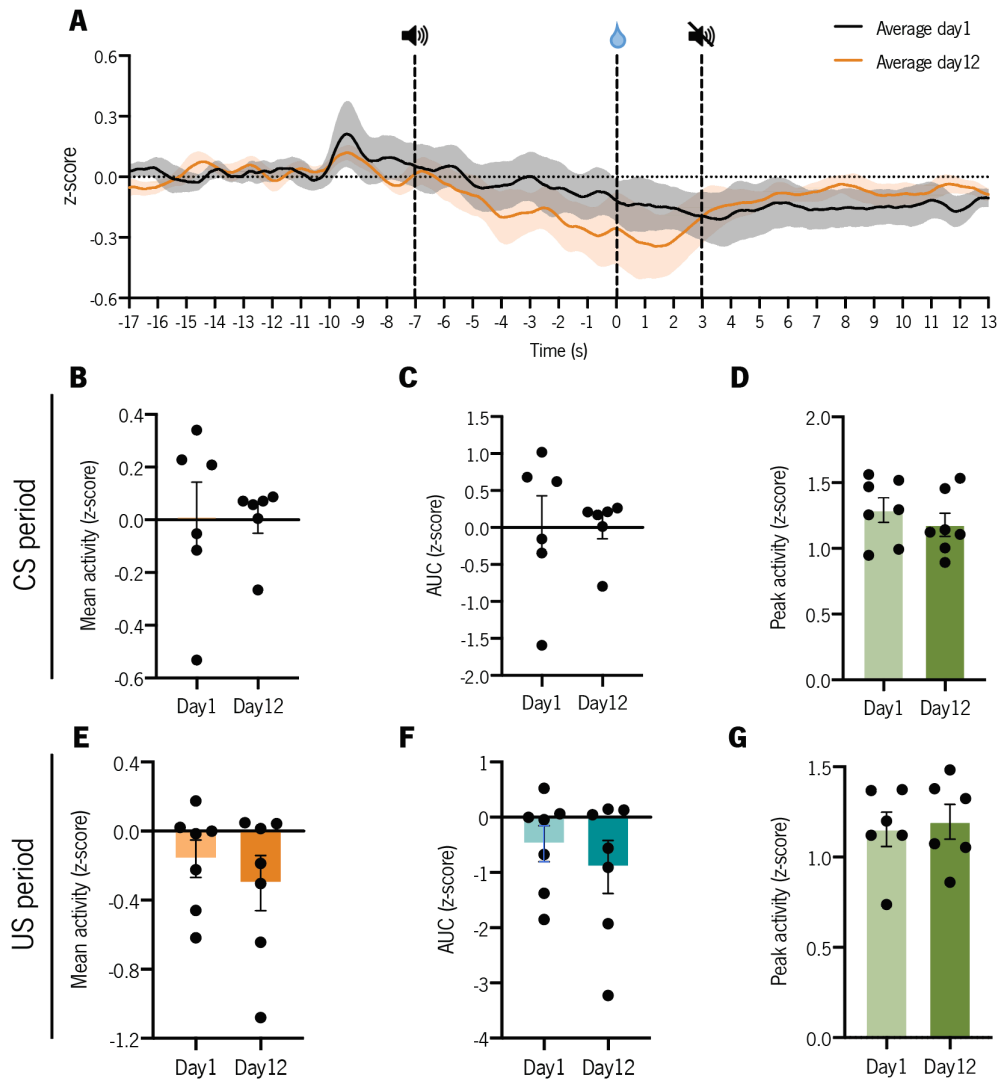


Figure 16 – D2-neurons activity decreases in response to CS and US from day 1 to day 12 of Pavlovian conditioning. **A)** Average of change in fluorescence during day1 (black) and day 12 (orange) of Pavlovian conditioning. **B)** Mean activity between day 1 and day 12 during CS period. **C)** same as in B) for AUC and **D)** peak activity. **E)** Mean activity between day 1 and day 12 during US period. **F)** same as in E) for AUC and **G)** peak activity. Data are represented as mean \pm SEM.

Overall, while animals learned to associate CS to the US as Pavlovian conditioning progressed, the activity of D2-neurons during CS presentation and reward delivery decreased.

4.2.3 D1-neurons activity changes in Pavlovian aversive conditioning

Next, we wanted to track the activity of D1-neurons during Pavlovian aversive conditioning. For that, D1-cre mice injected with GCaMP6f were subjected to 3 days of test in which a CS (tone plus a cue-light) was paired with a US (mild foot shock; 0.5mA for 1 sec) (**Figure 17A**). Freezing during the CS period was calculated for each day. All statistical data are summarized in **Table S14**.

On the first conditioning session, mice were exposed to 10 CS-US pairings, and an increase in freezing over the trials was developed (**Figure 17B**; $F_{(4,0,27,8)} = 7.991$, $p < 0.0001$). In addition, significantly higher percentage of freezing in the last trial is observed when compared with the first trial (**Figure 17C**; $t_{(8)} = 5.641$, $p = 0.0024$).

On the second day of test, mice received 30 trials – 20 CS-US and 10 trials of CS only, i.e., that were not followed by an electric foot shock; CS-US and CS trials were randomly assigned. Mice do not show any difference in freezing behavior between the trials with or without foot shock (**Figure 17D**).

On the third day, animals went through an extinction session in which they were exposed to 30 trials of CS only. Mice do not show a significant difference in percentage of freezing between the first trial and last trial (**Figure 17E**). Finally, no difference is detected in the percentage of freezing between day 1 and day 3 (**Figure 17F**).

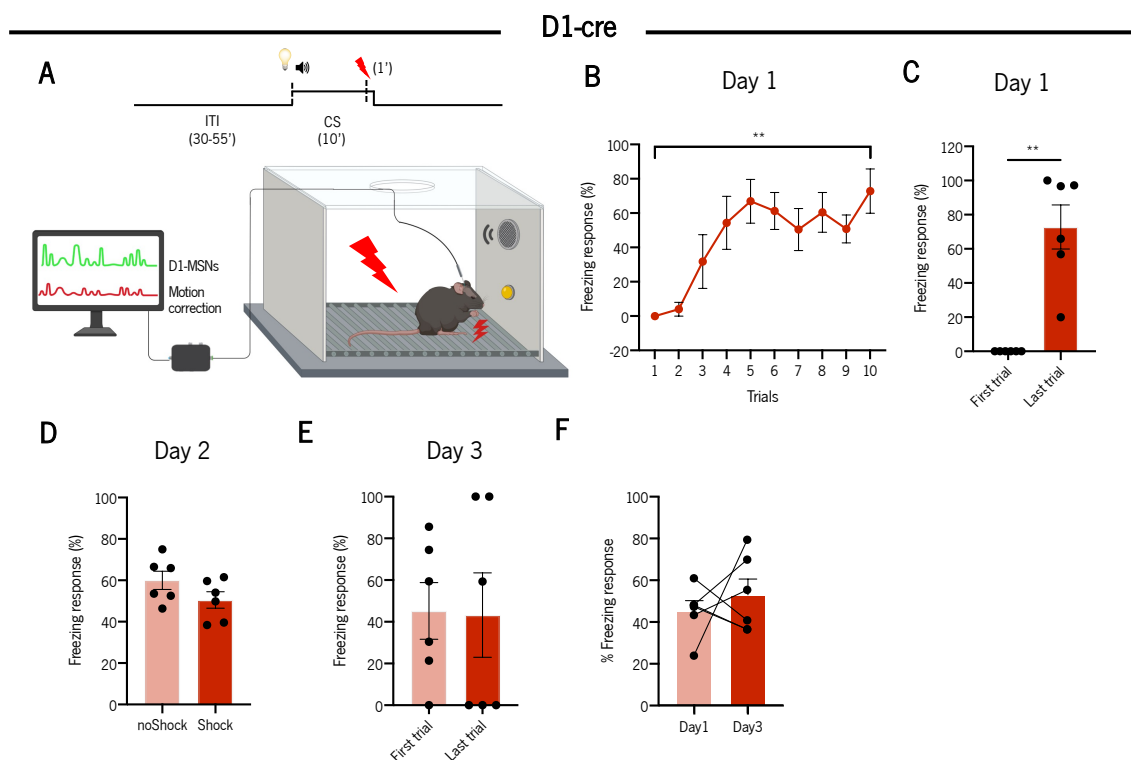


Figure 17 – Behavior of D1-cre mice injected with GCaMP6f during Pavlovian aversive conditioning. A) Schematic representation of the Pavlovian aversive conditioning. Each trial consisted of a random ITI period (45-50s) followed by a 10s CS (80dB, 3kHz tone plus a cue-light), co-terminated with a foot shock (US; 0.5mA, 1s). **B)** Percentage of freezing

response across trials on the first conditioning session (day 1); **C**) Percentage of freezing response in the first trial *versus* the last trial on day 1. **D**) Percentage of freezing response between trials without shock and trials with shock on day 2. **E**) Percentage of freezing response in the first trial *versus* last trial on day 3. **F**) Percentage of freezing response between day 1 (first conditioning session) and day 3 (extinction session). (D1-cre mice $n = 6$). Data are represented as mean \pm SEM ** $p \leq 0.01$.

During behavior, fiber photometry recordings of NAc D1-neurons were performed. The average activity of the CS period [-10 to -7s] was compared with the activity immediately before CS onset, baseline [-13 to -10]. All statistical data are summarized in **Table S15**.

During days 1, day 2 (both noshock and shock trials) and day 3, the average activity of D1-neurons during CS period increased when compared to the baseline period considering the average of all trial (**Figure 18A-B**; all trials: $W = 30959$, $p < 0.0001$; **Figure 18C-D**; all trials: $W = 0$, $p < 0.0001$; **Figure 18E-F**; all trials: $W = 0$, $p < 0.0001$; **Figure 18G-H**; all trials: $W = 0$, $p < 0.0001$).

Next, the average activity of the US period [0 to 3s] was compared with the activity immediately before the foot shock, baseline [-3 to 0s]. The average activity of D1-neurons increased in response to the shock on the sessions with shock delivery (**Figure 18A-B**; all trials: $W = 1431$, $p < 0.0001$; **Figure 18C-D**; all trials: $W = 0$, $p < 0.0001$). On trials where the shock was omitted, the activity of D1-neurons during US period is decreased comparatively to the baseline considering the average of all trials (**Figure 18E-F**; all trials: $W = 2469$, $p < 0.0001$; **Figure 18G-H**; all trials: $W = 0$, $p < 0.0001$); except for the first trial on day 2_noshock ($W = 2729$, $p < 0.0001$) and on day 3 ($W = 14116$, $p < 0.0001$) where the activity was increased.

Overall, the activity of D1-neurons during CS presentation and shock delivery is increased.

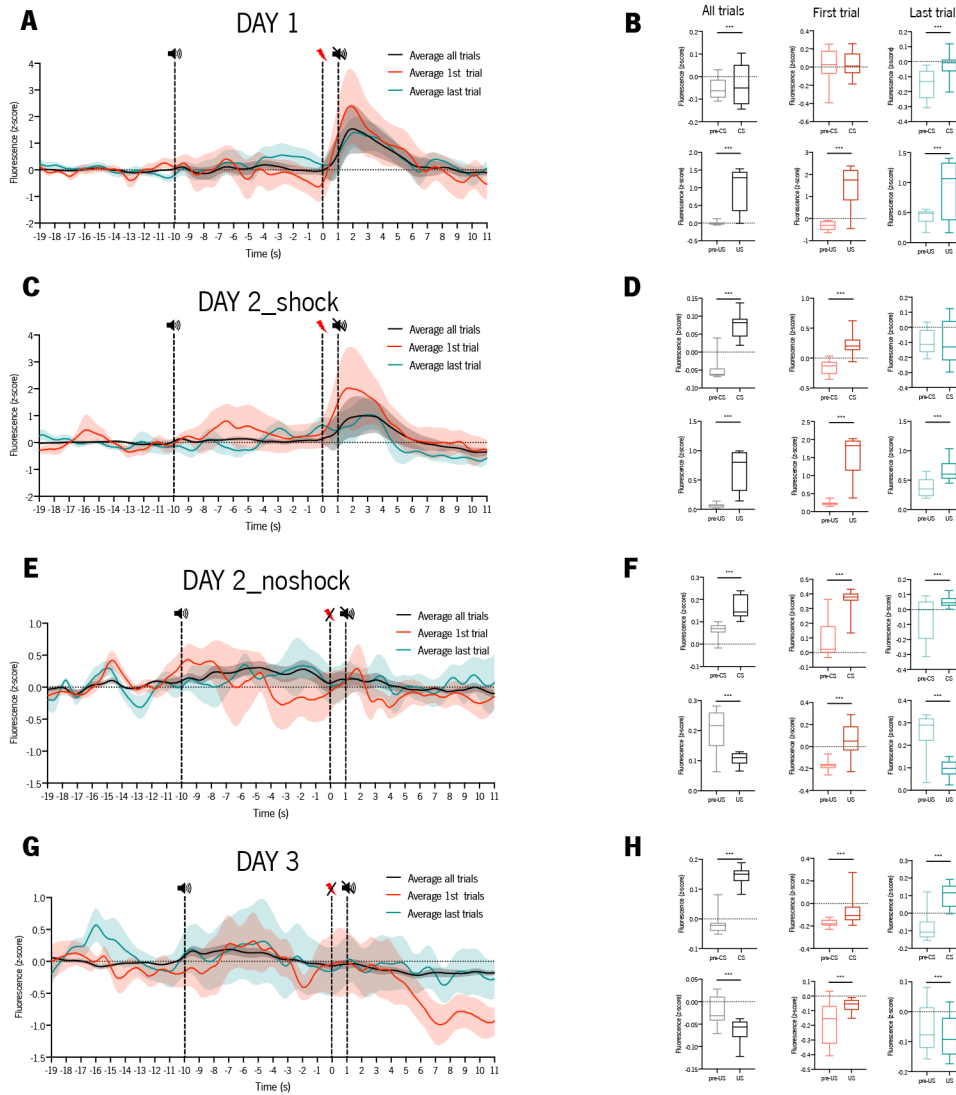


Figure 18 – Average activity of D1-neurons during Pavlovian aversive conditioning. Normalized activity (z-score) of D1-neurons evaluated by measuring GCaMP6f signal with fiber photometry. The activity during the first trial is marked in red, the last trial in blue, and average of all trials in black. **A)** Normalized activity of day 1; **B)** Boxplot showing the normalized activity between the period before CS (pre-CS) [-13 to -10s] and CS period (CS) [-10, to -7s], and between the period before US (pre-US) [-3 to 0s] and US period (US) [0 to 3s] during day 1; **C)** Same as in A) for day 2_shock; **D)** Same as in B) for day 2_shock; **E)** Same as in A) for day 2_noshock; **F)** Same as in B) for day 2_noshock; **G)** Same as in A) for day 3); **H)** Same as in B) for day3. Data are represented as mean \pm SEM for A), C), E) and G); Data are represented as median \pm Min to Max for B), D), F) and H) * $p \leq 0.0001$. - shock; - noshock; - cue start; - cue stopped.

During the first conditioning session, the activity of D1-neurons remains close to the baseline during CS onset. However, this activity increases as animals associate the CS with the US, as shown by the increase in the activity over day 2 and day 3 (**Figure 19**). D1-neurons exhibit an evident increase in the activity immediately after the foot shock delivery (CS-US group) in day 1 and day 2. On the contrary

on day 3, the activity of D1-neurons decreases after the period when foot shock was expected but was omitted.

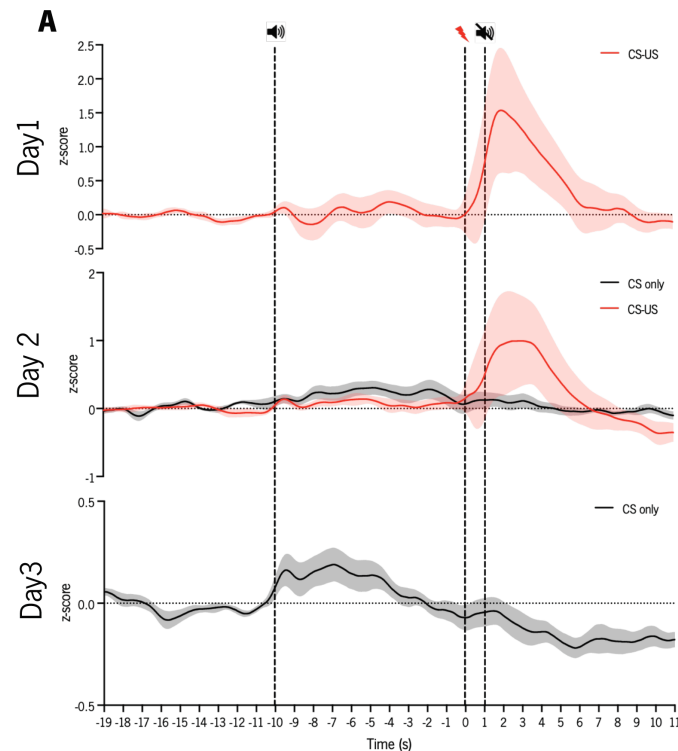


Figure 19 – Activity of D1-neurons during Pavlovian aversive conditioning. Normalized activity of D1-neurons evaluated by measuring GCaMP6f signal with fiber photometry. The average of all trials with CS-US pairings are marked in red, and with CS only in black. **A)** Normalized activity of day 1, 2 and 3 during Pavlovian aversive conditioning. Data are represented as mean \pm SEM. ⚡ – shock; 🔊 - cue start; 🔇 - cue stopped.

Next, the mean activity, AUC and peak activity of D1-neurons in response to the CS was compared with the baseline period (same periods in the analysis as describe above). All statistical data are summarized in **Table S16**.

No significant differences between mean activity during baseline period and CS period was found, though there is a trend on day 3 to increase in response to the CS (**Figure 20A**; Day 3: $t_{(3)} = 2.072$, $p = 0.0930$).

Similarly, the AUC exhibits no significant differences between baseline and CS periods, and the same trend was observed on day 3 (**Figure 20B**; Day 3: $t_{(3)} = 2.072$, $p = 0.0932$).

Regarding peak activity, there is no significant difference between baseline and CS period (**Figure 20C**).

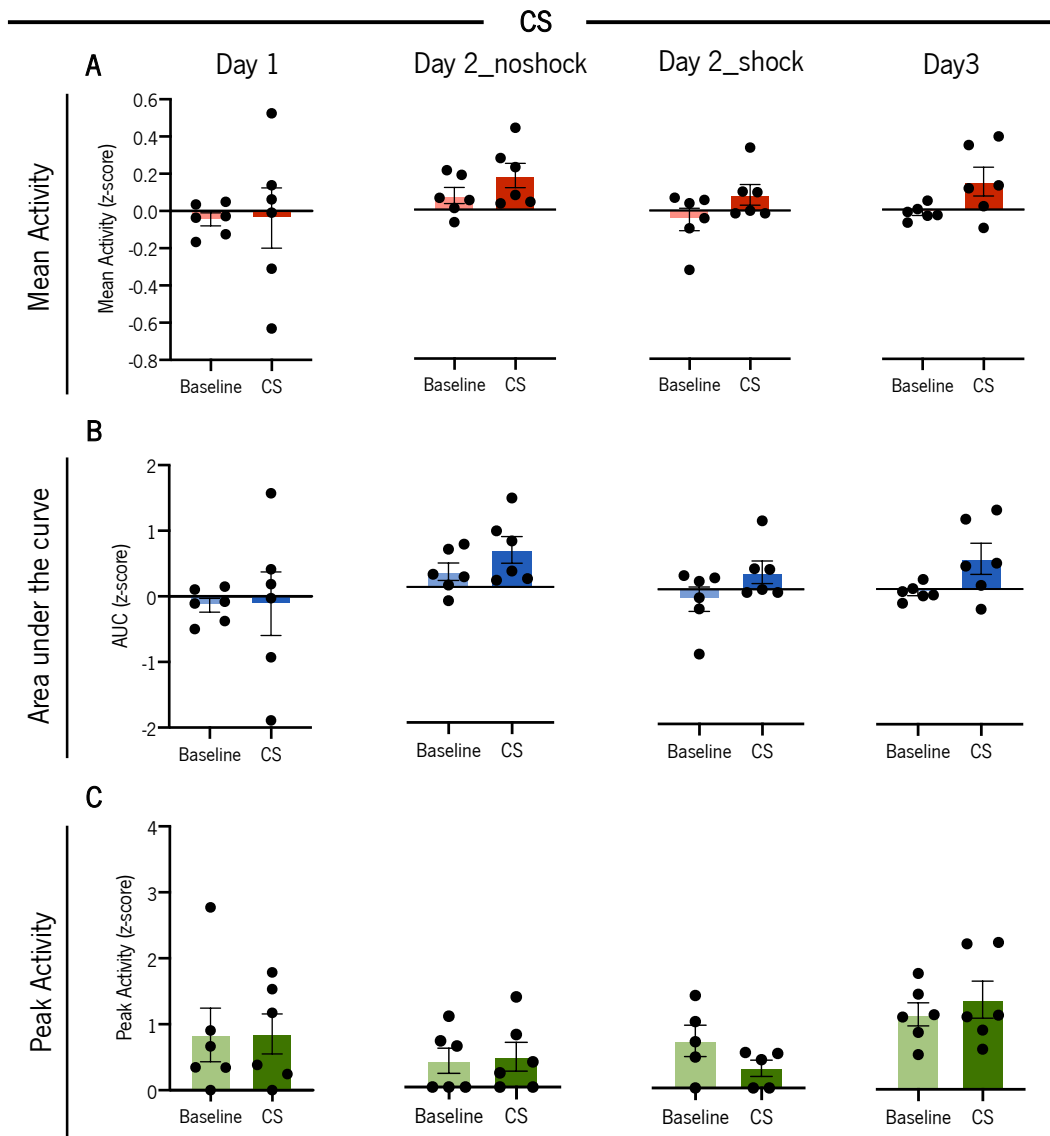


Figure 20 – Activity of D1-neurons increases in response to the CS. A) Mean activity between baseline period [-13, -10] and CS period [-10, -7] during day 1, day 2_noshock, day 2_shock and day 3. **B)** Same as in A) for AUC. **C)** Same as in A) for peak activity. Data are represented as mean \pm SEM.

Afterwards, we compared the mean activity of D1-neurons in the US period with the baseline period. All statistical data are summarized in **Table S17**. No significant differences between mean activity during baseline period and US period were found (**Figure 21A**). Similarly, the AUC presents no significant differences between baseline and US periods (**Figure 21B**).

Regarding peak activity, no statistically significant differences between the baseline and US period were found, with the exception of day 3, where the peak activity in response to the US decreases compared to the baseline period (**Figure 21C**; Day 1: $t_{(3)} = 1.323$, $p = 0.2430$; Day 2_noshock: $t_{(3)} = 0.4979$, $p = 0.6397$; Day 2_shock: $t_{(3)} = 1.563$, $p = 0.1788$; Day 3: $t_{(3)} = 3.030$, $p = 0.0291$).

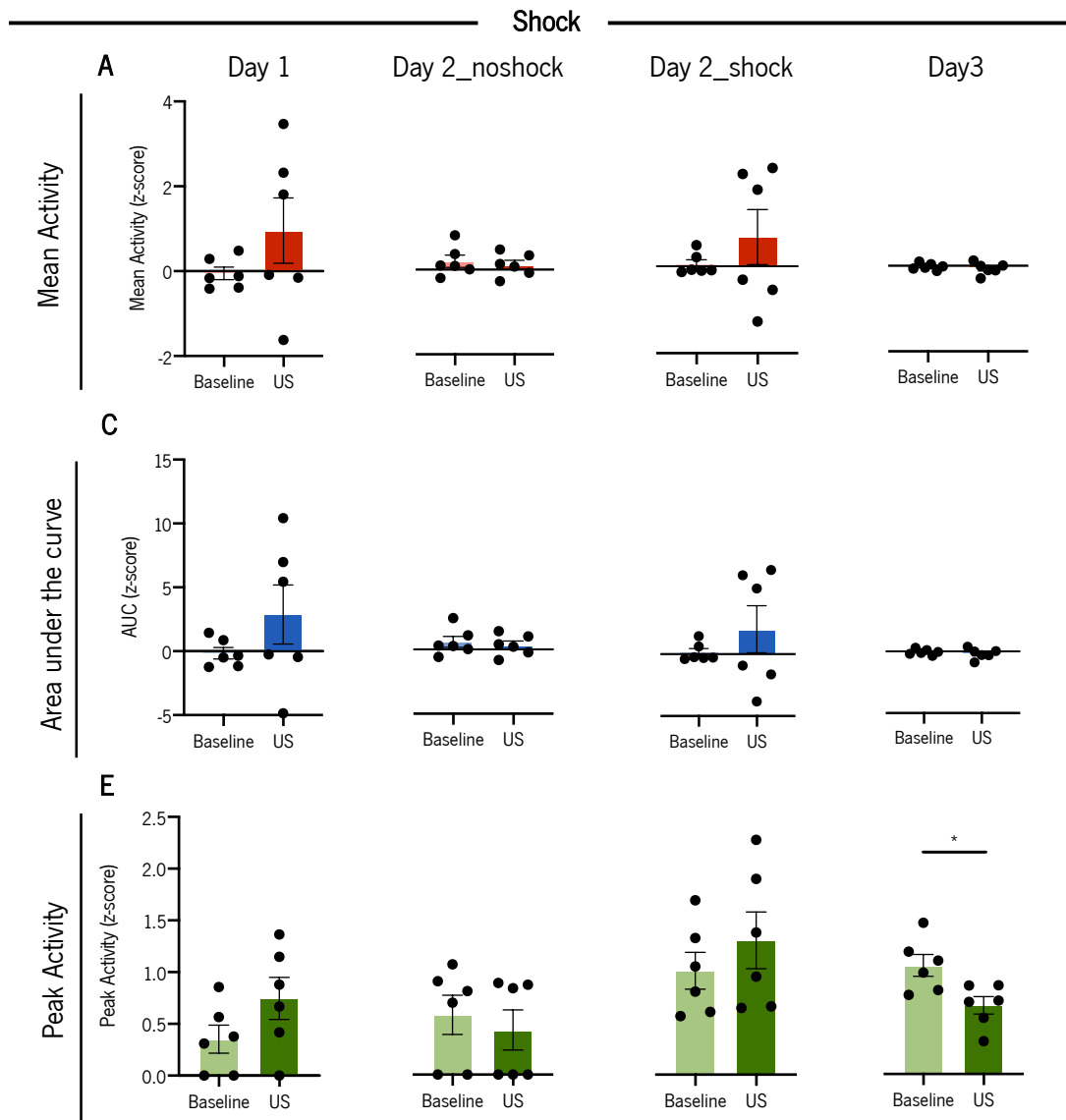


Figure 21 – Activity of D1-neurons increases in response to foot shock. A) Mean activity between baseline period [-3, 0] and US period [0, 3] during day 1, day 2_noshock, day 2_shock and day 3. **B)** Same as in A) for AUC. **C)** Same as in A) for peak activity. Data are represented as mean \pm SEM * $p < 0.05$.

Finally, we compared D1-neurons activity in response to the CS and to the US between day 1 (trials with CS paired with shock) and day 3 (trials with only CS exposure) of Pavlovian aversive conditioning. All statistical data are summarized in **Table S18**. The mean activity (**Figure 22A**), the AUC (**Figure 22B**) and peak activity (**Figure 22C**), show no significant differences in response to the CS between days. The mean activity (**Figure 22D**), the AUC (**Figure 22E**) and peak activity (**Figure 22F**), show no significant differences in response to the US between Day 1 and Day 3.

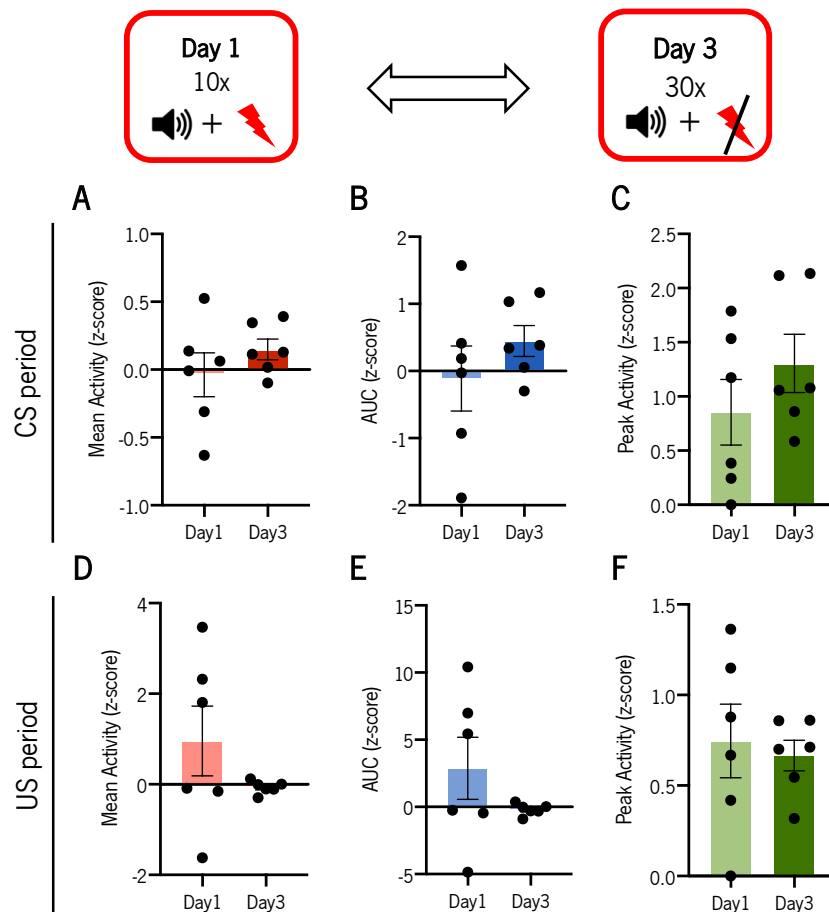


Figure 22 – D1-neurons activity in day 1 and day 3 in response to CS and to US (shock). **A)** Mean activity between day 1 and day 3 during CS period. **B)** same as in A) for AUC and **C)** for peak activity. **D)** Mean activity between on day 1 and day 3 during US period. **E)** same as in D) for AUC and **F)** for peak activity. Data are represented as mean \pm SEM.

In sum, D1-neurons increases their activity during CS onset as animals associate the CS with the US and it also increases in response to the shock, for the sessions where the shock was delivered.

4.2.4. D2-neurons respond to Pavlovian aversive conditioning

Next, we wanted to follow the activity of D2-neurons during Pavlovian aversive conditioning. For that D2-cre mice were subjected to 3 days of fear conditioning test as described for D1-cre mice (**Figure 23A**). All statistical data are summarized in **Table S19**.

On the first conditioning session, mice show a significant increase in the percentage of freezing over trials (**Figure 23B**; $F_{(2.45,13.07)} = 10.77$, $p = 0.0012$). In addition, a significantly higher percentage of freezing is observed in the last trial when compared to the first trial (**Figure 23C**; $t_{(6)} = 8.634$, $p = 0.0001$).

On the second day, mice were exposed to 20 CS-US trials and 10 CS only trials, (randomly). Mice do not show any difference in freezing between the trials with or without foot shock (**Figure 23D**). On

day 3, CS only, mice do not show a significant difference in percentage of freezing between the first and last trials (**Figure 23E**). No difference in the percentage of freezing between day 1 and day 3 were found (**Figure 23F**).

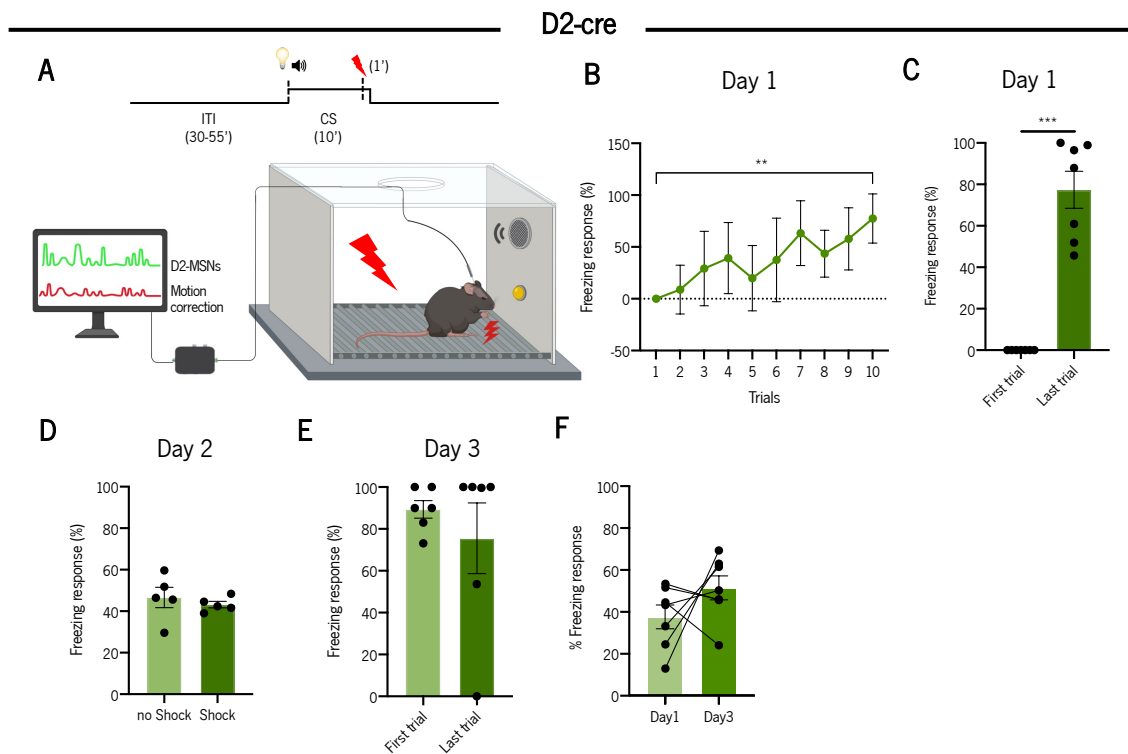


Figure 23- Behavior of D2-cre mice injected with GCaMP6f during Pavlovian aversive conditioning. A) Schematic representation of the Pavlovian aversive conditioning. Each trial consisted of a random ITI period (45-50s) followed by a 10s CS (80dB, 3kHz tone plus a cue-light), co-terminated with a foot shock (US; 0.5mA, 1s). **B)** Percentage of freezing response across trials on the first conditioning session (day 1); **C)** Percentage of freezing response in the first trial *versus* the last trial on day 1. **D)** Percentage of freezing response between trials without shock and trials with shock on day 2. **E)** Percentage of freezing response in the first trial *versus* last trial on day 3. **F)** Percentage of freezing response between day 1 (first conditioning session) and day 3 (extinction session). (D2-cre mice n= 7). Data are represented as mean \pm SEM ** $p \leq 0.01$, *** $p \leq 0.001$.

Fiber photometry recordings were performed every day for D2-neurons. Analysis was done exactly the same as for D1-neurons. All statistical data are summarized in **Table S20**.

During the 3 sessions, the average activity of D2-neurons during the CS period increases (**Figure 24A-B**; all trials: $W = 29237$, $p < 0.0001$; **Figure 24C-D**; all trials: $W = 0$, $p < 0.0001$; **Figure 24E-F**; all trials: $W = 0$, $p < 0.0001$; **Figure 24G-H**; all trials: $W = 0$, $p < 0.0001$), except for the first trial during the first conditioning session, where the activity decreases (**Figure 24A-B**; first trial: $W = 22020$, $p < 0.0001$).

The average activity of D2-neurons in the US increases only in sessions with shock delivery (**Figure 24A-B**; all trials: $W = 768$, $p < 0.0001$; **Figure 24C-D**; all trials: $W = 2680$, $p < 0.0001$). On the contrary, in the sessions where the shock was omitted the average activity of D2-neurons during the US period decreases (**Figure 24E-F**; all trials: $W = 0$, $p < 0.0001$; **Figure 24G-H**; all trials: $W = 0$, $p < 0.0001$).

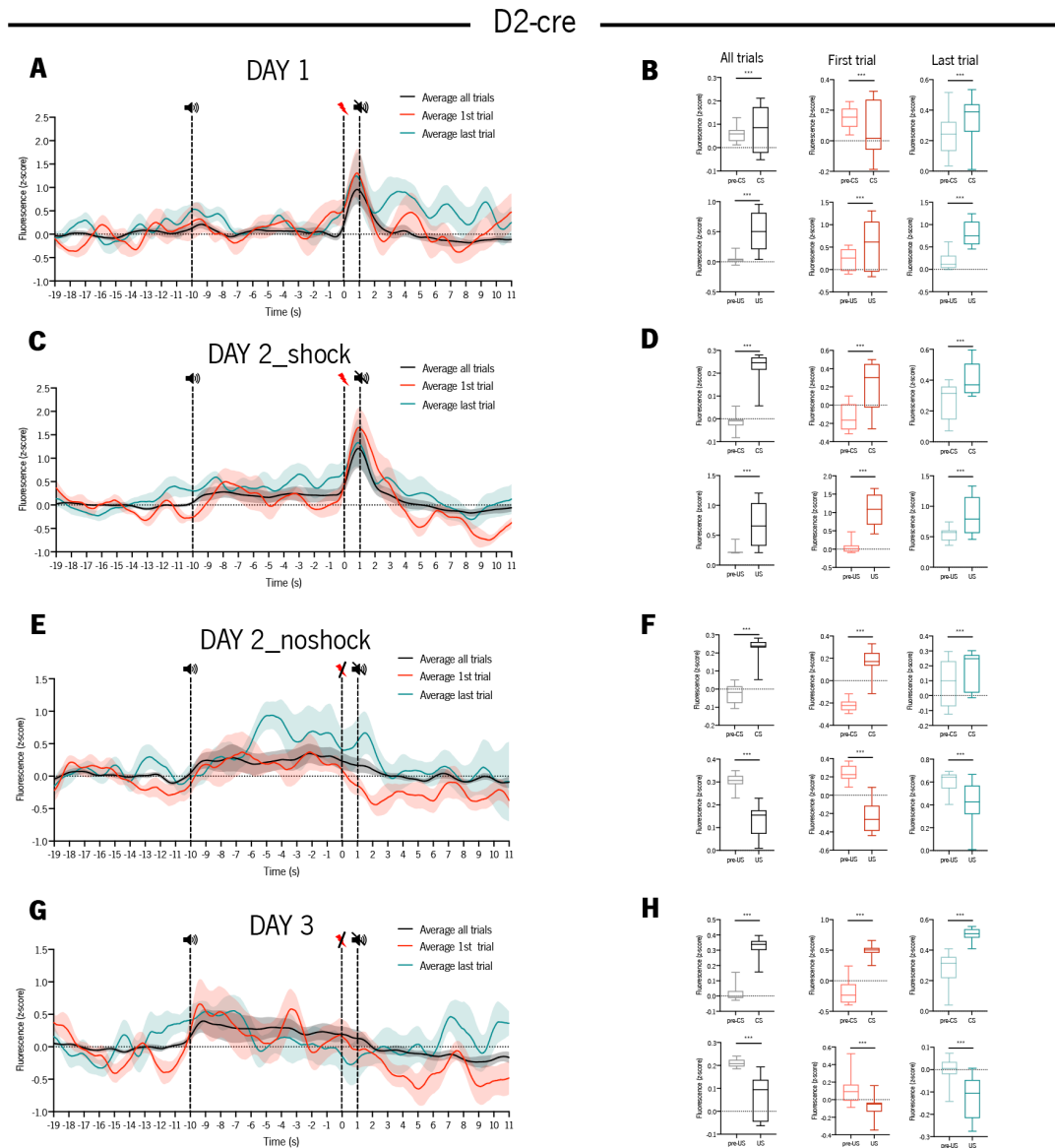


Figure 24 – Average activity of D2-neurons during Pavlovian aversive conditioning. Normalized activity (z-score) of D2-neurons evaluated by measuring GCaMP6f signal with fiber photometry. The activity during the first trial is marked in red, the last trial in blue, and average of all trials in black. **A)** Normalized activity of day 1; **B)** Boxplot showing the normalized activity between the period before CS (pre-CS) [-13 to -10s] and CS period (CS) [-10 to -7s], and between the period before US (pre-US) [-3 to 0s] and US period (US) [0 to 3s] during day 1; **C)** Same as in A) for day 2_shock; **D)** Same as in B) for day 2_shock; **E)** Same as in A) for day 2_noshock; **F)** Same as in B) for day 2_noshock; **G)** Same as in A) for day 3; **H)** Same

as in B) for day3. Data are represented as mean \pm SEM for A), C), E) and G); Data are represented as median \pm Min to Max for B), D), F) and H) *** $p \leq 0.0001$. ⚡ - shock; ⚡ - noshock; 🔊 - cue start; 🔊 - cue stopped.

During the first conditioning session, the activity of D2-neurons increases immediately after the CS onset but returns to baseline before shock delivery (**Figure 25**). On the contrary, on day 2 and day 3, the activity of D2-neurons increases immediately after the CS onset and continues high during the entire CS period. In addition, D2-neurons exhibit an evident increase in the activity immediately after the shock is delivery (CS-US in day 1 and day 2).

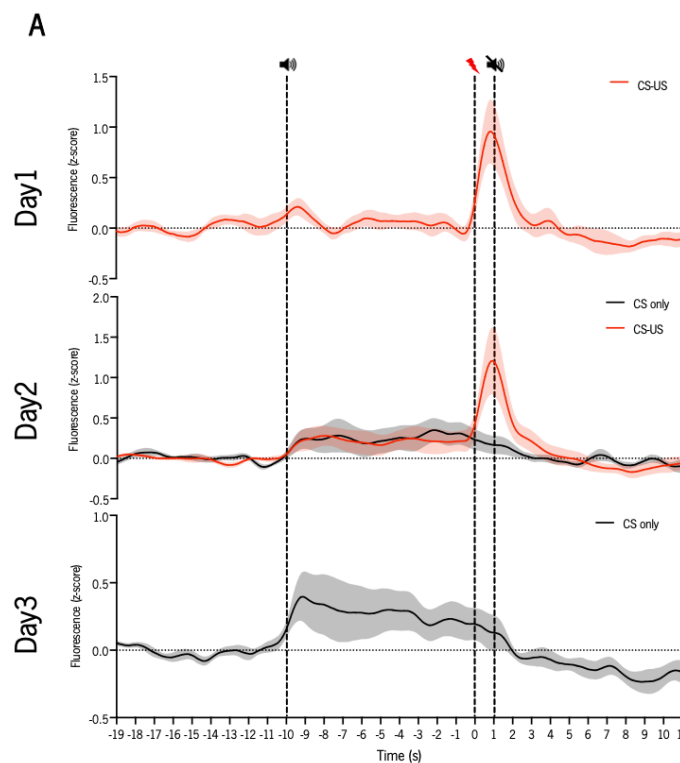


Figure 25 – Activity of D2-neurons during Pavlovian aversive conditioning. Normalized activity of D2-neurons evaluated by measuring GCaMP6f signal with fiber photometry. The average activity of all trials with CS-US pairings is marked in red, and with CS only in black. **A)** Normalized activity of day 1, 2 and 3 during Pavlovian aversive conditioning. Data are represented as mean \pm SEM. ⚡ – shock; 🔊 - cue start; 🔊 - cue stopped.

Next, the mean activity, AUC and peak activity of D2-neurons in response to the CS was compared with the baseline period. All statistical data are summarized in **Table S21**.

On day 2_shock, there is a significant increase in activity during the CS period compared with the baseline period (**Figure 26A**; Day 2_shock: $W = 24$, $p = 0.0469$). No significant differences between the mean activity during baseline period and CS period were found for the other sessions (**Figure 26A**).

Similarly, no significant differences between baseline and CS periods were found for the AUC, except for day 2_shock (**Figure 26B** Day 1: $t_{\theta} = 0.2355$, $p = 0.8217$; Day 2_noshock: $t_{\theta} = 1.829$, $p = 0.1172$; Day 2_shock: $W = 24$, $p = 0.0469$; Day 3: $W = 13$, $p = 0.1562$).

Regarding peak activity, there are no statistically significant difference between baseline and CS period, with the exception of day 2_shock, where the peak activity in response to the CS increases compared to the baseline period (**Figure 26C** Day 1: $W = 3$, $p = 0.5000$; Day 2_noshock: $t_{\theta} = 1.749$, $p = 0.1407$; Day 2_shock: $W = 26$, $p = 0.0312$; Day 3: $t_{\theta} = 0.2570$, $p = 0.8058$).

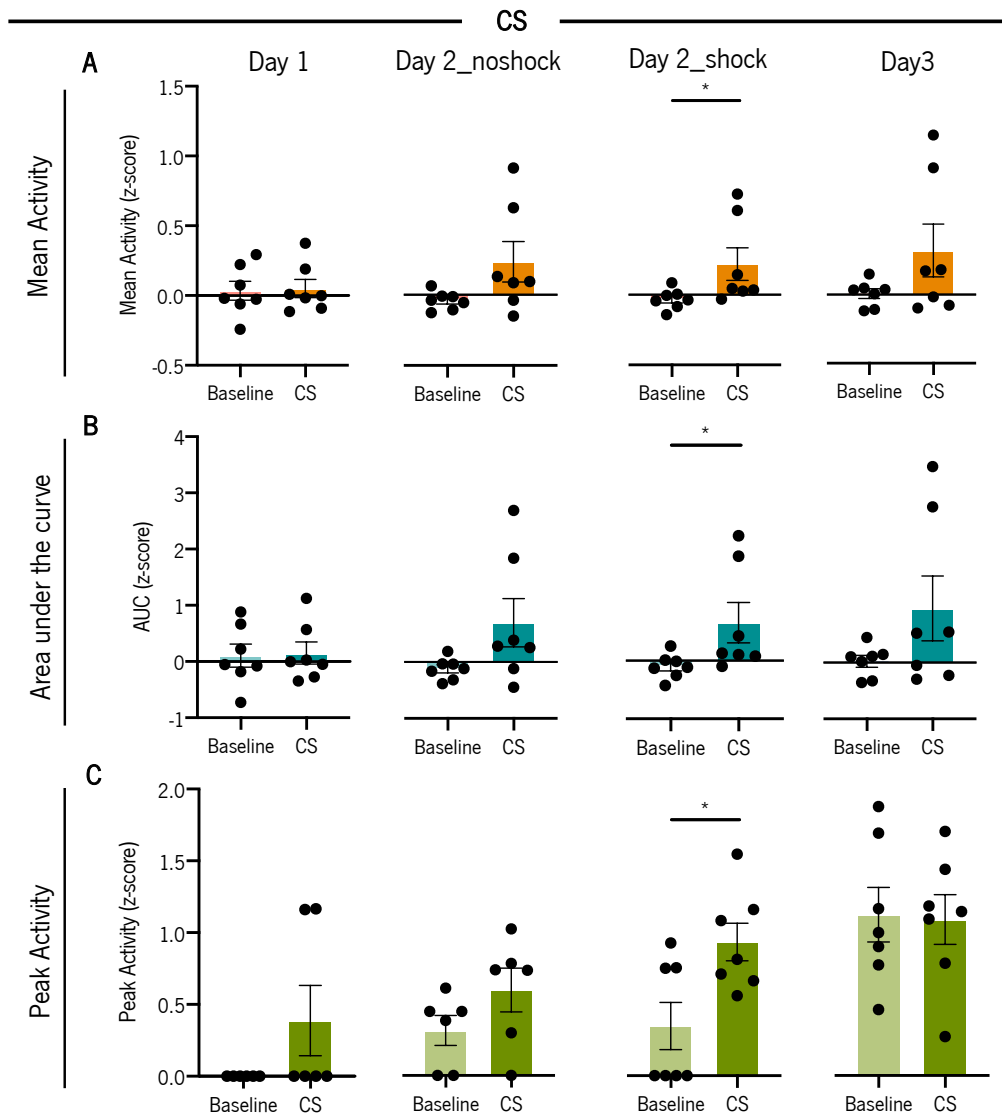


Figure 26 – Activity of D2-neurons increases in response to the CS. A) Mean activity between baseline period [-13, -10] and CS period [-10, -7] during day 1, day 2_noshock, day 2_shock and day 3. **B)** Same as in A) for AUC. **C)** Same as in A) for peak activity. Data are represented as mean ± SEM * $p < 0.05$.

After, the activity of D2-neurons in response to the US was compared with the baseline period. All statistical data are summarized in **Table S22**.

The mean activity of D2-neurons significantly increases in response to the shock on day 1, but not on other days (**Figure 27A**; Day 1: $t_{(6)} = 2.783$, $p = 0.0319$; Day 2_noshock: $t_{(6)} = 1.846$, $p = 0.1242$; Day 2_shock: $t_{(6)} = 1.680$, $p = 0.1538$; Day 3: $t_{(6)} = 2.062$, $p = 0.0941$).

The AUC is similar between baseline and US periods, except for day 1 which shows a significant increase when compared to the baseline (**Figure 27B**; Day 1: $t_{(6)} = 2.791$, $p = 0.0315$; Day 2_noshock: $t_{(6)} = 1.844$, $p = 0.1245$; Day 2_shock: $t_{(6)} = 1.672$, $p = 0.1554$; Day 3: $t_{(6)} = 2.064$, $p = 0.0940$).

Regarding peak fluorescence activity, there is no statistically significant difference between baseline and US period (**Figure 27C**).

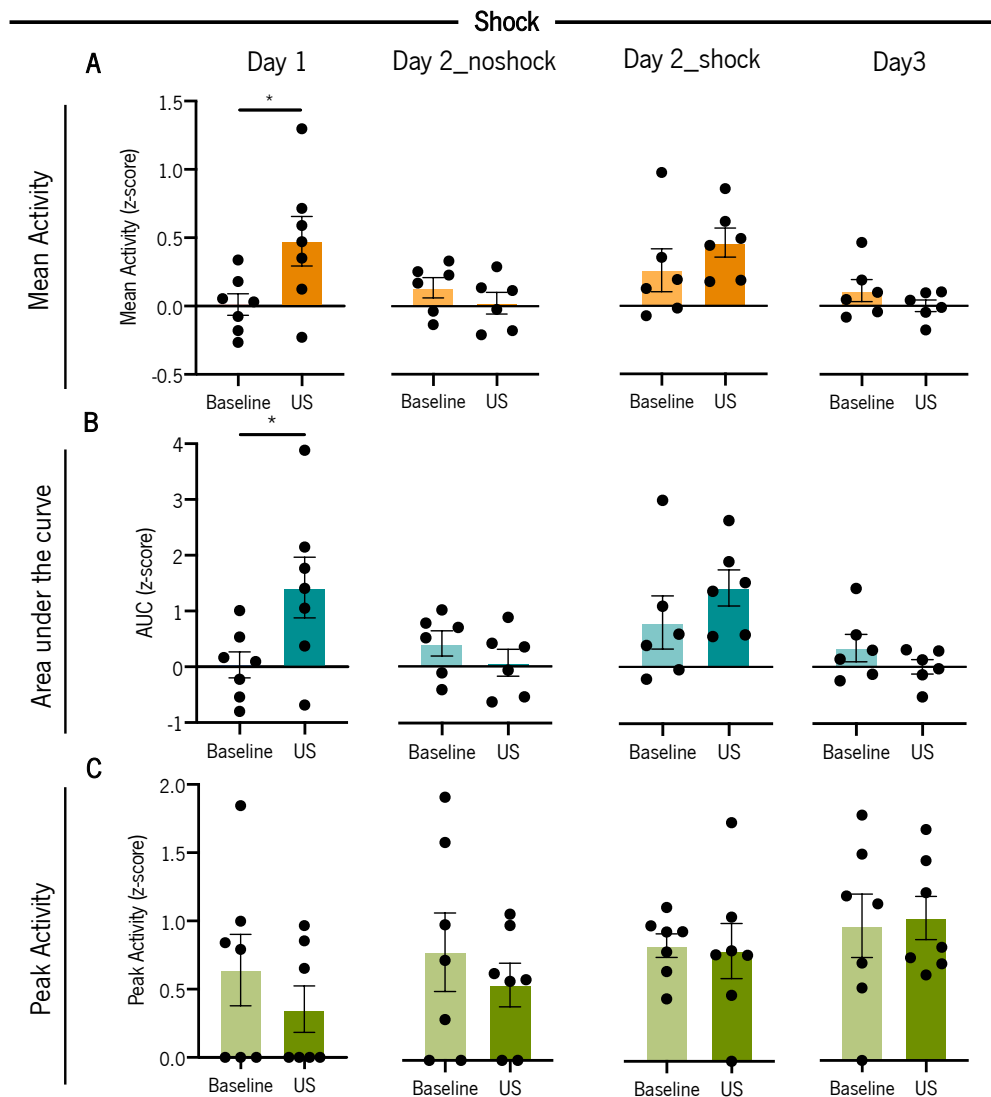


Figure 27 – Activity of D2-neurons increases in response to foot shock. A) Mean activity between baseline period [-3, 0] and US period [0, 3] during day 1, day 2_noshock, day 2_shock and day 3. **B)** Same as in A) for AUC. **C)** Same as in A) for peak activity. Data are represented as mean \pm SEM * $p < 0.05$.

Finally, D2-neurons activity in response to the CS and to the US between day 1 (trials with CS-US) and day 3 (CS only) was compared. All statistical data are summarized in **Table S23**.

D2-neurons mean activity (**Figure 28A**), the AUC (**Figure 28B**), and peak activity (**Figure 28C**) show no significant differences in response to the CS between day 1 and 3.

Regarding the US period, comparisons of mean activity (**Figure 28D**; $t_{(9)} = 2.530$, $p = 0.0500$) and AUC (**Figure 28E**; $t_{(10)} = 2.536$, $p = 0.0500$) between day 1 and 3 revealed that the activity of D2-neurons significantly decrease. Peak activity (**Figure 28F**; $W = 24$, $p = 0.0469$) show an increase in the activity on day 3.

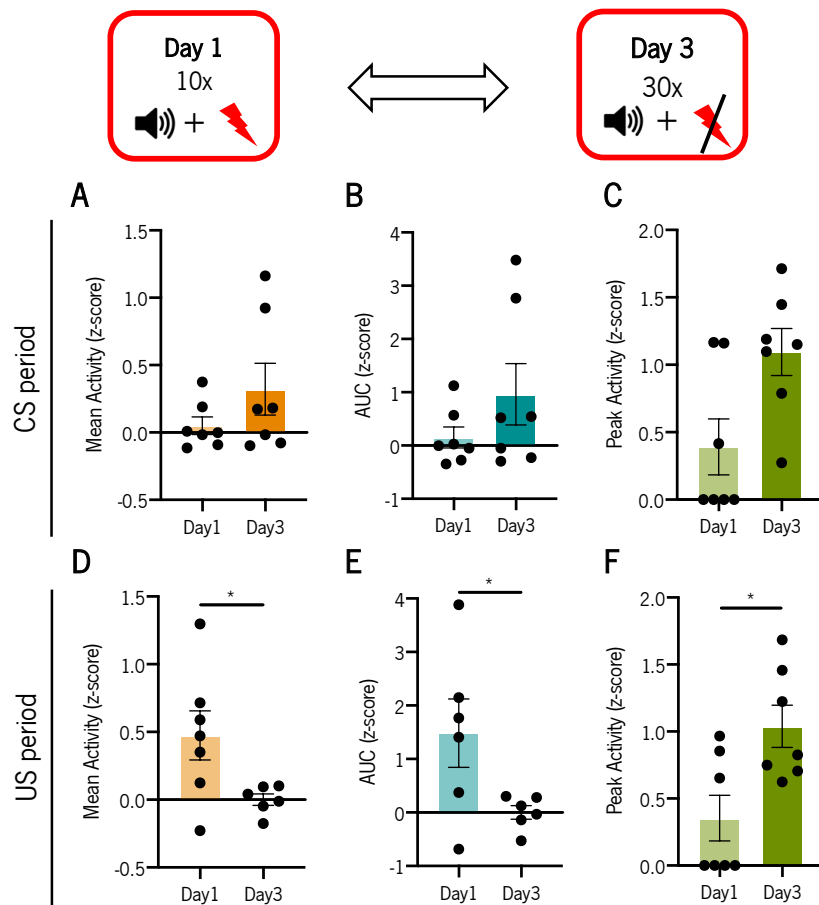


Figure 28 – D2-neurons activity in day 1 and day 3 in response to CS and to the US (shock). **A)** Mean activity between day 1 and day 3 during CS period. **B)** Same as in A) for AUC and **C)** for peak activity. **D)** Mean activity between day 1 and day 3 during US period. **E)** Same as in D) for AUC and **F)** for peak activity. Data are represented as mean \pm SEM * $p \leq 0.05$.

Similar to D1-neurons, the activity of D2-neurons increases during CS onset as animals learned to associate the CS with the US, and it also increases in response to the shock, particularly during the first conditioning session.

***CHAPTER 5 – Discussion, Conclusion
and Future Perspectives***

5.1 Discussion

Associations between natural rewards or aversive outcomes and predictive environmental cues are crucial for survival in an external environment (Day & Carelli, 2007; Soares-Cunha et al., 2020; Zessen et al., 2021). These are classical cases of Pavlovian conditioning, in which a neutral cue is assigned to predict something to be either positive/rewarding or negative/aversive (Day & Carelli, 2007; Hanley & Garland, 2019). As a result, Pavlovian learning is the basis for both normal and maladaptive human behaviors. Thus, understanding cue-outcome associative learning may help us better comprehend a wide range of human behaviors.

Evidence has shown that NAc plays an important role in mediating Pavlovian associations (Day et al., 2006a; Day & Carelli, 2007; Roitman et al., 2005; Wan & Peoples, 2006). Thus, the present work focuses on identifying what are the NAc neurons that are responsive to cue-outcome associations.

NAc neuronal ensembles responding to early versus late learning during Pavlovian conditioning associations

The NAc is involved in processing information about USs and to learn associations between these rewards and external stimuli. Intraoral administration of a sucrose solution (Roitman et al., 2005), self-administration of sucrose (Nicola et al., 2004c) or water and food (Roitman et al., 2005) during an operant task results in a reduction of NAc neuronal activity (Roitman et al., 2005). In addition, these firing patterns are thought to be differentially distributed in the NAc core and shell, suggesting that these subregions play different roles in this process (Ikemoto, 2007; McFarland et al., 2003; Robbins et al., 2008; Rodd-Henricks et al., 2002; Sellings & Clarke, 2003; Xia et al., 2020).

A common strategy used to understand how neuronal populations responding to certain stimuli or behavior are anatomically distributed is the examination of the pattern of expression of immediately early genes (IEG) and markers of neuronal activity such as for example the evaluation of endogenous c-fos⁺ cells. Due to its rapid mRNA accumulation (around 30-45min) and peak of protein expression (60-90min after the onset of stimulation) c-fos is frequently used to identify neuronal activation after a stimulus or behavioral conditioning (Bullitt, 1990; Perrin-Terrin et al., 2016; Zangenehpour & Chaudhuri, 2002).

In this work we first aimed to identify the anatomical distribution of NAc neuronal ensembles that are activated in early *versus* late learning of Pavlovian conditioning. To achieve that, B6 wild-type mice were subjected to a Pavlovian conditioning test and were sacrificed 90 min after the second session (day 2) or the last session (day 12), and then endogenous c-fos labelling was done to quantify neuronal activation in the NAc core, medial shell, and lateral shell.

Our data showed that at early learning (Pav_d2 group), there are no statistical differences in c-fos⁺ cells when compared to the control group (noPav_d2 group) for neither NAc subregion. However, c-fos⁺ cells tend to increase during early learning, whereas in late learning (Pav_d12 group), c-fos⁺ cells tend to decrease, though no statistically significant effect was found. Although this decrease is not significant in this present work, this result was previously reported by another study, in where authors found lower c-Fos density in the NAc and NAcc of mice that performed a classical conditioning in comparison to the control groups. Additionally, this decrease was also observed when other IEG from the same family was analysed (Fos B) (Noye Tuplin et al., 2018). On the contrary, other study shows an increase in the number of c-fos⁺ cells in NAc after exposure to sucrose (Koekkoek et al., 2021). Furthermore, cues associated with rewarding foods, which have acquired incentive value, have shown to induce c-fos mRNA and c-Fos protein expression within the NAc (Finglewicz et al., 2011; Flagel, Cameron, et al., 2011). This may suggest that c-fos is not the best marker for neuronal activation within the NAc during cue-reward associations, and that others IEGs, such as Arc or Zif268, may be more sensitive to this type of activity expression pattern (Gore et al., 2015; Lv et al., 2011; Noe et al., 2019; J.-J. Wang et al., 2014).

Interestingly, if we observe our fiber photometry data, we also find a decrease in the activity of NAc D1-and D2-neurons in response to the CS and to the US from day 1 to day 12, which somehow matches the observed trend for decreased c-fos⁺ cells in day 12. One could assume that there is no significant neuronal recruitment within the NAc during Pavlovian conditioning, which does not fit the electrophysiological data available to date (Carelli et al., 2000; Carelli & Deadwyler, 1994; Carelli & West, 2014; Carelli & Wondolowski, 2003). Or one could hypothesize that at late stages of Pavlovian conditioning, neurons in the NAc are inhibited, which is reflected by a decrease in c-fos expression. Therefore, one question arises: is there any correlation between the decrease in activity of NAc ensembles across learning and c-fos expression? This is a question that remains to be answered in future studies.

Electrophysiological studies revealed that the majority (79%) of NAc responses to reward, as well CS responses, were inhibitory (Wan & Peoples, 2006). Similarly, other Pavlovian conditioning study that examined accumbal activity at reward exposure shows that NAc neurons were typically inhibited by sucrose (75% of cells) (Roitman et al., 2005); or revealed both increase or decrease in firing rate during the CS presentation (Day et al., 2006a). However, so far, there has been no study showing how neuronal inhibition is correlated with c-fos expression. According to the literature, simultaneous NAc activation and inhibition may occur during cue-reward associations (Carlezon & Thomas, 2009; Day et al., 2006b; Kutlu,

Zachry, Melugin, Cajigas, Chevee, Kelly, et al., 2021; Patriarchi et al., 2018b), which could explain the variety of c-fos expression patterns existing in different studies.

Thus, one should increase the number of animals, since using a low number may mask some potential differences regarding c-fos⁺ cells density in the NAc. Furthermore, c-fos analysis performed in animals in which neuronal activity was recorded using fiber photometry, could be helpful to understand what is the correlation between neuronal activity and c-fos expression.

Finally, it is also important to consider that the NAc is composed by a variety of neuronal subpopulations – MSNs, cholinergic interneurons and several sub-groups of GABAergic interneurons. Thus, it would be important to determine if c-fos expression is different between these genetically-distinct neuronal populations.

Functional relevance of D1- and D2 neurons responding to Pavlovian conditioning associations

We next aimed to determine the functional relevance of accumbal D1- and D2-neurons for the acquisition of CS-US associative learning, by recording the activity in real time of these specific accumbal population during Pavlovian conditioning. We used D1-cre and D2-cre lines to drive expression of the GECI. Though D1 are apparently restricted to D1-MSNs, D2 receptor is also expressed in cholinergic interneurons, this is the reason why we do not state D2-MSNs but opted for D2-neurons (and concomitantly D1-neurons).

Before proceeding the analysis of neuronal activity, we confirmed that the animals exhibit, as expected, an increase in the number of nose pokes during CS presentation, showing that animals distinguish the CS-US paired period from the ITI period and that association between CS and reward delivery was learned. Accordingly, the same behavior outcome was observed in Patriarchi *et al.* by showing an increase in the numbers of licks during CS over the course of training (Patriarchi et al., 2018a). Additionally, this present work extend that this behavioral effect was accompanied by a gradual decrease in D1 and D2-neurons activity as animals learned the associations between CS and US, suggesting that these two NAc subpopulations of neurons are involved in mediating Pavlovian associations.

Traditionally, these subpopulations have been assigned two opposite functions: D1-MSNs were associated with reward and positive reinforcement and D2-MSNs with aversion and negative reinforcement (Hikida et al., 2010, 2016; Kravitz et al., 2012; Volman et al., 2013). However, our data showed that D1 and D2-neurons exhibit a similar pattern of activity during Pavlovian conditioning. As the learning process is consolidated, the activity of D1- and D2 neurons decreases in response to the cue

and to the reward. In addition, their activity appears to have a particularly relevant role in the early stages of cue-reward acquisition. There is an increase in the activity of D1-neurons during the CS in the first day, and a decrease over the rest of the sessions. This effect observed in day 1 is not evident in D2-neurons, suggesting different activity dynamics during Pavlovian learning. Interestingly, the activity of D1- or D2-neurons in day 12 is more similar than in day 1.

Furthermore, there is also significant difference between day 1 and day 12. In agreement with our data, in ventrolateral striatum, D1- and D2-MSNs exhibit event-related concurrent Ca^{2+} activities during food-incentive and goal-directed behavior. Both types of MSNs in the VLS positively encode the action initiation, but only D1-MSNs positively encode the sustainment of goal directed behavior (Natsubori et al., 2017). Thus, both D1- and D2-MSNs positively encode food-incentive behavior and do not support the opposing functional roles of D1- *versus* D2-MSNs. These results show a similar encoding profile for D1- and D2-MSNs in food-incentive and goal-directed behaviour, similarly to what we report in this study for Pavlovian conditioning associative learning.

On the contrary, another study using Ca^{2+} fiber photometry demonstrated distinct patterns of D1- and D2-MSNs signaling in NAc during cocaine reward learning. Acute cocaine administration enhances D1- and suppresses D2-MSN activity, and cocaine-induced facilitation of D1-MSN activity is required for the formation of cocaine-context associations. Accordingly, D1- and D2-MSNs display distinct temporal profile of activity during a cocaine conditioned place preference (CPP) protocol choice session: increased D1-MSN activity immediately preceded entry into the drug-paired context, whereas D2-MSN activity was suppressed only after entry into the compartment (Calipari et al., 2016). Despite these opposing results, it is important to point out that Calipari *et al.* used a drug reward (cocaine), which, by itself causes significant and opposing changes in the activity of accumbal D1- and D2-MSNs (Creed et al., 2016), potentially contributing for the pronounced opposing function of these two neuronal sub-types.

However, fiber photometry data are not robust enough to reveal possible individual neuronal subtype differences within NAc MSNs. Indeed, a study using single cell RNA sequencing revealed a tremendous diversity in neuronal subtypes with distinct molecular and spatial features. In addition, they were also able to link gene expression and spatial distribution of these neuron subtypes to the anatomic and functional complexity of the NAc, providing insights into how NAc achieves its observed structural and functional diversity despite having an apparently simple neuronal composition (D1 and D2 MSNs) (R. Chen et al., 2021). Thus, it is plausible to assume that the mild changes in bulk activity recorded in our study using fiber photometry result from the opposing contribution of distinct sub-populations within D1/D2 neurons for Pavlovian conditioning.

In sum, although D1- and D2-MSNs have classically been described as having a dichotomous function in reward, this work showed similar patterns of bulk activity between the two populations during Pavlovian conditioning. These results are in fact in accordance with previous data using optogenetics in which we showed that increasing the activity of either D1- or D2-neurons results in increased motivational levels (Soares-Cunha et al., 2020).

Functional relevance of D1- and D2 neurons responding to Pavlovian aversive conditioning

We next aimed to determine the functional relevance of accumbal D1- and D2-neurons for the acquisition of cue-aversive associative learning. For that the same animals were subjected to a Pavlovian aversive conditioning test and the activity of D1- and D2-neurons was measured during response to the cue (CS) and to the shock (US). As expected (de Jong et al., 2019), animals exhibit more freezing behavior in response to the cue after conditioning (last shock trial) than before conditioning session (first shock trial), showing that cue predicts foot shock delivery.

Our data showed again a similar pattern of activity between D1- and D2-neurons for cue-aversive learning. A gradually increase across sessions in the activity of both D1- and D2-neurons in response to CS and a prominent increase following shock delivery.

In agreement with our data, electrophysiological recordings in the NAc show that the delivery of quinine (unpleasant taste stimuli) without prior exposure, elicits an excitatory response in NAc neurons (Roitman et al., 2005). In addition, increase in NAc firing rates was also observed in response to other aversive stimuli like air puff (Yanagimoto & Maeda, 2003). Moreover, data shows the existence of NAc neuronal subpopulations that respond to aversion-predictive cues. This response grows as learning progresses and associations between cue and the aversive stimuli (quinine) occur (Roitman et al., 2005; Setlow et al., 2003). Thus, electrophysiological recordings reflect similarly what we saw with fiber photometry recordings. Still, in our work, we went one step further and showed that this encoding occurs in both D1- and D2-neurons.

These results, in parallel with results from the Pavlovian conditioning further corroborate the premise of a coexisting role of D1- and D2-MSNs in encoding aversion, since both populations show similar patterns of activity during Pavlovian aversive conditioning. Again, our results further support data from our group that shows that NAc D1- and D2-neurons can contribute for both reward and aversion (Soares-Cunha et al., 2020), depending on their patterns of activity. Thus, together, these studies reveal a more complex role played by accumbal D1- and D2-MSNs in encoding reward and aversion than the initial model.

5.2 Conclusion

Evidence so far strongly suggests that NAc is involved in processing information about unconditioned rewards and to learn associations between these rewards and CSs. Here, we showed that c-fos expression does not significantly change during Pavlovian conditioning at early and in late phases of training. However, a trend for increased c-fos expression at early learning and decrease at late learning was observed. This trend was previously reported, but contradicting reports also exist.

Fiber photometry analysis of D1- and D2-neurons activity in the NAc during cue-outcome associations reveal a decrease in activity in response to the cue and to the reward delivery as Pavlovian learning occurs. Additionally, there is a gradual increase in the activity of both D1- and D2-neurons in response to CS across sessions, as well as a significant increase following shock delivery, during cue-aversive associations. These results show that both D1- and D2-neurons activity contributes to reward and aversion processing and that these genetically-distinct populations show similar patterns of bulk activity. Important to refer that most likely this is not the case if we look to individual neurons. Preliminary data from our team using GCAMP6f with miniscopes has shown that at least 3 subpopulations of D1- and D2-MSNs exist in terms of responses to Pavlovian conditioning (Soares-Cunha, Domingues et al, unpublished observations).

In conclusion, our data support the notion that a dichotomous function of D1- and D2-MSNs is too simplistic and that these neurons are co-activated during both positive and negative associative conditioning (results summarized in **Table 1**).

Table 1 - Summary of the main results obtained from c-fos expression in NAc neurons responding to early versus late learning, and bulk activity of NAc D1- and D2-neurons during Pavlovian conditioning and Pavlovian aversive conditioning, recorded with fiber photometry. = no changes; $\approx\uparrow$ tendency to increase; $\approx\downarrow$ tendency to decrease; \uparrow increase; \downarrow decrease

NAc subregions	c-fos+ cell density													
	Early learning						Late learning							
NAcc	=						=							
NAcsm	$\approx\uparrow$						=							
NAcsl	=						=							
NAc neurons	Pavlovian conditioning						Pavlovian aversive conditioning							
	CS			Sucrose			CS			Shock				
	Day1	Day6	Day12	Day1	Day6	Day12	Day1	Day2	Day3	Day1	Day2	Day3		
							noshock	shock			noshock	shock		
D1	\uparrow	\downarrow	\downarrow	\downarrow	\uparrow	\downarrow	\uparrow	\uparrow	\uparrow	\uparrow	\uparrow	\downarrow	\uparrow	\downarrow
D2	\downarrow	\downarrow	\downarrow	\downarrow	\downarrow	\downarrow	\uparrow	\uparrow	\uparrow	\uparrow	\uparrow	\downarrow	\uparrow	\downarrow

5.3 Future perspectives

Although our results allowed to go one step further in understanding if/how D1- and D2-neurons within the NAc encode CS-US associations, additional studies are still necessary to answer some questions raised during the course of the work: 1) what is the relationship between neuronal inhibition and c-fos expression?; 2) Is the pattern of bulk activity of accumbal neurons a reflex of what is happening at the single cell level? (apparently not); 3) are D1- and D2-neurons responsive to rewarding or aversion events anatomically and functionally segregated in the NAc? These are all open questions that we will tackle in the future.

One possible strategy that could be used to investigate how neuronal inhibition is reflected in c-fos expression could be correlating neuronal recruitment/activation with c-fos expression after Pavlovian conditioning. In addition, it would also be interesting to determine the patterns of c-fos expression in the distinct neuronal sub-populations of the NAc. The use of specific markers of accumbal neurons and c-fos could allow elucidate if genetically-distinct neurons within the NAc are similarly or differentially recruited for appropriate behavioral performance. Finally, it would also be relevant to assess neuronal recruitment, through c-fos expression, in mice exposed to Pavlovian aversive conditioning (negative cue-outcome association) and to compare with patterns of expression in mice exposed to Pavlovian conditioning (positive cue-outcome association).

In recent years, many methodological advances in brain imaging have been made, allowing for more accurate and clear identification of neuronal activity. In addition to the fiber photometry data, it would be very interesting to map the neuronal activity of the NAc with electrophysiological recordings in awake animals to obtain a higher temporal resolution regarding the patterns of activity of MSNs. Coupling electrophysiological recordings with Photostimulation-assisted Identification of Neuronal Populations (PINP) would enable the tagging/identification of genetically-defined neuronal populations during *in vivo* electrophysiological recordings (Lima et al., 2009).

While fiber photometry neural activity analysis is restricted to an average bulk Ca^{2+} signal across NAc, the application of *in vivo* calcium imaging using miniaturized microscopes (miniscopes) would enable to have, not only single cell resolution, but also spatial and temporal resolution. The application of this technique would allow to determine the involvement of single neurons in processing of rewarding and aversive associative learning. In continuation of this work, this technique would be a better approach since it would allow the identification of the recruitment of individual D1- and D2-neurons in precise moments of CS-US reward and aversive-cue related behaviors. Interestingly, recent preliminary data from our team, using calcium transient recordings with miniscopes, indicate that distinct D1- and D2-MSN sub-

populations respond differently to the same behavioral events (e.g.: cue, outcome), with some neurons increasing activity, while others decreased (and others did not change).

Finally, it would also be very important to define the genetic traits of neuronal ensembles of positive and negative associative learning, though, for example, the use of single-cell RNA sequencing (scRNA-seq). This tool allows genetic characterization of single cells from a wide transcriptome after obtaining mRNA from single cells, providing detailed molecular profiling of distinct cell types present in any brain region (R. Chen et al., 2021; Kolodziejczyk et al., 2015; Ziegenhain et al., 2017). Results obtained could be useful for identification of the neuronal populations involved in rewarding or aversive behaviours and for generation of new genetic tools to target/study these specific ensembles.

CHAPTER 6 – References

6. References

- Airan, R. D., Thompson, K. R., Fenno, L. E., Bernstein, H., & Deisseroth, K. (2009). Temporally precise in vivo control of intracellular signalling. *Nature*, *458*(7241), 1025–1029. <https://doi.org/10.1038/nature07926>
- Akam, T., & Walton, M. E. (2019). pyPhotometry: Open source Python based hardware and software for fiber photometry data acquisition. *Scientific Reports*, *9*, 3521. <https://doi.org/10.1038/s41598-019-39724-y>
- Al-Hasani, R., Gowrishankar, R., Schmitz, G. P., Pedersen, C. E., Marcus, D. J., Shirley, S. E., Hobbs, T. E., Elerding, A. J., Renaud, S. J., Jing, M., Li, Y., Alvarez, V. A., Lemos, J. C., & Bruchas, M. R. (2021). Ventral tegmental area GABAergic inhibition of cholinergic interneurons in the ventral nucleus accumbens shell promotes reward reinforcement. *Nature Neuroscience*, *24*(10), 1414–1428. <https://doi.org/10.1038/s41593-021-00898-2>
- Al-Hasani, R., McCall, J. G., Shin, G., Gomez, A. M., Schmitz, G. P., Bernardi, J. M., Pyo, C.-O., Park, S. I., Marcinkiewicz, C. M., Crowley, N. A., Krashes, M. J., Lowell, B. B., Kash, T. L., Rogers, J. A., & Bruchas, M. R. (2015). Distinct Subpopulations of Nucleus Accumbens Dynorphin Neurons Drive Aversion and Reward. *Neuron*, *87*(5), 1063–1077. <https://doi.org/10.1016/j.neuron.2015.08.019>
- Ambroggi, F., Ghazizadeh, A., Nicola, S. M., & Fields, H. L. (2011). Roles of Nucleus Accumbens Core and Shell in Incentive-Cue Responding and Behavioral Inhibition. *Journal of Neuroscience*, *31*(18), 6820–6830. <https://doi.org/10.1523/JNEUROSCI.6491-10.2011>
- Apicella, P., Scarnati, E., Ljungberg, T., & Schultz, W. (1992). Neuronal activity in monkey striatum related to the expectation of predictable environmental events. *Journal of Neurophysiology*, *68*(3), 945–960. <https://doi.org/10.1152/jn.1992.68.3.945>
- Balleine, B. W., & Killcross, S. (2006). Parallel incentive processing: An integrated view of amygdala function. *Trends in Neurosciences*, *29*(5), 272–279. <https://doi.org/10.1016/j.tins.2006.03.002>
- Beier, K. T., Steinberg, E. E., DeLoach, K. E., Xie, S., Miyamichi, K., Schwarz, L., Gao, X. J., Kremer, E. J., Malenka, R. C., & Luo, L. (2015). Circuit Architecture of VTA Dopamine Neurons Revealed by Systematic Input-Output Mapping. *Cell*, *162*(3), 622–634. <https://doi.org/10.1016/j.cell.2015.07.015>
- Berendse, H. W., & Groenewegen, H. J. (1990). Organization of the thalamostriatal projections in the rat, with special emphasis on the ventral striatum. *The Journal of Comparative Neurology*, *299*(2), 187–228. <https://doi.org/10.1002/cne.902990206>
- Berridge, K. C., & Kringelbach, M. L. (2015). Pleasure systems in the brain. *Neuron*, *86*(3), 646–664. <https://doi.org/10.1016/j.neuron.2015.02.018>
- Berrios, J., Stamatakis, A. M., Kantak, P. A., McElligott, Z. A., Judson, M. C., Aita, M., Rougie, M., Stuber,

- G. D., & Philpot, B. D. (2016). Loss of UBE3A from TH-expressing neurons suppresses GABA co-release and enhances VTA-NAc optical self-stimulation. *Nature Communications*, *7*, 10702. <https://doi.org/10.1038/ncomms10702>
- Bertran-Gonzalez, J., Bosch, C., Maroteaux, M., Matamales, M., Hervé, D., Valjent, E., & Girault, J.-A. (2008). Opposing patterns of signaling activation in dopamine D1 and D2 receptor-expressing striatal neurons in response to cocaine and haloperidol. *The Journal of Neuroscience: The Official Journal of the Society for Neuroscience*, *28*(22), 5671–5685. <https://doi.org/10.1523/JNEUROSCI.1039-08.2008>
- Bock, R., Shin, J. H., Kaplan, A. R., Dobi, A., Markey, E., Kramer, P. F., Gremel, C. M., Christensen, C. H., Adrover, M. F., & Alvarez, V. A. (2013). Strengthening the accumbal indirect pathway promotes resilience to compulsive cocaine use. *Nature Neuroscience*, *16*(5), 632–638. <https://doi.org/10.1038/nn.3369>
- Bowman, E. M., Aigner, T. G., & Richmond, B. J. (1996). Neural signals in the monkey ventral striatum related to motivation for juice and cocaine rewards. *Journal of Neurophysiology*, *75*(3), 1061–1073. <https://doi.org/10.1152/jn.1996.75.3.1061>
- Brown, M. T. C., Tan, K. R., O'Connor, E. C., Nikonenko, I., Muller, D., & Lüscher, C. (2012). Ventral tegmental area GABA projections pause accumbal cholinergic interneurons to enhance associative learning. *Nature*, *492*(7429), 452–456. <https://doi.org/10.1038/nature11657>
- Bullitt, E. (1990). Expression of c-fos-like protein as a marker for neuronal activity following noxious stimulation in the rat. *The Journal of Comparative Neurology*, *296*(4), 517–530. <https://doi.org/10.1002/cne.902960402>
- Burgoyne, R. D. (2007). Neuronal Calcium Sensor Proteins: Generating Diversity in Neuronal Ca²⁺ Signalling. *Nature reviews. Neuroscience*, *8*(3), 182–193. <https://doi.org/10.1038/nrn2093>
- Caboche, J., Vernier, P., Rogard, M., & Besson, M. J. (1993). Haloperidol increases PPE mRNA levels in the caudal part of the nucleus accumbens in the rat. *Neuroreport*, *4*(5), 551–554. <https://doi.org/10.1097/00001756-199305000-00022>
- Calipari, E. S., Bagot, R. C., Purushothaman, I., Davidson, T. J., Yorgason, J. T., Peña, C. J., Walker, D. M., Pirpinias, S. T., Guise, K. G., Ramakrishnan, C., Deisseroth, K., & Nestler, E. J. (2016). In vivo imaging identifies temporal signature of D1 and D2 medium spiny neurons in cocaine reward. *Proceedings of the National Academy of Sciences of the United States of America*, *113*(10), 2726–2731. <https://doi.org/10.1073/pnas.1521238113>
- Carelli, R. M., & Deadwyler, S. A. (1994). A comparison of nucleus accumbens neuronal firing patterns during cocaine self-administration and water reinforcement in rats. *The Journal of Neuroscience: The*

Official Journal of the Society for Neuroscience, 14(12), 7735–7746.

Carelli, R. M., Ijames, S. G., & Crumling, A. J. (2000). Evidence that separate neural circuits in the nucleus accumbens encode cocaine versus «natural» (water and food) reward. *The Journal of Neuroscience: The Official Journal of the Society for Neuroscience*, 20(11), 4255–4266.

Carelli, R. M., & West, E. A. (2014). When a good taste turns bad: Neural mechanisms underlying the emergence of negative affect and associated natural reward devaluation by cocaine. *Neuropharmacology*, 76 Pt B, 360–369. <https://doi.org/10.1016/j.neuropharm.2013.04.025>

Carelli, R. M., & Wondolowski, J. (2003). Selective encoding of cocaine versus natural rewards by nucleus accumbens neurons is not related to chronic drug exposure. *The Journal of Neuroscience: The Official Journal of the Society for Neuroscience*, 23(35), 11214–11223.

Carlezon, W. A., & Thomas, M. J. (2009). Biological substrates of reward and aversion: A nucleus accumbens activity hypothesis. *Neuropharmacology*, 56(Suppl 1), 122–132. <https://doi.org/10.1016/j.neuropharm.2008.06.075>

Castro, D. C., Oswell, C. S., Zhang, E. T., Pedersen, C. E., Piantadosi, S. C., Rossi, M. A., Hunker, A. C., Guglin, A., Morón, J. A., Zweifel, L. S., Stuber, G. D., & Bruchas, M. R. (2021). An endogenous opioid circuit determines state-dependent reward consumption. *Nature*, 598(7882), Art. 7882. <https://doi.org/10.1038/s41586-021-04013-0>

Cerri, D. H., Saddoris, M. P., & Carelli, R. M. (2014). Nucleus accumbens core neurons encode value-independent associations necessary for sensory preconditioning. *Behavioral Neuroscience*, 128(5), 567–578. <https://doi.org/10.1037/a0037797>

Chandra, R., Lenz, J. D., Gancarz, A. M., Chaudhury, D., Schroeder, G. L., Han, M.-H., Cheer, J. F., Dietz, D. M., & Lobo, M. K. (2013). Optogenetic inhibition of D1R containing nucleus accumbens neurons alters cocaine-mediated regulation of Tiam1. *Frontiers in Molecular Neuroscience*, 6, 13. <https://doi.org/10.3389/fnmol.2013.00013>

Chen, R., Blosser, T. R., Djekidel, M. N., Hao, J., Bhattacharjee, A., Chen, W., Tuesta, L. M., Zhuang, X., & Zhang, Y. (2021). Decoding molecular and cellular heterogeneity of mouse nucleus accumbens. *Nature Neuroscience*, 24(12), 1757–1771. <https://doi.org/10.1038/s41593-021-00938-x>

Chen, T.-W., Wardill, T. J., Sun, Y., Pulver, S. R., Renninger, S. L., Baohan, A., Schreiter, E. R., Kerr, R. A., Orger, M. B., Jayaraman, V., Looger, L. L., Svoboda, K., & Kim, D. S. (2013). Ultrasensitive fluorescent proteins for imaging neuronal activity. *Nature*, 499(7458), Art. 7458. <https://doi.org/10.1038/nature12354>

Churchill, L., Cross, R. S., Pazdernik, T. L., Nelson, S. R., Zahm, D. S., Heimer, L., & Kalivas, P. W.

(1992). Patterns of glucose use after bicuculline-induced convulsions in relationship to γ -aminobutyric acid and μ -opioid receptors in the ventral pallidum—Functional markers for the ventral pallidum. *Brain Research*, *581*(1), 39–45. [https://doi.org/10.1016/0006-8993\(92\)90341-6](https://doi.org/10.1016/0006-8993(92)90341-6)

Cole, S. L., Robinson, M. J. F., & Berridge, K. C. (2018). Optogenetic self-stimulation in the nucleus accumbens: D1 reward versus D2 ambivalence. *PLoS ONE*, *13*(11), e0207694. <https://doi.org/10.1371/journal.pone.0207694>

Cooper, S., Robison, A. J., & Mazei-Robison, M. S. (2017). Reward Circuitry in Addiction. *Neurotherapeutics*, *14*(3), 687–697. <https://doi.org/10.1007/s13311-017-0525-z>

Creed, M., Ntamati, N. R., Chandra, R., Lobo, M. K., & Lüscher, C. (2016). Convergence of Reinforcing and Anhedonic Cocaine Effects in the Ventral Pallidum. *Neuron*, *92*(1), 214–226. <https://doi.org/10.1016/j.neuron.2016.09.001>

Cromwell, H. C., & Schultz, W. (2003). Effects of expectations for different reward magnitudes on neuronal activity in primate striatum. *Journal of Neurophysiology*, *89*(5), 2823–2838. <https://doi.org/10.1152/jn.01014.2002>

Cui, G., Jun, S. B., Jin, X., Pham, M. D., Vogel, S. S., Lovinger, D. M., & Costa, R. M. (2013). Concurrent activation of striatal direct and indirect pathways during action initiation. *Nature*, *494*(7436), Art. 7436. <https://doi.org/10.1038/nature11846>

Dautan, D., Huerta-Ocampo, I., Witten, I. B., Deisseroth, K., Bolam, J. P., Gerdjikov, T., & Mena-Segovia, J. (2014). A major external source of cholinergic innervation of the striatum and nucleus accumbens originates in the brainstem. *The Journal of Neuroscience: The Official Journal of the Society for Neuroscience*, *34*(13), 4509–4518. <https://doi.org/10.1523/JNEUROSCI.5071-13.2014>

Day, J. J., & Carelli, R. M. (2007). The Nucleus Accumbens and Pavlovian Reward Learning. *The Neuroscientist: a review journal bringing neurobiology, neurology and psychiatry*, *13*(2), 148–159. <https://doi.org/10.1177/1073858406295854>

Day, J. J., Jones, J. L., & Carelli, R. M. (2011). Nucleus accumbens neurons encode predicted and ongoing reward costs in rats. *The European Journal of Neuroscience*, *33*(2), 308–321. <https://doi.org/10.1111/j.1460-9568.2010.07531.x>

Day, J. J., Wheeler, R. A., Roitman, M. F., & Carelli, R. M. (2006a). Nucleus accumbens neurons encode Pavlovian approach behaviors: Evidence from an autoshaping paradigm. *European Journal of Neuroscience*, *23*(5), 1341–1351. <https://doi.org/10.1111/j.1460-9568.2006.04654.x>

Day, J. J., Wheeler, R. A., Roitman, M. F., & Carelli, R. M. (2006b). Nucleus accumbens neurons encode Pavlovian approach behaviors: Evidence from an autoshaping paradigm. *The European Journal of*

Neuroscience, 23(5), 1341–1351. <https://doi.org/10.1111/j.1460-9568.2006.04654.x>

de Jong, J. W., Afjei, S. A., Pollak Dorocic, I., Peck, J. R., Liu, C., Kim, C. K., Tian, L., Deisseroth, K., & Lammel, S. (2019). A Neural Circuit Mechanism for Encoding Aversive Stimuli in the Mesolimbic Dopamine System. *Neuron*, 101(1), 133-151.e7. <https://doi.org/10.1016/j.neuron.2018.11.005>

Deng, Y.-P., Lei, W.-L., & Reiner, A. (2006). Differential perikaryal localization in rats of D1 and D2 dopamine receptors on striatal projection neuron types identified by retrograde labeling. *Journal of Chemical Neuroanatomy*, 32(2–4), 101–116. <https://doi.org/10.1016/j.jchemneu.2006.07.001>

Deutch, A. Y., & Cameron, D. S. (1992). Pharmacological characterization of dopamine systems in the nucleus accumbens core and shell. *Neuroscience*, 46(1), 49–56. [https://doi.org/10.1016/0306-4522\(92\)90007-o](https://doi.org/10.1016/0306-4522(92)90007-o)

Dichter, G. S., Damiano, C. A., & Allen, J. A. (2012). Reward circuitry dysfunction in psychiatric and neurodevelopmental disorders and genetic syndromes: Animal models and clinical findings. *Journal of Neurodevelopmental Disorders*, 4(1), 19. <https://doi.org/10.1186/1866-1955-4-19>

Figlewicz, D. P., Bennett-Jay, J. L., Kittleson, S., Sipols, A. J., & Zavosh, A. (2011). Sucrose self-administration and CNS activation in the rat. *American Journal of Physiology. Regulatory, Integrative and Comparative Physiology*, 300(4), R876-884. <https://doi.org/10.1152/ajpregu.00655.2010>

Fiorillo, C. D. (2013). Two dimensions of value: Dopamine neurons represent reward but not aversiveness. *Science (New York, N.Y.)*, 341(6145), 546–549. <https://doi.org/10.1126/science.1238699>

Flagel, S. B., Cameron, C. M., Pickup, K. N., Watson, S. J., Akil, H., & Robinson, T. E. (2011). A FOOD PREDICTIVE CUE MUST BE ATTRIBUTED WITH INCENTIVE SALIENCE FOR IT TO INDUCE c-FOS mRNA EXPRESSION IN CORTICO-STRIATAL-THALAMIC BRAIN REGIONS. *Neuroscience*, 196, 80–96. <https://doi.org/10.1016/j.neuroscience.2011.09.004>

Flagel, S. B., Clark, J. J., Robinson, T. E., Mayo, L., Czuj, A., Willuhn, I., Akers, C. A., Clinton, S. M., Phillips, P. E. M., & Akil, H. (2011). A selective role for dopamine in stimulus–reward learning. *Nature*, 469(7328), Art. 7328. <https://doi.org/10.1038/nature09588>

Francis, T. C., Yano, H., Demarest, T. G., Shen, H., & Bonci, A. (2019). High-Frequency Activation of Nucleus Accumbens D1-MSNs Drives Excitatory Potentiation on D2-MSNs. *Neuron*, 103(3), 432-444.e3. <https://doi.org/10.1016/j.neuron.2019.05.031>

Fuller, T. A., Russchen, F. T., & Price, J. L. (1987). Sources of presumptive glutamergic/aspartergic afferents to the rat ventral striatopallidal region. *The Journal of Comparative Neurology*, 258(3), 317–338. <https://doi.org/10.1002/cne.902580302>

Galaj, E., & Ranaldi, R. (2021). Neurobiology of Reward-Related Learning. *Neuroscience and biobehavioral*

reviews, 124, 224–234. <https://doi.org/10.1016/j.neubiorev.2021.02.007>

Gale, J., Shields, D., Ishizawa, Y., & Eskandar, E. (2014). Reward and reinforcement activity in the nucleus accumbens during learning. *Frontiers in Behavioral Neuroscience*, 8. <https://www.frontiersin.org/article/10.3389/fnbeh.2014.00114>

Gangarossa, G., Espallergues, J., de Kerchove d'Exaerde, A., El Mestikawy, S., Gerfen, C. R., Hervé, D., Girault, J.-A., & Valjent, E. (2013). Distribution and compartmental organization of GABAergic medium-sized spiny neurons in the mouse nucleus accumbens. *Frontiers in Neural Circuits*, 7, 22. <https://doi.org/10.3389/fncir.2013.00022>

Gerfen, C. R. (1992). The neostriatal mosaic: Multiple levels of compartmental organization. *Trends in Neurosciences*, 15(4), 133–139. [https://doi.org/10.1016/0166-2236\(92\)90355-c](https://doi.org/10.1016/0166-2236(92)90355-c)

Gerfen, C. R., Engber, T. M., Mahan, L. C., Susel, Z., Chase, T. N., Monsma, F. J., & Sibley, D. R. (1990). D1 and D2 dopamine receptor-regulated gene expression of striatonigral and striatopallidal neurons. *Science (New York, N.Y.)*, 250(4986), 1429–1432. <https://doi.org/10.1126/science.2147780>

Gertler, T. S., Chan, C. S., & Surmeier, D. J. (2008). Dichotomous Anatomical Properties of Adult Striatal Medium Spiny Neurons. *Journal of Neuroscience*, 28(43), 10814–10824. <https://doi.org/10.1523/JNEUROSCI.2660-08.2008>

Ghitza, U. E., Fabbriatore, A. T., Prokopenko, V., Pawlak, A. P., & West, M. O. (2003). Persistent cue-evoked activity of accumbens neurons after prolonged abstinence from self-administered cocaine. *The Journal of Neuroscience: The Official Journal of the Society for Neuroscience*, 23(19), 7239–7245.

Gore, F., Schwartz, E. C., & Salzman, C. D. (2015). Manipulating neural activity in physiologically classified neurons: Triumphs and challenges. *Philosophical Transactions of the Royal Society B: Biological Sciences*, 370(1677), 20140216. <https://doi.org/10.1098/rstb.2014.0216>

Graveland, G. A., & DiFiglia, M. (1985). The frequency and distribution of medium-sized neurons with indented nuclei in the primate and rodent neostriatum. *Brain Research*, 327(1–2), 307–311. [https://doi.org/10.1016/0006-8993\(85\)91524-0](https://doi.org/10.1016/0006-8993(85)91524-0)

Grienberger, C., & Konnerth, A. (2012). Imaging Calcium in Neurons. *Neuron*, 73(5), 862–885. <https://doi.org/10.1016/j.neuron.2012.02.011>

Groenewegen, H. J., & Russchen, F. T. (1984). Organization of the efferent projections of the nucleus accumbens to pallidal, hypothalamic, and mesencephalic structures: A tracing and immunohistochemical study in the cat. *The Journal of Comparative Neurology*, 223(3), 347–367. <https://doi.org/10.1002/cne.902230303>

Haber, S. N., & Knutson, B. (2010). The Reward Circuit: Linking Primate Anatomy and Human Imaging.

- Neuropsychopharmacology*, 35(1), Art. 1. <https://doi.org/10.1038/npp.2009.129>
- Hanley, A. W., & Garland, E. L. (2019). Mindfulness training disrupts Pavlovian conditioning. *Physiology & Behavior*, 204, 151–154. <https://doi.org/10.1016/j.physbeh.2019.02.028>
- Hassani, O. K., Cromwell, H. C., & Schultz, W. (2001). Influence of expectation of different rewards on behavior-related neuronal activity in the striatum. *Journal of Neurophysiology*, 85(6), 2477–2489. <https://doi.org/10.1152/jn.2001.85.6.2477>
- Heidbreder, C. A., & Groenewegen, H. J. (2003). The medial prefrontal cortex in the rat: Evidence for a dorso-ventral distinction based upon functional and anatomical characteristics. *Neuroscience and Biobehavioral Reviews*, 27(6), 555–579. <https://doi.org/10.1016/j.neubiorev.2003.09.003>
- Heiman, M., Schaefer, A., Gong, S., Peterson, J. D., Day, M., Ramsey, K. E., Suárez-Fariñas, M., Schwarz, C., Stephan, D. A., Surmeier, D. J., Greengard, P., & Heintz, N. (2008). A translational profiling approach for the molecular characterization of CNS cell types. *Cell*, 135(4), 738–748. <https://doi.org/10.1016/j.cell.2008.10.028>
- Heimer, L., & Alheid, G. F. (1991). Piecing together the puzzle of basal forebrain anatomy. *Advances in Experimental Medicine and Biology*, 295, 1–42. https://doi.org/10.1007/978-1-4757-0145-6_1
- Hikida, T., Kimura, K., Wada, N., Funabiki, K., & Nakanishi, S. (2010). Distinct roles of synaptic transmission in direct and indirect striatal pathways to reward and aversive behavior. *Neuron*, 66(6), 896–907. <https://doi.org/10.1016/j.neuron.2010.05.011>
- Hikida, T., Morita, M., & Macpherson, T. (2016). Neural mechanisms of the nucleus accumbens circuit in reward and aversive learning. *Neuroscience Research*, 108, 1–5. <https://doi.org/10.1016/j.neures.2016.01.004>
- Hnasko, T. S., Hjelmstad, G. O., Fields, H. L., & Edwards, R. H. (2012). Ventral Tegmental Area Glutamate Neurons: Electrophysiological Properties and Projections. *Journal of Neuroscience*, 32(43), 15076–15085. <https://doi.org/10.1523/JNEUROSCI.3128-12.2012>
- Hollerman, J. R., Tremblay, L., & Schultz, W. (1998). Influence of reward expectation on behavior-related neuronal activity in primate striatum. *Journal of Neurophysiology*, 80(2), 947–963. <https://doi.org/10.1152/jn.1998.80.2.947>
- Hu, H. (2016). Reward and Aversion. *Annual Review of Neuroscience*, 39, 297–324. <https://doi.org/10.1146/annurev-neuro-070815-014106>
- Ibáñez-Sandoval, O., Xenias, H. S., Tepper, J. M., & Koós, T. (2015). Dopaminergic and cholinergic modulation of striatal tyrosine hydroxylase interneurons. *Neuropharmacology*, 95, 468–476. <https://doi.org/10.1016/j.neuropharm.2015.03.036>

- Ikemoto, S. (2007). Dopamine reward circuitry: Two projection systems from the ventral midbrain to the nucleus accumbens-olfactory tubercle complex. *Brain Research Reviews*, *56*(1), 27–78. <https://doi.org/10.1016/j.brainresrev.2007.05.004>
- Ito, R., & Hayen, A. (2011). Opposing roles of nucleus accumbens core and shell dopamine in the modulation of limbic information processing. *The Journal of Neuroscience: The Official Journal of the Society for Neuroscience*, *31*(16), 6001–6007. <https://doi.org/10.1523/JNEUROSCI.6588-10.2011>
- Jacob, A. D., Ramsaran, A. I., Mocle, A. J., Tran, L. M., Yan, C., Frankland, P. W., & Josselyn, S. A. (2018a). A Compact Head-Mounted Endoscope for In Vivo Calcium Imaging in Freely Behaving Mice. *Current Protocols in Neuroscience*, *84*(1), e51. <https://doi.org/10.1002/cpns.51>
- Jacob, A. D., Ramsaran, A. I., Mocle, A. J., Tran, L. M., Yan, C., Frankland, P. W., & Josselyn, S. A. (2018b). A Compact Head-Mounted Endoscope for In Vivo Calcium Imaging in Freely Behaving Mice. *Current Protocols in Neuroscience*, *84*(1), e51. <https://doi.org/10.1002/cpns.51>
- Kawaguchi, Y. (1997). Neostriatal cell subtypes and their functional roles. *Neuroscience Research*, *27*(1), 1–8. [https://doi.org/10.1016/s0168-0102\(96\)01134-0](https://doi.org/10.1016/s0168-0102(96)01134-0)
- Kelley, A. E., & Domesick, V. B. (1982). The distribution of the projection from the hippocampal formation to the nucleus accumbens in the rat: An anterograde- and retrograde-horseradish peroxidase study. *Neuroscience*, *7*(10), 2321–2335. [https://doi.org/10.1016/0306-4522\(82\)90198-1](https://doi.org/10.1016/0306-4522(82)90198-1)
- Kim, T. H., & Schnitzer, M. J. (2022). Fluorescence imaging of large-scale neural ensemble dynamics. *Cell*, *185*(1), 9–41. <https://doi.org/10.1016/j.cell.2021.12.007>
- Koekkoek, L. L., Masís-Vargas, A., Kool, T., Eggels, L., van der Gun, L. L., Lamuadni, K., Slomp, M., Diepenbroek, C., Kalsbeek, A., & la Fleur, S. E. (2021). Sucrose drinking mimics effects of nucleus accumbens μ -opioid receptor stimulation on fat intake and brain c-Fos-expression. *Nutritional Neuroscience*, 1–13. <https://doi.org/10.1080/1028415X.2021.1975365>
- Kolodziejczyk, A. A., Kim, J. K., Svensson, V., Marioni, J. C., & Teichmann, S. A. (2015). The Technology and Biology of Single-Cell RNA Sequencing. *Molecular Cell*, *58*(4), 610–620. <https://doi.org/10.1016/j.molcel.2015.04.005>
- Koob, G. F., & Le Moal, M. (2008). Addiction and the Brain Antireward System. *Annual Review of Psychology*, *59*(1), 29–53. <https://doi.org/10.1146/annurev.psych.59.103006.093548>
- Kravitz, A. V., Freeze, B. S., Parker, P. R. L., Kay, K., Thwin, M. T., Deisseroth, K., & Kreitzer, A. C. (2010). Regulation of parkinsonian motor behaviours by optogenetic control of basal ganglia circuitry. *Nature*, *466*(7306), 622–626. <https://doi.org/10.1038/nature09159>
- Kravitz, A. V., Moorman, D. E., Simpson, A., & Peoples, L. L. (2006). Session-long modulations of

accumbal firing during sucrose-reinforced operant behavior. *Synapse (New York, N.Y.)*, *60*(6), 420–428. <https://doi.org/10.1002/syn.20311>

Kravitz, A. V., Tye, L. D., & Kreitzer, A. C. (2012). Distinct roles for direct and indirect pathway striatal neurons in reinforcement. *Nature Neuroscience*, *15*(6), 816–818. <https://doi.org/10.1038/nn.3100>

Kreitzer, A. C. (2009). Physiology and pharmacology of striatal neurons. *Annual Review of Neuroscience*, *32*, 127–147. <https://doi.org/10.1146/annurev.neuro.051508.135422>

Kringelbach, M. L., & Berridge, K. C. (2010). The Functional Neuroanatomy of Pleasure and Happiness. *Discovery medicine*, *9*(49), 579–587.

Krukoff, T. L. (1999). C-fos Expression as a Marker of Functional Activity in the Brain. In A. A. Boulton, G. B. Baker, & A. N. Bateson (Eds.), *Cell Neurobiology Techniques* (pp. 213–230). Humana Press. <https://doi.org/10.1385/0-89603-510-7:213>

Kupchik, Y. M., Brown, R. M., Heinsbroek, J. A., Lobo, M. K., Schwartz, D. J., & Kalivas, P. W. (2015). Coding the direct/indirect pathways by D1 and D2 receptors is not valid for accumbens projections. *Nature neuroscience*, *18*(9), 1230–1232. <https://doi.org/10.1038/nn.4068>

Kutlu, M. G., Zachry, J. E., Melugin, P. R., Cajigas, S. A., Chevee, M. F., Kelley, S. J., Kutlu, B., Tian, L., Siciliano, C. A., & Calipari, E. S. (2021). Dopamine release in the nucleus accumbens core signals perceived saliency. *Current biology: CB*, *31*(21), 4748-4761.e8. <https://doi.org/10.1016/j.cub.2021.08.052>

Kutlu, M. G., Zachry, J. E., Melugin, P. R., Cajigas, S. A., Chevee, M. F., Kelly, S. J., Kutlu, B., Tian, L., Siciliano, C. A., & Calipari, E. S. (2021). Dopamine release in the nucleus accumbens core signals perceived saliency. *Current Biology: CB*, *31*(21), 4748-4761.e8. <https://doi.org/10.1016/j.cub.2021.08.052>

Lafferty, C. K., Yang, A. K., Mendoza, J. A., & Britt, J. P. (2020). Nucleus Accumbens Cell Type- and Input-Specific Suppression of Unproductive Reward Seeking. *Cell Reports*, *30*(11), 3729-3742.e3. <https://doi.org/10.1016/j.celrep.2020.02.095>

Lammel, S., Ion, D. I., Roeper, J., & Malenka, R. C. (2011). Projection-specific modulation of dopamine neuron synapses by aversive and rewarding stimuli. *Neuron*, *70*(5), 855–862. <https://doi.org/10.1016/j.neuron.2011.03.025>

Lammel, S., Lim, B. K., Ran, C., Huang, K. W., Betley, M. J., Tye, K. M., Deisseroth, K., & Malenka, R. C. (2012). Input-specific control of reward and aversion in the ventral tegmental area. *Nature*, *491*(7423), Art. 7423. <https://doi.org/10.1038/nature11527>

Lanciego, J. L., Gonzalo, N., Castle, M., Sanchez-Escobar, C., Aymerich, M. S., & Obeso, J. A. (2004).

- Thalamic innervation of striatal and subthalamic neurons projecting to the rat entopeduncular nucleus. *European Journal of Neuroscience*, *19*(5), 1267–1277. <https://doi.org/10.1111/j.1460-9568.2004.03244.x>
- Lee, J. H., Ribeiro, E. A., Kim, J., Ko, B., Kronman, H., Jeong, Y. H., Kim, J. K., Janak, P. H., Nestler, E. J., Koo, J. W., & Kim, J.-H. (2020). Dopaminergic Regulation of Nucleus Accumbens Cholinergic Interneurons Demarcates Susceptibility to Cocaine Addiction. *Biological Psychiatry*, *88*(10), 746–757. <https://doi.org/10.1016/j.biopsych.2020.05.003>
- Lewis, R. G., Florio, E., Punzo, D., & Borrelli, E. (2021). The Brain's Reward System in Health and Disease. *Advances in experimental medicine and biology*, *1344*, 57–69. https://doi.org/10.1007/978-3-030-81147-1_4
- Li, Y., Liu, Z., Guo, Q., & Luo, M. (2019). Long-term Fiber Photometry for Neuroscience Studies. *Neuroscience Bulletin*, *35*(3), 425–433. <https://doi.org/10.1007/s12264-019-00379-4>
- Lima, S. Q., Hromádka, T., Znamenskiy, P., & Zador, A. M. (2009). PINP: A New Method of Tagging Neuronal Populations for Identification during In Vivo Electrophysiological Recording. *PLoS ONE*, *4*(7), e6099. <https://doi.org/10.1371/journal.pone.0006099>
- Lobo, M. K., Covington, H. E., Chaudhury, D., Friedman, A. K., Sun, H., Damez-Werno, D., Dietz, D. M., Zaman, S., Koo, J. W., Kennedy, P. J., Mouzon, E., Mogri, M., Neve, R. L., Deisseroth, K., Han, M.-H., & Nestler, E. J. (2010). Cell type-specific loss of BDNF signaling mimics optogenetic control of cocaine reward. *Science (New York, N.Y.)*, *330*(6002), 385–390. <https://doi.org/10.1126/science.1188472>
- Lobo, M. K., Karsten, S. L., Gray, M., Geschwind, D. H., & Yang, X. W. (2006). FACS-array profiling of striatal projection neuron subtypes in juvenile and adult mouse brains. *Nature Neuroscience*, *9*(3), 443–452. <https://doi.org/10.1038/nn1654>
- Lu, X. Y., Ghasemzadeh, M. B., & Kalivas, P. W. (1998). Expression of D1 receptor, D2 receptor, substance P and enkephalin messenger RNAs in the neurons projecting from the nucleus accumbens. *Neuroscience*, *82*(3), 767–780. [https://doi.org/10.1016/s0306-4522\(97\)00327-8](https://doi.org/10.1016/s0306-4522(97)00327-8)
- Lv, X.-F., Xu, Y., Han, J.-S., & Cui, C.-L. (2011). Expression of activity-regulated cytoskeleton-associated protein (Arc/Arg3.1) in the nucleus accumbens is critical for the acquisition, expression and reinstatement of morphine-induced conditioned place preference. *Behavioural Brain Research*, *223*(1), 182–191. <https://doi.org/10.1016/j.bbr.2011.04.029>
- McDonald, A. J. (1991). Organization of amygdaloid projections to the prefrontal cortex and associated striatum in the rat. *Neuroscience*, *44*(1), 1–14. [https://doi.org/10.1016/0306-4522\(91\)90247-I](https://doi.org/10.1016/0306-4522(91)90247-I)
- McFarland, K., Lapish, C. C., & Kalivas, P. W. (2003). Prefrontal glutamate release into the core of the

nucleus accumbens mediates cocaine-induced reinstatement of drug-seeking behavior. *The Journal of Neuroscience: The Official Journal of the Society for Neuroscience*, *23*(8), 3531–3537.

McGeorge, A. J., & Faull, R. L. (1989). The organization of the projection from the cerebral cortex to the striatum in the rat. *Neuroscience*, *29*(3), 503–537. [https://doi.org/10.1016/0306-4522\(89\)90128-0](https://doi.org/10.1016/0306-4522(89)90128-0)

Mogenson, G. J., Swanson, L. W., & Wu, M. (1983). Neural projections from nucleus accumbens to globus pallidus, substantia innominata, and lateral preoptic-lateral hypothalamic area: An anatomical and electrophysiological investigation in the rat. *The Journal of Neuroscience: The Official Journal of the Society for Neuroscience*, *3*(1), 189–202.

Mogenson, G., Jones, D., & Yim, C. (1980). From motivation to action: Functional interface between the limbic system and the motor system. *Progress in Neurobiology*, *14*(2–3), 69–97. [https://doi.org/10.1016/0301-0082\(80\)90018-0](https://doi.org/10.1016/0301-0082(80)90018-0)

Mondoloni, S., Mameli, M., & Congiu, M. (2022). Reward and aversion encoding in the lateral habenula for innate and learned behaviours. *Translational Psychiatry*, *12*, 3. <https://doi.org/10.1038/s41398-021-01774-0>

Morgane, P. J., Galler, J. R., & Mokler, D. J. (2005). A review of systems and networks of the limbic forebrain/limbic midbrain. *Progress in Neurobiology*, *75*(2), 143–160. <https://doi.org/10.1016/j.pneurobio.2005.01.001>

Namburi, P., Al-Hasani, R., Calhoun, G. G., Bruchas, M. R., & Tye, K. M. (2016). Architectural Representation of Valence in the Limbic System. *Neuropsychopharmacology*, *41*(7), 1697–1715. <https://doi.org/10.1038/npp.2015.358>

Namburi, P., Beyeler, A., Yorozu, S., Calhoun, G. G., Halbert, S. A., Wichmann, R., Holden, S. S., Mertens, K. L., Anahtar, M., Felix-Ortiz, A. C., Wickersham, I. R., Gray, J. M., & Tye, K. M. (2015). A circuit mechanism for differentiating positive and negative associations. *Nature*, *520*(7549), Art. 7549. <https://doi.org/10.1038/nature14366>

Namvar, P., Zarrabian, S., Nazari-Serenjeh, F., Sadeghzadeh, F., & Haghparast, A. (2019). Involvement of D1- and D2-like dopamine receptors within the rat nucleus accumbens in the maintenance of morphine rewarding properties in the rats. *Behavioral Neuroscience*, *133*(6), 556–562. <https://doi.org/10.1037/bne0000336>

Natsubori, A., Tsutsui-Kimura, I., Nishida, H., Bouchekioua, Y., Sekiya, H., Uchigashima, M., Watanabe, M., de Kerchove d'Exaerde, A., Mimura, M., Takata, N., & Tanaka, K. F. (2017). Ventrolateral Striatal Medium Spiny Neurons Positively Regulate Food-Incentive, Goal-Directed Behavior Independently of D1 and D2 Selectivity. *The Journal of Neuroscience: The Official Journal of the Society for Neuroscience*,

37(10), 2723–2733. <https://doi.org/10.1523/JNEUROSCI.3377-16.2017>

Nauta, W. J., Smith, G. P., Faull, R. L., & Domesick, V. B. (1978). Efferent connections and nigral afferents of the nucleus accumbens septi in the rat. *Neuroscience*, 3(4–5), 385–401. [https://doi.org/10.1016/0306-4522\(78\)90041-6](https://doi.org/10.1016/0306-4522(78)90041-6)

Nicola, S. M. (2007). The nucleus accumbens as part of a basal ganglia action selection circuit. *Psychopharmacology*, 191(3), 521–550. <https://doi.org/10.1007/s00213-006-0510-4>

Nicola, S. M., Yun, I. A., Wakabayashi, K. T., & Fields, H. L. (2004a). Cue-evoked firing of nucleus accumbens neurons encodes motivational significance during a discriminative stimulus task. *Journal of Neurophysiology*, 91(4), 1840–1865. <https://doi.org/10.1152/jn.00657.2003>

Nicola, S. M., Yun, I. A., Wakabayashi, K. T., & Fields, H. L. (2004b). Firing of nucleus accumbens neurons during the consummatory phase of a discriminative stimulus task depends on previous reward predictive cues. *Journal of Neurophysiology*, 91(4), 1866–1882. <https://doi.org/10.1152/jn.00658.2003>

Nicola, S. M., Yun, I. A., Wakabayashi, K. T., & Fields, H. L. (2004c). Firing of nucleus accumbens neurons during the consummatory phase of a discriminative stimulus task depends on previous reward predictive cues. *Journal of Neurophysiology*, 91(4), 1866–1882. <https://doi.org/10.1152/jn.00658.2003>

Nieh, E. H., Kim, S.-Y., Namburi, P., & Tye, K. M. (2013). Optogenetic dissection of neural circuits underlying emotional valence and motivated behaviors. *Brain research*, 1511, 73–92. <https://doi.org/10.1016/j.brainres.2012.11.001>

Noe, E., Bonneau, N., Fournier, M.-L., Caillé, S., Cador, M., & Le Moine, C. (2019). Arc reactivity in accumbens nucleus, amygdala and hippocampus differentiates cue over context responses during reactivation of opiate withdrawal memory. *Neurobiology of Learning and Memory*, 159, 24–35. <https://doi.org/10.1016/j.nlm.2019.02.007>

Noye Tuplin, E. W., Lightfoot, S. H. M., & Holahan, M. R. (2018). Comparison of the Time-Dependent Changes in Immediate Early Gene Labeling and Spine Density Following Abstinence From Contingent or Non-contingent Chocolate Pellet Delivery. *Frontiers in Behavioral Neuroscience*, 12, 144. <https://doi.org/10.3389/fnbeh.2018.00144>

Oades, R. D., & Halliday, G. M. (1987). Ventral tegmental (A10) system: Neurobiology. 1. Anatomy and connectivity. *Brain Research*, 434(2), 117–165. [https://doi.org/10.1016/0165-0173\(87\)90011-7](https://doi.org/10.1016/0165-0173(87)90011-7)

Olds, J., & Milner, P. (1954). Positive reinforcement produced by electrical stimulation of septal area and other regions of rat brain. *Journal of Comparative and Physiological Psychology*, 47(6), 419–427. <https://doi.org/10.1037/h0058775>

- O'Neal, T. J., Bernstein, M. X., MacDougall, D. J., & Ferguson, S. M. (2022). A Conditioned Place Preference for Heroin Is Signaled by Increased Dopamine and Direct Pathway Activity and Decreased Indirect Pathway Activity in the Nucleus Accumbens. *The Journal of Neuroscience: The Official Journal of the Society for Neuroscience*, *42*(10), 2011–2024. <https://doi.org/10.1523/JNEUROSCI.1451-21.2021>
- O'Neill, P.-K., Gore, F., & Salzman, C. D. (2018). Basolateral amygdala circuitry in positive and negative valence. *Current opinion in neurobiology*, *49*, 175–183. <https://doi.org/10.1016/j.conb.2018.02.012>
- Owesson-White, C., Belle, A. M., Herr, N. R., Peele, J. L., Gowrishankar, P., Carelli, R. M., & Wightman, R. M. (2016). Cue-Evoked Dopamine Release Rapidly Modulates D2 Neurons in the Nucleus Accumbens During Motivated Behavior. *The Journal of Neuroscience: The Official Journal of the Society for Neuroscience*, *36*(22), 6011–6021. <https://doi.org/10.1523/JNEUROSCI.0393-16.2016>
- Pakhotin, P., & Bracci, E. (2007). Cholinergic Interneurons Control the Excitatory Input to the Striatum. *The Journal of Neuroscience*, *27*(2), 391–400. <https://doi.org/10.1523/JNEUROSCI.3709-06.2007>
- Patel, S., Roberts, J., Moorman, J., & Reavill, C. (1995). Localization of serotonin-4 receptors in the striatonigral pathway in rat brain. *Neuroscience*, *69*(4), 1159–1167. [https://doi.org/10.1016/0306-4522\(95\)00314-9](https://doi.org/10.1016/0306-4522(95)00314-9)
- Patriarchi, T., Cho, J. R., Merten, K., Howe, M. W., Marley, A., Xiong, W.-H., Folk, R. W., Broussard, G. J., Liang, R., Jang, M. J., Zhong, H., Dombeck, D., von Zastrow, M., Nimmerjahn, A., Gradinaru, V., Williams, J. T., & Tian, L. (2018a). Ultrafast neuronal imaging of dopamine dynamics with designed genetically encoded sensors. *Science (New York, N.Y.)*, *360*(6396), eaat4422. <https://doi.org/10.1126/science.aat4422>
- Patriarchi, T., Cho, J. R., Merten, K., Howe, M. W., Marley, A., Xiong, W.-H., Folk, R. W., Broussard, G. J., Liang, R., Jang, M. J., Zhong, H., Dombeck, D., von Zastrow, M., Nimmerjahn, A., Gradinaru, V., Williams, J. T., & Tian, L. (2018b). Ultrafast neuronal imaging of dopamine dynamics with designed genetically encoded sensors. *Science (New York, N.Y.)*, *360*(6396), eaat4422. <https://doi.org/10.1126/science.aat4422>
- Pavlov (1927), P. I. (2010). Conditioned reflexes: An investigation of the physiological activity of the cerebral cortex. *Annals of Neurosciences*, *17*(3), 136–141. <https://doi.org/10.5214/ans.0972-7531.1017309>
- Paxinos, G., & Franklin, K. B. J. (2001). *The Mouse Brain in Stereotaxic Coordinates, Second Edition* (2nd edition). Academic Press.
- Pearce, J. M., & Hall, G. (1980). A model for Pavlovian learning: Variations in the effectiveness of

conditioned but not of unconditioned stimuli. *Psychological Review*, 87(6), 532–552. <https://doi.org/10.1037/0033-295X.87.6.532>

Pennartz, C. M., Groenewegen, H. J., & Lopes da Silva, F. H. (1994). The nucleus accumbens as a complex of functionally distinct neuronal ensembles: An integration of behavioural, electrophysiological and anatomical data. *Progress in Neurobiology*, 42(6), 719–761. [https://doi.org/10.1016/0301-0082\(94\)90025-6](https://doi.org/10.1016/0301-0082(94)90025-6)

Perreault, M., Hasbi, A., O’Dowd, B., & George, S. (2011). The Dopamine D1–D2 Receptor Heteromer in Striatal Medium Spiny Neurons: Evidence for a Third Distinct Neuronal Pathway in Basal Ganglia. *Frontiers in Neuroanatomy*, 5. <https://www.frontiersin.org/article/10.3389/fnana.2011.00031>

Perrin-Terrin, A.-S., Jeton, F., Pichon, A., Frugière, A., Richalet, J.-P., Bodineau, L., & Voituron, N. (2016). The c-FOS Protein Immunohistological Detection: A Useful Tool As a Marker of Central Pathways Involved in Specific Physiological Responses In Vivo and Ex Vivo. *Journal of Visualized Experiments : JoVE*, 110, 53613. <https://doi.org/10.3791/53613>

Phillipson, O. T., & Griffiths, A. C. (1985). The topographic order of inputs to nucleus accumbens in the rat. *Neuroscience*, 16(2), 275–296. [https://doi.org/10.1016/0306-4522\(85\)90002-8](https://doi.org/10.1016/0306-4522(85)90002-8)

Poulin, J.-F., Caronia, G., Hofer, C., Cui, Q., Helm, B., Ramakrishnan, C., Chan, C. S., Dombeck, D., Deisseroth, K., & Awatramani, R. (2018). Mapping projections of molecularly defined dopamine neuron subtypes using intersectional genetic approaches. *Nature neuroscience*, 21(9), 1260–1271. <https://doi.org/10.1038/s41593-018-0203-4>

Prensa, L., Richard, S., & Parent, A. (2003). Chemical anatomy of the human ventral striatum and adjacent basal forebrain structures. *The Journal of Comparative Neurology*, 460(3), 345–367. <https://doi.org/10.1002/cne.10627>

Qi, J., Zhang, S., Wang, H.-L., Barker, D. J., Miranda-Barrientos, J., & Morales, M. (2016). VTA glutamatergic inputs to nucleus accumbens drive aversion by acting on GABAergic interneurons. *Nature Neuroscience*, 19(5), 725–733. <https://doi.org/10.1038/nn.4281>

Quiroz, C., Orrú, M., Rea, W., Ciudad-Roberts, A., Yepes, G., Britt, J. P., & Ferré, S. (2016). Local Control of Extracellular Dopamine Levels in the Medial Nucleus Accumbens by a Glutamatergic Projection from the Infralimbic Cortex. *The Journal of Neuroscience: The Official Journal of the Society for Neuroscience*, 36(3), 851–859. <https://doi.org/10.1523/JNEUROSCI.2850-15.2016>

Resendez, S. L., & Stuber, G. D. (2015). In vivo Calcium Imaging to Illuminate Neurocircuit Activity Dynamics Underlying Naturalistic Behavior. *Neuropsychopharmacology*, 40(1), Art. 1. <https://doi.org/10.1038/npp.2014.206>

- Robbins, T. W., Ersche, K. D., & Everitt, B. J. (2008). Drug addiction and the memory systems of the brain. *Annals of the New York Academy of Sciences*, *1141*, 1–21. <https://doi.org/10.1196/annals.1441.020>
- Rodd-Henricks, Z. A., McKinzie, D. L., Li, T.-K., Murphy, J. M., & McBride, W. J. (2002). Cocaine is self-administered into the shell but not the core of the nucleus accumbens of Wistar rats. *The Journal of Pharmacology and Experimental Therapeutics*, *303*(3), 1216–1226. <https://doi.org/10.1124/jpet.102.038950>
- Rogard, M., Caboche, J., Julien, J. F., & Besson, M. J. (1993). The rat nucleus accumbens: Two levels of complexity in the distribution of glutamic acid decarboxylase (67 kDa) and preproenkephalin messenger RNA. *Neuroscience Letters*, *155*(1), 81–86. [https://doi.org/10.1016/0304-3940\(93\)90678-e](https://doi.org/10.1016/0304-3940(93)90678-e)
- Roitman, M. F., Wheeler, R. A., & Carelli, R. M. (2005). Nucleus Accumbens Neurons Are Innately Tuned for Rewarding and Aversive Taste Stimuli, Encode Their Predictors, and Are Linked to Motor Output. *Neuron*, *45*(4), 587–597. <https://doi.org/10.1016/j.neuron.2004.12.055>
- Roitman, M. F., Wheeler, R. A., Tiesinga, P. H. E., Roitman, J. D., & Carelli, R. M. (2010). Hedonic and nucleus accumbens neural responses to a natural reward are regulated by aversive conditioning. *Learning & Memory*, *17*(11), 539–546. <https://doi.org/10.1101/lm.1869710>
- Russell, J. T. (2011). Imaging calcium signals in vivo: A powerful tool in physiology and pharmacology. *British Journal of Pharmacology*, *163*(8), 1605–1625. <https://doi.org/10.1111/j.1476-5381.2010.00988.x>
- Russo, S. J., & Nestler, E. J. (2013). The Brain Reward Circuitry in Mood Disorders. *Nature reviews. Neuroscience*, *14*(9), 10.1038/nrn3381. <https://doi.org/10.1038/nrn3381>
- Schall, T. A., Wright, W. J., & Dong, Y. (2021). Nucleus accumbens fast-spiking interneurons in motivational and addictive behaviors. *Molecular Psychiatry*, *26*(1), 234–246. <https://doi.org/10.1038/s41380-020-0683-y>
- Schindelin, J., Arganda-Carreras, I., Frise, E., Kaynig, V., Longair, M., Pietzsch, T., Preibisch, S., Rueden, C., Saalfeld, S., Schmid, B., Tinevez, J.-Y., White, D. J., Hartenstein, V., Eliceiri, K., Tomancak, P., & Cardona, A. (2012). Fiji: An open-source platform for biological-image analysis. *Nature Methods*, *9*(7), 676–682. <https://doi.org/10.1038/nmeth.2019>
- Schultz, W. (1998). Predictive reward signal of dopamine neurons. *Journal of Neurophysiology*, *80*(1), 1–27. <https://doi.org/10.1152/jn.1998.80.1.1>
- Schultz, W. (2000). Multiple reward signals in the brain. *Nature Reviews Neuroscience*, *1*(3), Art. 3. <https://doi.org/10.1038/35044563>

Sellings, L. H. L., & Clarke, P. B. S. (2003). Segregation of amphetamine reward and locomotor stimulation between nucleus accumbens medial shell and core. *The Journal of Neuroscience: The Official Journal of the Society for Neuroscience*, *23*(15), 6295–6303.

Sesack, S. R., & Grace, A. A. (2010). Cortico-Basal Ganglia Reward Network: Microcircuitry. *Neuropsychopharmacology*, *35*(1), 27–47. <https://doi.org/10.1038/npp.2009.93>

Setlow, B. (1997). The nucleus accumbens and learning and memory. *Journal of Neuroscience Research*, *49*(5), 515–521. [https://doi.org/10.1002/\(SICI\)1097-4547\(19970901\)49:5<515::AID-JNR1>3.0.CO;2-E](https://doi.org/10.1002/(SICI)1097-4547(19970901)49:5<515::AID-JNR1>3.0.CO;2-E)

Setlow, B., Schoenbaum, G., & Gallagher, M. (2003). Neural Encoding in Ventral Striatum during Olfactory Discrimination Learning. *Neuron*, *38*(4), 625–636. [https://doi.org/10.1016/S0896-6273\(03\)00264-2](https://doi.org/10.1016/S0896-6273(03)00264-2)

Sherathiya, V. N., Schaid, M. D., Seiler, J. L., Lopez, G. C., & Lerner, T. N. (2021). GuPPy, a Python toolbox for the analysis of fiber photometry data. *Scientific Reports*, *11*, 24212. <https://doi.org/10.1038/s41598-021-03626-9>

Šimić, G., Tkalčić, M., Vukić, V., Mulc, D., Španić, E., Šagud, M., Olucha-Bordonau, F. E., Vukšić, M., & R. Hof, P. (2021). Understanding Emotions: Origins and Roles of the Amygdala. *Biomolecules*, *11*(6), 823. <https://doi.org/10.3390/biom11060823>

Soares-Cunha, C., Coimbra, B., David-Pereira, A., Borges, S., Pinto, L., Costa, P., Sousa, N., & Rodrigues, A. J. (2016). Activation of D2 dopamine receptor-expressing neurons in the nucleus accumbens increases motivation. *Nature Communications*, *7*, 11829. <https://doi.org/10.1038/ncomms11829>

Soares-Cunha, C., Coimbra, B., Domingues, A. V., Vasconcelos, N., Sousa, N., & Rodrigues, A. J. (2018). Nucleus Accumbens Microcircuit Underlying D2-MSN-Driven Increase in Motivation. *eNeuro*, *5*(2), ENEURO.0386-18.2018. <https://doi.org/10.1523/ENEURO.0386-18.2018>

Soares-Cunha, C., Coimbra, B., Sousa, N., & Rodrigues, A. J. (2016). Reappraising striatal D1- and D2-neurons in reward and aversion. *Neuroscience and Biobehavioral Reviews*, *68*, 370–386. <https://doi.org/10.1016/j.neubiorev.2016.05.021>

Soares-Cunha, C., de Vasconcelos, N. A. P., Coimbra, B., Domingues, A. V., Silva, J. M., Loureiro-Campos, E., Gaspar, R., Sotiropoulos, I., Sousa, N., & Rodrigues, A. J. (2020). Nucleus accumbens medium spiny neurons subtypes signal both reward and aversion. *Molecular Psychiatry*, *25*(12), Art. 12. <https://doi.org/10.1038/s41380-019-0484-3>

Soares-Cunha, C., Domingues, A. V., Correia, R., Coimbra, B., Vieitas-Gaspar, N., de Vasconcelos, N. A. P., Pinto, L., Sousa, N., & Rodrigues, A. J. (2022). Distinct role of nucleus accumbens D2-MSN projections to ventral pallidum in different phases of motivated behavior. *Cell Reports*, *38*(7), 110380.

<https://doi.org/10.1016/j.celrep.2022.110380>

Song, S. S., Kang, B. J., Wen, L., Lee, H. J., Sim, H., Kim, T. H., Yoon, S., Yoon, B.-J., Augustine, G. J., & Baik, J.-H. (2014). Optogenetics reveals a role for accumbal medium spiny neurons expressing dopamine D2 receptors in cocaine-induced behavioral sensitization. *Frontiers in Behavioral Neuroscience*, *8*, 336. <https://doi.org/10.3389/fnbeh.2014.00336>

Steinberg, E. E., Boivin, J. R., Saunders, B. T., Witten, I. B., Deisseroth, K., & Janak, P. H. (2014). Positive Reinforcement Mediated by Midbrain Dopamine Neurons Requires D1 and D2 Receptor Activation in the Nucleus Accumbens. *PLOS ONE*, *9*(4), e94771. <https://doi.org/10.1371/journal.pone.0094771>

Strong, C. E., Hagarty, D. P., Brea Guerrero, A., Schoepfer, K. J., Cajuste, S. M., & Kabbaj, M. (2020). Chemogenetic selective manipulation of nucleus accumbens medium spiny neurons bidirectionally controls alcohol intake in male and female rats. *Scientific Reports*, *10*(1), Art. 1. <https://doi.org/10.1038/s41598-020-76183-2>

Stuber, G. D., Sparta, D. R., Stamatakis, A. M., van Leeuwen, W. A., Hardjoprajitno, J. E., Cho, S., Tye, K. M., Kempadoo, K. A., Zhang, F., Deisseroth, K., & Bonci, A. (2011). Excitatory transmission from the amygdala to nucleus accumbens facilitates reward seeking. *Nature*, *475*(7356), 377–380. <https://doi.org/10.1038/nature10194>

Swanson, L. W. (1982). The projections of the ventral tegmental area and adjacent regions: A combined fluorescent retrograde tracer and immunofluorescence study in the rat. *Brain Research Bulletin*, *9*(1–6), 321–353. [https://doi.org/10.1016/0361-9230\(82\)90145-9](https://doi.org/10.1016/0361-9230(82)90145-9)

Tai, L.-H., Lee, A. M., Benavidez, N., Bonci, A., & Wilbrecht, L. (2012). Transient stimulation of distinct subpopulations of striatal neurons mimics changes in action value. *Nature Neuroscience*, *15*(9), 1281–1289. <https://doi.org/10.1038/nn.3188>

Tecuapetla, F., Patel, J. C., Xenias, H., English, D., Tadros, I., Shah, F., Berlin, J., Deisseroth, K., Rice, M. E., Tepper, J. M., & Koos, T. (2010). Glutamatergic signaling by mesolimbic dopamine neurons in the nucleus accumbens. *The Journal of Neuroscience*, *30*(20), 7105–7110. <https://doi.org/10.1523/jneurosci.0265-10.2010>

Tepper, J. M., & Bolam, J. P. (2004). Functional diversity and specificity of neostriatal interneurons. *Current Opinion in Neurobiology*, *14*(6), 685–692. <https://doi.org/10.1016/j.conb.2004.10.003>

Threlfell, S., Lalic, T., Platt, N. J., Jennings, K. A., Deisseroth, K., & Cragg, S. J. (2012). Striatal dopamine release is triggered by synchronized activity in cholinergic interneurons. *Neuron*, *75*(1), 58–64. <https://doi.org/10.1016/j.neuron.2012.04.038>

Tindell, A. J., Smith, K. S., Peciña, S., Berridge, K. C., & Aldridge, J. W. (2006). Ventral pallidum firing

codes hedonic reward: When a bad taste turns good. *Journal of Neurophysiology*, *96*(5), 2399–2409. <https://doi.org/10.1152/jn.00576.2006>

Tritsch, N. X., Ding, J. B., & Sabatini, B. L. (2012). Dopaminergic neurons inhibit striatal output through non-canonical release of GABA. *Nature*, *490*(7419), 262–266. <https://doi.org/10.1038/nature11466>

Tritsch, N. X., Oh, W.-J., Gu, C., & Sabatini, B. L. (2014). Midbrain dopamine neurons sustain inhibitory transmission using plasma membrane uptake of GABA, not synthesis. *eLife*, *3*, e01936. <https://doi.org/10.7554/eLife.01936>

Valjent, E., Bertran-Gonzalez, J., Hervé, D., Fisone, G., & Girault, J.-A. (2009). Looking BAC at striatal signaling: Cell-specific analysis in new transgenic mice. *Trends in Neurosciences*, *32*(10), 538–547. <https://doi.org/10.1016/j.tins.2009.06.005>

Van Bockstaele, E. J., & Pickel, V. M. (1995). GABA-containing neurons in the ventral tegmental area project to the nucleus accumbens in rat brain. *Brain Research*, *682*(1–2), 215–221. [https://doi.org/10.1016/0006-8993\(95\)00334-m](https://doi.org/10.1016/0006-8993(95)00334-m)

Vicente, A. M., Galvão-Ferreira, P., Tecuapetla, F., & Costa, R. M. (2016). Direct and indirect dorsolateral striatum pathways reinforce different action strategies. *Current Biology: CB*, *26*(7), R267-269. <https://doi.org/10.1016/j.cub.2016.02.036>

Volman, S. F., Lammel, S., Margolis, E. B., Kim, Y., Richard, J. M., Roitman, M. F., & Lobo, M. K. (2013). New insights into the specificity and plasticity of reward and aversion encoding in the mesolimbic system. *The Journal of Neuroscience*, *33*(45), 17569–17576. <https://doi.org/10.1523/JNEUROSCI.3250-13.2013>

Voorn, P., Gerfen, C. R., & Groenewegen, H. J. (1989). Compartmental organization of the ventral striatum of the rat: Immunohistochemical distribution of enkephalin, substance P, dopamine, and calcium-binding protein. *The Journal of Comparative Neurology*, *289*(2), 189–201. <https://doi.org/10.1002/cne.902890202>

Wan, X., & Peoples, L. L. (2006). Firing Patterns of Accumbal Neurons During a Pavlovian-Conditioned Approach Task. *Journal of Neurophysiology*, *96*(2), 652–660. <https://doi.org/10.1152/jn.00068.2006>

Wang, H. B., Laverghetta, A. V., Foehring, R., Deng, Y. P., Sun, Z., Yamamoto, K., Lei, W. L., Jiao, Y., & Reiner, A. (2006). Single-cell RT-PCR, in situ hybridization histochemical, and immunohistochemical studies of substance P and enkephalin co-occurrence in striatal projection neurons in rats. *Journal of Chemical Neuroanatomy*, *31*(3), 178–199. <https://doi.org/10.1016/j.jchemneu.2006.01.003>

Wang, H.-B., Deng, Y.-P., & Reiner, A. (2007). In situ Hybridization Histochemical and Immunohistochemical Evidence that Striatal Projection Neurons Co-containing Substance P and

Enkephalin are Overrepresented in the Striosomal Compartment of Striatum in Rats. *Neuroscience letters*, 425(3), 195–199. <https://doi.org/10.1016/j.neulet.2007.08.033>

Wang, J.-J., Yao, W.-Q., Chen, Y.-J., Ma, L., & Tao, Y.-Z. (2014). [Neurons in NAc core and BLA are activated during cocaine context-associated reward memory retrieval in mice]. *Sheng Li Xue Bao: [Acta Physiologica Sinica]*, 66(5), 545–558.

Wheeler, R. A., & Carelli, R. M. (2009). Dissecting motivational circuitry to understand substance abuse. *Neuropharmacology*, 56 Suppl 1, 149–159. <https://doi.org/10.1016/j.neuropharm.2008.06.028>

Wheeler, R. A., Twining, R. C., Jones, J. L., Slater, J. M., Grigson, P. S., & Carelli, R. M. (2008). Behavioral and electrophysiological indices of negative affect predict cocaine self-administration. *Neuron*, 57(5), 774–785. <https://doi.org/10.1016/j.neuron.2008.01.024>

Williams, D. J., Crossman, A. R., & Slater, P. (1977). The efferent projections of the nucleus accumbens in the rat. *Brain Research*, 130(2), 217–227. [https://doi.org/10.1016/0006-8993\(77\)90271-2](https://doi.org/10.1016/0006-8993(77)90271-2)

Wilson, D. I. G., & Bowman, E. M. (2004). Nucleus accumbens neurons in the rat exhibit differential activity to conditioned reinforcers and primary reinforcers within a second-order schedule of saccharin reinforcement. *The European Journal of Neuroscience*, 20(10), 2777–2788. <https://doi.org/10.1111/j.1460-9568.2004.03747.x>

Wise, R. A. (2002). Brain reward circuitry: Insights from unsensed incentives. *Neuron*, 36(2), 229–240. [https://doi.org/10.1016/s0896-6273\(02\)00965-0](https://doi.org/10.1016/s0896-6273(02)00965-0)

Xia, X., Fan, L., Cheng, C., Cheng, L., Cao, L., He, B., Chen, J., Li, H., & Jiang, T. (2020). Mapping Connectional Differences between Humans and Macaques in the Nucleus Accumbens Shell-Core Architecture. *bioRxiv*. <https://doi.org/10.1101/2020.06.12.147546>

Xu, L., Nan, J., & Lan, Y. (2020). The Nucleus Accumbens: A Common Target in the Comorbidity of Depression and Addiction. *Frontiers in Neural Circuits*, 14. <https://www.frontiersin.org/article/10.3389/fncir.2020.00037>

Yanagimoto, K., & Maeda, H. (2003). The nucleus accumbens unit activities related to the emotional significance of complex environmental stimuli in freely moving cats. *Neuroscience Research*, 46(2), 183–189. [https://doi.org/10.1016/s0168-0102\(03\)00058-0](https://doi.org/10.1016/s0168-0102(03)00058-0)

Yin, H. H., & Knowlton, B. J. (2006). The role of the basal ganglia in habit formation. *Nature Reviews. Neuroscience*, 7(6), 464–476. <https://doi.org/10.1038/nrn1919>

Yuan, L., Dou, Y.-N., & Sun, Y.-G. (2019). Topography of Reward and Aversion Encoding in the Mesolimbic Dopaminergic System. *The Journal of Neuroscience: The Official Journal of the Society for Neuroscience*, 39(33), 6472–6481. <https://doi.org/10.1523/JNEUROSCI.0271-19.2019>

- Záborszky, L., Alheid, G. F., Beinfeld, M. C., Eiden, L. E., Heimer, L., & Palkovits, M. (1985). Cholecystokinin innervation of the ventral striatum: A morphological and radioimmunological study. *Neuroscience*, *14*(2), 427–453. [https://doi.org/10.1016/0306-4522\(85\)90302-1](https://doi.org/10.1016/0306-4522(85)90302-1)
- Záborszky, L., & Cullinan, W. E. (1992). Projections from the nucleus accumbens to cholinergic neurons of the ventral pallidum: A correlated light and electron microscopic double-immunolabeling study in rat. *Brain Research*, *570*(1–2), 92–101. [https://doi.org/10.1016/0006-8993\(92\)90568-t](https://doi.org/10.1016/0006-8993(92)90568-t)
- Zahm, D. S., & Brog, J. S. (1992). On the significance of subterritories in the «accumbens» part of the rat ventral striatum. *Neuroscience*, *50*(4), 751–767. [https://doi.org/10.1016/0306-4522\(92\)90202-d](https://doi.org/10.1016/0306-4522(92)90202-d)
- Zahm, D. S., & Heimer, L. (1990). Two transpallidal pathways originating in the rat nucleus accumbens. *The Journal of Comparative Neurology*, *302*(3), 437–446. <https://doi.org/10.1002/cne.903020302>
- Zangenehpour, S., & Chaudhuri, A. (2002). Differential induction and decay curves of c-fos and zif268 revealed through dual activity maps. *Brain Research. Molecular Brain Research*, *109*(1–2), 221–225. [https://doi.org/10.1016/s0169-328x\(02\)00556-9](https://doi.org/10.1016/s0169-328x(02)00556-9)
- Zessen, R. van, Flores-Dourojeanni, J. P., Eekel, T., Reijen, S. van den, Lodder, B., Omrani, A., Smidt, M. P., Ramakers, G. M. J., Plasse, G. van der, Stuber, G. D., & Adan, R. A. H. (2021). Cue and Reward Evoked Dopamine Activity Is Necessary for Maintaining Learned Pavlovian Associations. *Journal of Neuroscience*, *41*(23), 5004–5014. <https://doi.org/10.1523/JNEUROSCI.2744-20.2021>
- Zhang, L., Liang, B., Barbera, G., Hawes, S., Zhang, Y., Stump, K., Baum, I., Yang, Y., Li, Y., & Lin, D.-T. (2019). Unit Title: Miniscope GRIN lens system for calcium imaging of neuronal activity from deep brain structures in behaving animals. *Current protocols in neuroscience*, *86*(1), e56. <https://doi.org/10.1002/cpns.56>
- Zhang, X., & Li, B. (2018). Population coding of valence in the basolateral amygdala. *Nature Communications*, *9*, 5195. <https://doi.org/10.1038/s41467-018-07679-9>
- Zhou, L., Furuta, T., & Kaneko, T. (2003). Chemical organization of projection neurons in the rat accumbens nucleus and olfactory tubercle. *Neuroscience*, *120*(3), 783–798. [https://doi.org/10.1016/s0306-4522\(03\)00326-9](https://doi.org/10.1016/s0306-4522(03)00326-9)
- Ziegenhain, C., Vieth, B., Parekh, S., Reinius, B., Guillaumet-Adkins, A., Smets, M., Leonhardt, H., Heyn, H., Hellmann, I., & Enard, W. (2017). Comparative Analysis of Single-Cell RNA Sequencing Methods. *Molecular Cell*, *65*(4), 631-643.e4. <https://doi.org/10.1016/j.molcel.2017.01.023>

***CHAPTER 7 – Supplementary
information***

Supplementary information

Table S1. Summary of statistical data from the main figures

Figure 4 – Animals learn the association between cue and reward throughout training			
Figure	Statistical test	Test Value	Post hoc
Figure 4C	Two-way ANOVA	Pav_d2 - CS vs ITI: $F_{(1,5)} = 15.49, p = 0.0110^*$ Pav_d12 - CS vs ITI: $F_{(1,5)} = 8.687, p = 0.0320^*$	Pav_d2-CS vs ITI, day 1: $p=0.0155^*$; day 2: $p=0.0876$ Pav_d12-CS vs ITI, day 1: $p>0.9999$; day 2: $p>0.9999$; day 3: $p>0.9999$; day 4: $p=0.0763$; day 5: $p=0.1819$; day 6: $p=0.0087^*$; day 7: $p=0.0026^*$; day 8: $p=0.0074^*$; day 9: $p=0.0019^*$; day 10: $p < 0.0001^*$; day 11: $p < 0.0001^*$; day 12: $p < 0.0001^*$
Figure 4D	Linear regression	Pav_d2_CS: $r^2 = 0.0273, s = 67.08, p = 0.6081$ Pav_d12_CS: $r^2 = 0.1892, s = 190, p = 0.0002^*$ Pav_d12_ITI: $r^2 = 0.0012, s = 254.1, p = 0.3655$	

Table S2. Summary of statistical data from the main figures

Figure 5 – Quantification of c-fos⁺ cell density in the NAc of mice in early learning (day 2)			
Figure	Statistical test	Test Value	Descriptive statistics
Figure 5C	Unpaired t-test	$t_{(9)} = 1.239, p = 0.2615$	noPav_d2: 23.80 ± 5.389 cells/mm ² ; Pav_d2: 37.33 ± 11.26 cells/mm ²
Figure 5E	Unpaired t-test	$t_{(9)} = 2.133, p = 0.0769$	noPav_d2: 18.00 ± 3.592 cells/mm ² ; Pav_d2: 44.67 ± 15.81 cells/mm ²
Figure 5G	Unpaired t-test	$t_{(9)} = 0.413, p = 0.6937$	noPav_d2: 18.20 ± 7.151 cells/mm ² ; Pav_d2: 22.67 ± 6.960 cells/mm ²
			Post hoc
Figure 5D	Two way ANOVA	Coordinates: $F_{(3,7)} = 3.518, p = 0.0230^*$	1.9-1.8: $p > 0.9999$ 1.7-1.5: $p > 0.9999$ 1.4-1.3: $p = 0.9591$ 1.2-1.1: $p = 0.7941$ 1-0.9: $p = 0.0765$ 0.7-0.6: $p > 0.9999$
Figure 5F	Two way ANOVA	Coordinates: $F_{(3,7)} = 11.15, p = 0.0110^*$	1.9-1.8: $p > 0.9999$ 1.7-1.5: $p > 0.9999$ 1.4-1.3: $p > 0.9999$ 1.2-1.1: $p = 0.5873$ 1-0.9: $p = 0.0430^*$
Figure 5H	Two way ANOVA	Coordinates: $F_{(3,7)} = 4.936, p = 0.0159^*$	1.7-1.5: $p = 0.0181^*$ 1.4-1.3: $p > 0.9999$ 1.2-1.1: $p > 0.9999$ 1-0.9: $p = 0.0621$ 0.7-0.6: $p > 0.9999$

Table S3. Summary of statistical data from the main figures

Figure 6 - Quantification of c-fos⁺ cell density in the NAc of mice in late learning (day 12)			
Figure	Statistical test	Test Value	Descriptive statistics
Figure 6C	Unpaired t-test	$t_{(19)} = 0.6303, p = 0.5426$	noPav_d12: 31.40 ± 10.03 cells/mm ² ; Pav_d12: 24.14 ± 6.646 cells/mm ²

Figure 6E	Unpaired t-test	$t_{(29)} = 0.0886, p = 0.9312$	noPav_d12: 29.40±6.454 cells/mm ² ; Pav_d12: 28.57±6.399 cells/mm ²
Figure 6G	Unpaired t-test	$t_{(28)} = 0.1138, p = 0.9117$	noPav_d12: 15.60±4.718 cells/mm ² ; Pav_d12: 15.00±2.952 cells/mm ²
			Post hoc
Figure 6D	Two way ANOVA	Coordinates: $F_{(6,25)} = 2.947, p = 0.0317^*$	1.9-1.8: $p > 0.9999$ 1.7-1.5: $p > 0.9999$ 1.4-1.3: $p > 0.9999$ 1.2-1.1: $p > 0.9999$ 1-0.9: $p > 0.9999$ 0.7-0.6: $p > 0.9999$
Figure 6F	Two way ANOVA	Coordinates: $F_{(4,20)} = 3.489, p = 0.0257^*$	1.9-1.8: $p > 0.9999$ 1.7-1.5: $p > 0.9999$ 1.4-1.3: $p > 0.9999$ 1.2-1.1: $p > 0.9999$ 1-0.9: $p > 0.9999$
Figure 6H	Two way ANOVA	Coordinates: $F_{(4,20)} = 1.492, p = 0.2422$	1.7-1.5: $p = 0.1931$ 1.4-1.3: $p = 0.7112$ 1.2-1.1: $p > 0.9999$ 1-0.9: $p > 0.9999$ 0.7-0.6: $p > 0.9999$

Table S4. Summary of statistical data from the main figures

Figure 7 - Behavior of D1-cre mice during positive Pavlovian conditioning			
Figure	Statistical test	Test Value	Post hoc
Figure 7C	Two-way ANOVA	CS vs ITI: $F_{(1,8)} = 4.633, p = 0.0635^*$	day 1: $p > 0.9999$ day 2: $p > 0.9999$ day 3: $p > 0.9999$ day 4: $p > 0.9999$ day 5: $p > 0.9999$ day 6: $p = 0.1259$ day 7: $p = 0.0045^*$ day 8: $p = 0.0430^*$ day 9: $p = 0.0001^*$ day 10: $p < 0.0001^*$ day 11: $p = 0.0005^*$ day 12: $p < 0.0001^*$
Figure 7D	Linear Regression	$r^2 = 0.02094, s = 123.6, p = 0.1370$	

Table S5. Summary of statistical data from the main figures

Figure 8 – Activity of D1-neurons during Pavlovian conditioning			
Figure	Statistical test	Test Value	
		CS	US
Figure 8A-B	Wilcoxon signed rank	first 5 trials: $W = 0, p < 0.0001^*$ last 5 trials: $W = 0, p < 0.0001^*$ all trials: $W = 0, p < 0.0001^*$	first 5 trials: $W = 0, p < 0.0001^*$ last 5 trials: $W = 35037, p = 0.1660$ all trials: $W = 0, p < 0.0001^*$
Figure 8C-D	Wilcoxon signed rank	first 5 trials: $W = 26950, p < 0.0001^*$ last 5 trials: $W = 0, p < 0.0001^*$ all trials: $W = 58, p < 0.0001^*$	first 5 trials: $W = 9640, p < 0.0001^*$ last 5 trials: $W = 0, p < 0.0001^*$ all trials: $W = 22779, p < 0.0001^*$
Figure 8E-F	Wilcoxon signed rank	first 5 trials: $W = 22983, p < 0.0001^*$ last 5 trials: $W = 11933, p < 0.0001^*$ all trials: $W = 17445, p < 0.0001^*$	first 5 trials: $W = 0, p < 0.0001^*$ last 5 trials: $W = 17211, p < 0.0001^*$ all trials: $W = 799, p < 0.0001^*$

Table S6. Summary of statistical data from the main figures

Figure 9 – Activity of D1-neurons decreases in response to the CS		
Figure	Statistical test	Test Value
Figure 9A	Linear Regression	$r = 0.07561, s = 0.2134, p = 0.0124^*$
Figure 9B	Paired t-test	Day1: $t_{(8)} = 1.874, p = 0.1101$ Day6: $t_{(8)} = 1.672, p = 0.1456$ Day12: $t_{(8)} = 1.089, p = 0.3259$
Figure 9C	Linear Regression	$r = 0.07561, s = 0.6386, p = 0.0124^*$
Figure 9D	Paired t-test	Day1: $t_{(8)} = 1.873, p = 0.1102$ Day6: $t_{(8)} = 1.672, p = 0.1456$ Day12: $t_{(8)} = 1.083, p = 0.3281$
Figure 9E	Linear Regression	$r = 0.00461, s = 0.4510, p = 0.5419$
Figure 9F	Paired t-test	Day1: $t_{(8)} = 0.418, p = 0.6903$ Day6: $t_{(8)} = 0.143, p = 0.8909$ Day12: $t_{(8)} = 1.519, p = 0.1796$

Table S7. Summary of statistical data from the main figures

Figure 10 – Activity of D1-neurons decreases in response to the US		
Figure	Statistical test	Test Value
Figure 10A	Linear Regression	$r = 0.1186, s = 0.2495, p = 0.0016^*$
Figure 10B	Paired t-test	Day1: $t_{(8)} = 1.045, p = 0.3364$ Day6: $t_{(8)} = 0.279, p = 0.7897$ Day12: $t_{(8)} = 2.038, p = 0.0877$
Figure 10C	Linear Regression	$r = 0.1185, s = 0.7464, p = 0.0017^*$
Figure 10D	Paired t-test	Day1: $t_{(8)} = 1.046, p = 0.3358$ Day6: $t_{(8)} = 0.280, p = 0.7888$ Day12: $t_{(8)} = 2.034, p = 0.0882$
Figure 10E	Linear Regression	$r = 0.04277, s = 0.4062, p = 0.0674$
Figure 10F	Paired t-test	Day1: $t_{(8)} = 0.112, p = 0.9143$ Day6: $t_{(8)} = 0.274, p = 0.7953$ Day12: $t_{(8)} = 1.563, p = 0.1789$

Table S8. Summary of statistical data from the main figures

Figure11- D1-neurons activity decreases in response to CS and US from day 1 to day 12 of Pavlovian conditioning		
Figure	Statistical test	Test Value
Figure 11A	Wilcoxon signed rank	$W=100, p < 0.0001^*$
Figure 11B	Paired t-test	Day 1 vs Day 12: $t_{(8)} = 2.370; p = 0.0500^*$
Figure 11C	Paired t-test	Day 1 vs Day 12: $t_{(8)} = 2.370; p = 0.0500^*$
Figure 11D	Paired t-test	Day 1 vs Day 12: $t_{(8)} = 0.759, p = 0.4764$
Figure 11E	Paired t-test	Day 1 vs Day 12: $t_{(8)} = 2.573; p = 0.0422^*$
Figure 11F	Paired t-test	Day 1 vs Day 12: $t_{(8)} = 2.572, p = 0.0422^*$
Figure 11G	Paired t-test	Day 1 vs Day 12: $t_{(8)} = 0.765, p = 0.4730$

Table S9. Summary of statistical data from the main figures

Figure 12 - Behavior of D2-cre during positive Pavlovian conditioning			
Figure	Statistical test	Test Value	Post hoc
Figure 12C	Two-way ANOVA	CS vs ITI: $F_{(1,6)} = 2.584, p = 0.1591$	day 1: $p > 0.9999$ day 2: $p > 0.9999$ day 3: $p > 0.9999$ day 4: $p > 0.9999$ day 5: $p > 0.9999$ day 6: $p > 0.9999$ day 7: $p = 0.2345$ day 8: $p = 0.0990$ day 9: $p = 0.1549$ day 10: $p = 0.0147$ day 11: $p = 0.0017$ day 12: $p = 0.0012$
Figure 12D	Linear Regression	$r^2 = 0.07348, s = 94.27, p = 0.0132^*$	

Table S10. Summary of statistical data from the main figures

Figure 13 – Activity of D2-neurons during Pavlovian conditioning			
Figure	Statistical test	Test Value	
		CS	US
Figure 13A-B	Wilcoxon signed rank	first 5 trials: $W = 1482, p < 0.0001^*$ last 5 trials: $W = 0, p < 0.0001^*$ all trials: $W = 0, p < 0.0001^*$	first 5 trials: $W = 8889, p < 0.0001^*$ last 5 trials: $W = 14086, p < 0.0001^*$ all trials: $W = 0, p < 0.0001^*$
Figure 13C-D	Wilcoxon signed rank	first 5 trials: $W = 10558, p < 0.0001^*$ last 5 trials: $W = 9630, p < 0.0001^*$ all trials: $W = 0, p < 0.0001^*$	first 5 trials: $W = 0, p < 0.0001^*$ last 5 trials: $W = 0, p < 0.0001^*$ all trials: $W = 0, p < 0.0001^*$
Figure 13E-F	Wilcoxon signed rank	first 5 trials: $W = 26324, p < 0.0001^*$ last 5 trials: $W = 28294, p < 0.0001^*$ all trials: $W = 0, p < 0.0001^*$	first 5 trials: $W = 4967, p < 0.0001^*$ last 5 trials: $W = 16248, p < 0.0001^*$ all trials: $W = 7040, p < 0.0001^*$

Table S11. Summary of statistical data from the main figures

Figure 14 – Activity of D2-neurons decreases in response to the CS		
Figure	Statistical test	Test Value
Figure 14A	Linear Regression	$r^2 = 0.06563, s = 0.1934, p = 0.0218^*$
Figure 14B	Paired t-test	Day 1: $t_{(9)} = 2.959, p = 0.0315^*$ Day 6: $t_{(9)} = 2.212, p = 0.0689$ Day 12: $W = -11, p = 0.3125$
Figure 14C	Linear Regression	$r^2 = 0.03223, s = 0.5642, p = 0.1134$
Figure 14D	Paired t-test	Day 1: $t_{(9)} = 2.962, p = 0.0314^*$ Day 6: $t_{(9)} = 3.034, p = 0.0289^*$ Day 12: $W = -11, p = 0.3125$
Figure 14E	Linear Regression	$r^2 = 7.789e^{-005}, s = 0.3550, p = 0.9365$
Figure 14F	Paired t-test	Day 1: $t_{(9)} = 0.2689, p = 0.7970$ Day 6: $t_{(9)} = 0.0408, p = 0.9690$ Day 12: $t_{(9)} = 1.438, p = 0.2099$

Table S12. Summary of statistical data from the main figures

Figure 15 – Activity of D2-neurons decreases in response to the US		
Figure	Statistical test	Test Value
Figure 15A	Linear Regression	$r^2 = 0.03835$, $s = 0.2528$, $p = 0.0778$
Figure 15B	Paired t-test	Day 1: $t_{(9)} = 0.6741$, $p = 0.5254$ Day 6: $t_{(9)} = 1.971$, $p = 0.0962$ Day 12: $t_{(9)} = 0.9326$, $p = 0.3870$
Figure 15C	Linear Regression	$r^2 = 0.02961$, $s = 0.7192$, $p = 0.1222$
Figure 15D	Paired t-test	Day 1: $t_{(9)} = 0.6762$, $p = 0.5241$ Day 6: $t_{(9)} = 0.9676$, $p = 0.3777$ Day 12: $t_{(9)} = 0.9291$, $p = 0.3887$
Figure 15E	Linear Regression	$r^2 = 1.405e^{005}$, $s = 0.3560$, $p = 0.9735$
Figure 15F	Paired t-test	Day 1: $t_{(9)} = 1.395$, $p = 0.2355$ Day 6: $t_{(9)} = 2.069$, $p = 0.0840$ Day 12: $t_{(9)} = 0.300$, $p = 0.7763$

Table S13. Summary of statistical data from the main figures

Figure16- D2-neurons activity decreases in response to CS and US from day 1 to day 12 of Pavlovian conditioning		
Figure	Statistical test	Test Value
Figure 16A	Wilcoxon signed rank	$W=150$ $p < 0.0001$
Figure 16B	Wilcoxon test	Day 1 vs Day 12: $W = -3$, $p = 0.8438$
Figure 16C	Wilcoxon test	Day 1 vs Day 12: $W = -3$, $p = 0.8438$
Figure 16D	Paired t-test	Day 1 vs Day 12: $t_{(9)} = 0.9340$, $p = 0.3863$
Figure 16E	Paired t-test	Day 1 vs Day 12: $t_{(9)} = 1.218$; $p = 0.2690$
Figure 16F	Paired t-test	Day 1 vs Day 12: $t_{(9)} = 1.214$, $p = 0.2703$
Figure 16G	Paired t-test	Day 1 vs Day 12: $t_{(9)} = 0.3441$, $p = 0.7448$

Table S14. Summary of statistical data from the main figures

Figure 17 – Behavior of D1-cre mice during Pavlovian aversive conditioning			
Figure	Statistical test	Test Value	Post hoc
Figure 17B	Two-way ANOVA	$F_{(4,035,27,80)} = 7.991$, $p = 0.0002^*$	Trial 1 vs Trial 2: $p > 0.9999$ Trial 1 vs Trial 3: $p > 0.9999$ Trial 1 vs Trial 4: $p = 0.0430^*$ Trial 1 vs Trial 5: $p = 0.0035^*$ Trial 1 vs Trial 6: $p = 0.0110^*$ Trial 1 vs Trial 7: $p = 0.0895$ Trial 1 vs Trial 8: $p = 0.0130^*$ Trial 1 vs Trial 9: $p = 0.0844$ Trial 1 vs Trial 10: $p = 0.0010^*$ Trial 2 vs Trial 3: $p > 0.9999$ Trial 2 vs Trial 4: $p = 0.0726$ Trial 2 vs Trial 5: $p = 0.0069^*$ Trial 2 vs Trial 6: $p = 0.0204^*$ Trial 2 vs Trial 7: $p = 0.1432$ Trial 2 vs Trial 8: $p = 0.0238^*$ Trial 2 vs Trial 9: $p = 0.1356$ Trial 2 vs Trial 10: $p = 0.0022^*$ Trial 3 vs Trial 4: $p > 0.9999$ Trial 3 vs Trial 5: $p > 0.9999$ Trial 3 vs Trial 6: $p > 0.9999$

			Trial 3 vs Trial 7: $p > 0.9999$ Trial 3 vs Trial 8: $p > 0.9999$ Trial 3 vs Trial 9: $p > 0.9999$ Trial 3 vs Trial 10: $p = 0.4740$ Trial 4 vs Trial 5: $p > 0.9999$ Trial 4 vs Trial 6: $p > 0.9999$ Trial 4 vs Trial 7: $p > 0.9999$ Trial 4 vs Trial 8: $p > 0.9999$ Trial 4 vs Trial 9: $p > 0.9999$ Trial 4 vs Trial 10: $p > 0.9999$ Trial 5 vs Trial 6: $p > 0.9999$ Trial 5 vs Trial 7: $p > 0.9999$ Trial 5 vs Trial 8: $p > 0.9999$ Trial 5 vs Trial 9: $p > 0.9999$ Trial 5 vs Trial 10: $p > 0.9999$ Trial 6 vs Trial 7: $p > 0.9999$ Trial 6 vs Trial 8: $p > 0.9999$ Trial 6 vs Trial 9: $p > 0.9999$ Trial 6 vs Trial 10: $p > 0.9999$ Trial 7 vs Trial 8: $p > 0.9999$ Trial 7 vs Trial 9: $p > 0.9999$ Trial 7 vs Trial 10: $p > 0.9999$ Trial 8 vs Trial 9: $p > 0.9999$ Trial 8 vs Trial 10: $p > 0.9999$ Trial 9 vs Trial 10: $p > 0.9999$
Figure 17C	Paired t-test	$t_{(9)} = 5.641, p = 0.0024^*$	
Figure 17D	Paired t-test	$t_{(9)} = 1.742, p = 0.1420$	
Figure 17E	Paired t-test	$t_{(9)} = 0.08219, p = 0.9377$	
Figure 17F	Paired t-test	$t_{(9)} = 0.6736, p = 0.5304$	

Table S15. Summary of statistical data from the main figures

Figure 18 – Average activity of D1-neurons during Pavlovian aversive conditioning			
Figure	Statistical test	Test Value	
		CS	Shock
Figure 18A-B	Wilcoxon signed rank	first trial: $W = 37025, p = 0.6222$ last trial: $W = 5281, p < 0.0001^*$ all trials: $W = 30959, p < 0.0001^*$	first trial: $W = 1120, p < 0.0001^*$ last trial: $W = 11680, p < 0.0001^*$ all trials: $W = 1431, p < 0.0001^*$
Figure 18C-D	Wilcoxon signed rank	first trial: $W = 0, p < 0.0001^*$ last trial: $W = 36764, p = 0.5419$ all trials: $W = 0, p < 0.0001^*$	first trial: $W = 0, p < 0.0001^*$ last trial: $W = 0, p < 0.0001^*$ all trials: $W = 0, p < 0.0001^*$
Figure 18E-F	Wilcoxon signed rank	first trial: $W = 2612, p < 0.0001^*$ last trial: $W = 16382, p < 0.0001^*$ all trials: $W = 0, p < 0.0001^*$	first trial: $W = 2729, p < 0.0001^*$ last trial: $W = 1659, p < 0.0001^*$ all trials: $W = 2469, p < 0.0001^*$
Figure 18G-H	Wilcoxon signed rank	first trial: $W = 7771, p < 0.0001^*$ last trial: $W = 0, p < 0.0001^*$ all trials: $W = 0, p < 0.0001^*$	first trial: $W = 14116, p < 0.0001^*$ last trial: $W = 25493, p < 0.0001^*$ all trials: $W = 0, p < 0.0001^*$

Table S16. Summary of statistical data from the main figures

Figure 20 – Activity of D1-neurons increases in response to the CS		
Figure	Statistical test	Test Value
Figure 20A	Paired t-test	Day 1: $t_{(9)} = 0.05574, p = 0.9577$ Day 2_noshock: $t_{(9)} = 1.349, p = 0.2352$ Day 2_shock: $t_{(9)} = 1.804, p = 0.1311$

		Day 3: $t_{\beta} = 2.072, p = 0.0930$
Figure 20B	Paired t-test	Day 1: $t_{\beta} = 0.05438, p = 0.9587$; Day 2_noshock: $t_{\beta} = 1.348, p = 0.2355$; Day 2_shock: $t_{\beta} = 1.804, p = 0.1310$; Day 3: $t_{\beta} = 2.072, p = 0.0932$
Figure 20C	Paired t-test	Day 1: $t_{\beta} = 0.0463, p = 0.9649$; Day 2_noshock: $t_{\beta} = 0.1845, p = 0.8608$; Day 2_shock: $t_{\beta} = 1.905, p = 0.1296$; Day 3: $t_{\beta} = 1.550, p = 0.1819$

Table S17. Summary of statistical data from the main figures

Figure 21 – Activity of D1-neurons increases in response to foot shock		
Figure	Statistical test	Test Value
Figure 21A	Paired t-test	Day 1: $t_{\beta} = 1.501, p = 0.1937$ Day 2_noshock: $t_{\beta} = 1.061, p = 0.3373$ Day 2_shock: $W = 9, p = 0.4375$ Day 3: $t_{\beta} = 1.366, p = 0.2300$
Figure 21B	Paired t-test	Day 1: $t_{\beta} = 1.504, p = 0.1929$ Day 2_noshock: $t_{\beta} = 1.054, p = 0.3403$ Day 2_shock: $W = 9, p = 0.4375$ Day 3: $t_{\beta} = 1.370, p = 0.2290$
Figure 21C	Paired t-test	Day 1: $t_{\beta} = 1.323, p = 0.2430$ Day 2_noshock: $t_{\beta} = 0.4979, p = 0.6397$ Day 2_shock: $t_{\beta} = 1.563, p = 0.1788$ Day 3: $t_{\beta} = 3.030, p = 0.0291^*$

Table S18. Summary of statistical data from the main figures

Figure22- D1-neurons activity in day 1 and day 3 in response to CS and to US (shock)		
Figure	Statistical test	Test Value
Figure 22A	Paired t-test	Day 1 vs Day 3: $t_{\beta} = 1.608, p = 0.1688$
Figure 22B	Paired t-test	Day 1 vs Day 3: $t_{\beta} = 1.609, p = 0.1686$
Figure 22C	Paired t-test	Day 1 vs Day 3: $t_{\beta} = 0.8470, p = 0.4356$
Figure 22D	Paired t-test	Day 1 vs Day 3: $t_{\beta} = 1.313, p = 0.2461$
Figure 22E	Paired t-test	Day 1 vs Day 3: $t_{\beta} = 1.316, p = 0.2453$
Figure 22F	Paired t-test	Day 1 vs Day 3: $t_{\beta} = 0.442, p = 0.6768$

Table S19. Summary of statistical data from the main figures

Figure 23 – Behavior of D2-cre mice during Pavlovian aversive conditioning			
Figure	Statistical test	Test Value	Post hoc
Figure 23B	Two-way ANOVA	$F_{(2,45,110)} = 10.77, p = 0.0012^*$	Trial 1 vs Trial 2: $p > 0.9999$ Trial 1 vs Trial 3: $p > 0.9999$ Trial 1 vs Trial 4: $p > 0.9999$ Trial 1 vs Trial 5: $p > 0.9999$ Trial 1 vs Trial 6: $p > 0.9999$ Trial 1 vs Trial 7: $p = 0.0030^*$ Trial 1 vs Trial 8: $p = 0.0995$ Trial 1 vs Trial 9: $p = 0.0021^*$

			<p>Trial 1 vs Trial 10: $p = 0.0060^*$ Trial 2 vs Trial 3: $p > 0.9999$ Trial 2 vs Trial 4: $p = 0.6623$ Trial 2 vs Trial 5: $p > 0.9999$ Trial 2 vs Trial 6: $p > 0.9999$ Trial 2 vs Trial 7: $p = 0.0168^*$ Trial 2 vs Trial 8: $p = 0.0818$ Trial 2 vs Trial 9: $p = 0.0249^*$ Trial 2 vs Trial 10: $p = 0.0125^*$ Trial 3 vs Trial 4: $p > 0.9999$ Trial 3 vs Trial 5: $p > 0.9999$ Trial 3 vs Trial 6: $p > 0.9999$ Trial 3 vs Trial 7: $p = 0.1512$ Trial 3 vs Trial 8: $p > 0.9999$ Trial 3 vs Trial 9: $p = 0.7350$ Trial 3 vs Trial 10: $p = 0.1199$ Trial 4 vs Trial 5: $p > 0.9999$ Trial 4 vs Trial 6: $p > 0.9999$ Trial 4 vs Trial 7: $p > 0.9999$ Trial 4 vs Trial 8: $p > 0.9999$ Trial 4 vs Trial 9: $p > 0.9999$ Trial 4 vs Trial 10: $p > 0.9999$ Trial 5 vs Trial 6: $p > 0.9999$ Trial 5 vs Trial 7: $p = 0.0884$ Trial 5 vs Trial 8: $p > 0.9999$ Trial 5 vs Trial 9: $p = 0.1160$ Trial 5 vs Trial 10: $p = 0.0469^*$ Trial 6 vs Trial 7: $p = 0.8794$ Trial 6 vs Trial 8: $p > 0.9999$ Trial 6 vs Trial 9: $p > 0.9999$ Trial 6 vs Trial 10: $p = 0.1783$ Trial 7 vs Trial 8: $p > 0.9999$ Trial 7 vs Trial 9: $p > 0.9999$ Trial 7 vs Trial 10: $p > 0.9999$ Trial 8 vs Trial 9: $p > 0.9999$ Trial 8 vs Trial 10: $p > 0.9999$ Trial 9 vs Trial 10: $p > 0.9999$</p>
Figure 23C	Paired t-test	$t_{(8)} = 8.634, p = 0.0001^*$	
Figure 23D	Paired t-test	$t_{(8)} = 0.9286, p = 0.4057$	
Figure 23E	Paired t-test	$t_{(8)} = 0.9159, p = 0.4017$	
Figure 23F	Paired t-test	$t_{(8)} = 1.301, p = 0.2411$	

Table S20. Summary of statistical data from the main figures

Figure 24 – Average activity of D2-neurons during Pavlovian aversive conditioning			
Figure	Statistical test	Test Value	
		CS	Shock
Figure 24A-B	Wilcoxon signed rank	<p>first trial: $W = 22020, p < 0.0001^*$ last trial: $W = 21611, p < 0.0001^*$ all trials: $W = 29237, p < 0.0001$</p>	<p>first trial: $W = 18869, p < 0.0001^*$ last trial: $W = 0, p < 0.0001^*$ all trials: $W = 768, p < 0.0001^*$</p>
Figure 24C-D	Wilcoxon signed rank	<p>first trial: $W = 0, p < 0.0001^*$ last trial: $W = 4032, p < 0.0001^*$ all trials: $W = 0, p < 0.0001$</p>	<p>first trial: $W = 0, p < 0.0001^*$ last trial: $W = 13262, p < 0.0001^*$ all trials: $W = 2680, p < 0.0001^*$</p>
Figure 24E-F	Wilcoxon signed rank	<p>first trial: $W = 0, p < 0.0001^*$ last trial: $W = 21832, p < 0.0001^*$ all trials: $W = 0, p < 0.0001^*$</p>	<p>first trial: $W = 0, p < 0.0001^*$ last trial: $891, p < 0.0001^*$ all trials: $W = 0, p < 0.0001^*$</p>
Figure 24G-H	Wilcoxon signed rank	<p>first trial: $W = 0, p < 0.0001^*$ last trial: $W = 0, p < 0.0001^*$ all trials: $W = 0, p < 0.0001^*$</p>	<p>first trial: $W = 4685, p < 0.0001^*$ last trial: $W = 7327, p < 0.0001^*$ all trials: $W = 0, p < 0.0001^*$</p>

Table S21. Summary of statistical data from the main figures

Figure 26 – Activity of D2-neurons increases in response to the CS		
Figure	Statistical test	Test Value
Figure 26A	Paired t-test	Day 1: $t_{\beta} = 0.2367$, $p = 0.8207$ Day 2_noshock: $t_{\beta} = 1.828$, $p = 0.1173$ Day 2_shock: $W = 24$, $p = 0.0469^*$ Day 3: $W = 18$, $p = 0.1562$
Figure 26B	Paired t-test	Day 1: $t_{\beta} = 0.2355$, $p = 0.8217$ Day 2_noshock: $t_{\beta} = 1.829$, $p = 0.1172$ Day 2_shock: $W = 24$, $p = 0.0469^*$ Day 3: $W = 18$, $p = 0.1562$
Figure 26C	Paired t-test	Day 1: $W = 3$, $p = 0.5000$ Day 2_noshock: $t_{\beta} = 1.749$, $p = 0.1407$ Day 2_shock: $W = 26$, $p = 0.0312^*$ Day 3: $t_{\beta} = 0.2570$, $p = 0.8058$

Table S22. Summary of statistical data from the main figures

Figure 27 – Activity of D2-neurons increases in response to foot shock		
Figure	Statistical test	Test Value
Figure 27A	Paired t-test	Day 1: $t_{\beta} = 2.783$, $p = 0.0319^*$ Day 2_noshock: $t_{\beta} = 1.846$, $p = 0.1242$ Day 2_shock: $t_{\beta} = 1.680$, $p = 0.1538$ Day 3: $t_{\beta} = 2.062$, $p = 0.0941$
Figure 27B	Paired t-test	Day 1: $t_{\beta} = 2.791$, $p = 0.0315^*$ Day 2_noshock: $t_{\beta} = 1.844$, $p = 0.1245$ Day 2_shock: $t_{\beta} = 1.672$, $p = 0.1554$ Day 3: $t_{\beta} = 2.064$, $p = 0.0940$
Figure 27C	Paired t-test	Day 1: $W = -9$, $p = 0.3125$ Day 2_noshock: $t_{\beta} = 0.5947$, $p = 0.5738$ Day 2_shock: $t_{\beta} = 0.1889$, $p = 0.8564$ Day 3: $t_{\beta} = 0.2645$, $p = 0.8003$

Table S23. Summary of statistical data from the main figures

Figure 28- D2-neurons activity in day 1 and day 3 in response to CS and to US (shock)		
Figure	Statistical test	Test Value
Figure 28A	Wilcoxon test	Day 1 vs Day 3: $W = 14$, $p = 0.2969$
Figure 28B	Wilcoxon test	Day 1 vs Day 3: $W = 14$, $p = 0.2969$
Figure 28C	Wilcoxon test	Day 1 vs Day 3: $W = 22$, $p = 0.0781$
Figure 28D	Paired t-test	Day 1 vs Day 3: $t_{\beta} = 2.530$, $p = 0.0500^*$
Figure 28E	Paired t-test	Day 1 vs Day 3: $t_{\beta} = 2.536$, $p = 0.0500^*$
Figure 28F	Wilcoxon test	Day 1 vs Day 3: $W = 24$, $p = 0.0469^*$